SMART GRID POWER MARKET STUDY IN POWER TRANSMISSION, DISTRIBUTION AND DEMAND SYSTEMS

by

DONG ZHANG

SHUHUI LI, COMMITTEE CHAIR
JABER ABU QAHOUQ
FEI HU
XIAOYAN HONG
JUN MA

A DISSERTATION

Submitted in partial fulfillment of the requirements
for the degree of Doctor of Philosophy
in the Department of Electrical and Computer Engineering
in the Graduate School of
The University of Alabama

TUSCALOOSA, ALABAMA

2013

ABSTRACT

An electric power system is a meshed network which includes three major components: transmission, distribution, and demand systems. The future smart grid will be a highly intelligent electric power system that will have a profoundly impact on all the three areas. This dissertation focuses on 1) the competitive power market study, 2) optimal power management in microgrid, and 3) intelligent demand response strategies of residential system.

In the transmission system, generation companies and load serve entities are encouraged to compete for the amount of power generation and load demand. Therefore, utility companies require an efficient and reliable computational tool to analyze the competitive power markets. However, most of existing commercial power system simulators are unable to evaluate a competitive power market directly. This dissertation proposes a method to convert a competitive power market problem in such a way that PowerWorld can be used for broad competitive power market studies, including optimal power flow, unit commitment, and agent-based learning.

In the distribution system, it's urgent to develop an efficient computational tool that can be used in the energy management system to control different types of renewable energy in microgrid. This dissertation develops a mechanism to use PowerWorld for comprehensive analysis of microgrid power markets as well as optimal power flow under different power converter operating modes.

In the demand system, demand response (DR), a critical component for smart grid, will adjust the load power consumption pattern to achieve high economic efficiency. This dissertation proposes several different DR strategies for home appliance of the residential system.

DEDICATION

This dissertation is dedicated to my parents, Zhenzhong Zhang and Shujun Mi, who support and guide me through each step of my life. In particular, to Dr. Shuhui Li who introduced me to the world of Smart grid.

ACKNOWLEDGMENTS

Firstly, I would like to especially thank my advisor, Dr. Shuhui Li for helping me accomplish this dissertation. His innovative thinking and strong passion always inspire me to keep exploring the new solutions of the research issues in Smart grid.

Secondly, I would like to gratefully thank Dr. Fei Hu and Dr. Jaber Abu Qahouq for providing constructive advices and significant help on this dissertation.

Lastly, I would like to sincerely thank Dr. Xiaoyan Hong and Dr. Ma Jun for their willingness to serve as the committee members and useful comments on this dissertation.

CONTENTS

LIST OF TABLES

LIST OF FIGURES

1. SUMMARY OF RESEARCH

In an electric power grid, electric power delivers through transmission and distribution systems to energy consumers over a large geographically area. Today, the utility companies are facing many technological challenges in energy transmission, distribution and consumption systems. Smart grid is a highly modernized power grid, which is expected to be a revolution in each part of an electric power system by equipping numerous advanced technologies. The major subjects of this dissertation are the competitive power market study, microgrid power management system, and demand response for residential energy consumers.

In the transmission system, the competitive power market has the two-side biding rule for each market participator to issue bids offered by sellers and buyers. For the supply bid, each generation company (GenCo) is able to generate the reported marginal cost function as a bid for the amount of its power generation. For the demand bid, the load service entities (LSEs) use two types of loads, the fixed load and the price sensitive load, as a bid for the amount of load to be served. Both buyers (GenCos) and sellers (LSEs) will submit their bids to the regional independent system operators (ISOs) under the schedule of day-ahead market. After collecting all the bids, ISO will use unit commitment (UC) to determine the optimal sets of generation units to meet the demands in a 24-hour time period. In each hour, ISOs will also solve the optimal power dispatch to determine the power generation set points, the amount of load to be served, and the electricity price. Also, in order to bid rationally and intelligently, GenCos and LSEs are able to using the agent-learning module to adjust the bidding strategies based on the obtained net surpluses. However, today's most of the prevailing power system simulation software is not

designed to solve this agent-based competitive power market that can hinder the development of future smart grid. In this dissertation, a novel computational system was developed by converting a competitive power market's optimization problem into a format that can allow PowerWorld simulator to solve the optimization problem. This is discussed in the second chapter of the dissertation, which includes 1) studying what are characteristics and models associated with a competitive wholesale power market, 2) investigating how these models can be converted and transformed in such a way that PowerWorld simulator can be used for optimal power dispatch study of a competitive power market so as to take many advantages provided by the commercial software, and 3) exploring how PowerWorld and MatLab can be integrated together for combined unit commitment and optimal power dispatch study for a competitive power market. In the third chapter of the dissertation, details of the agent-based learning is investigated for a competitive power market.

In power distribution system, microgrid (MG) is able to integrate many different types of renewable energy to improve power efficiency, reliability, quality, and stability. Normally, MG has two operational modes: the grid connected and grid disconnected (islanding) modes. Therefore, utility companies needs to manage the energy exchange to achieve the best economical profit and energy efficiency under the two operational modes. The fourth chapter of this dissertation mainly focuses on MG power market research by using a commercial power system simulator, which includes 1) studying characteristics of inverter-interfaced DERs, 2) researching models associated with MG market policies, 3) exploring how to convert these market models into a formats that is compatible with a commercial power system simulator, and 4) investigating how to use the commercial power system simulator for MG market and power flow study with sufficient consideration of inverter-interfaced DER characteristics.

In the energy demand system, one of the biggest changes is that the electricity price will be a dynamic rate rather than a static rate over a day. To improve the energy efficiency is a big driven factor for new technologies for the end-users in order to reduce the cost during the peak load period. Demand response (DR) is expected to let the end users to use the home appliances in a smart way, which is the focus of Chapter 5. The dissertation first presents, in Section 5.2, heat transfer issues and how to use a home energy simulator to obtain energy consumption of a residential house. Then, Section 5.3 gives a computational experiment system that combines home energy simulation and dynamic electricity prices for DR evaluation. Section 5.4 illustrates how to use the computational experiment strategy to develop different DR policies based on optimization approach, particle swarm method, and a heuristic algorithm. The performance of different DR policies is evaluated in Section 5.5.

2. OPTIMAL DISPATCH AND UNIT COMMITMENT OF COMPETITIVE POWER MARKETS BY USING POWERWORLD SIMULATOR

2.1 Introduction

The Standard Market Design was proposed by the US Federal Energy Regulatory Commission (FERC) in 2002 [1, 2] by using locational marginal pricing (LMP), load serving entities (LSEs), and an independent system operator (ISO). Under this structure, the purpose of the ISO is to formulate the optimal power flow study and calculate the price by concerning both the location and time scheme of the injection and withdrawal of electric power in the grid.

Conceptually, LMP is the least cost to serve the next MW of load at a specific location under the limitations of transmission lines [3]. It has been widely implemented in the Mid-Atlantic states, Electric Reliability Council of Texas, New York, New England, California, and New Zealand [4]. Due to the severe congestion, LMPs of some constrained areas may be much higher than other areas with no or less congestion. Intuitively, LMPs can separate the whole power networks into different pricing zones or locations. With this mechanism, more energy efficiency and economic profit can be achieved, since it encourages a generator with cheap marginal price provide more energy to the grid.

Because of the divergence of LMPs, buyer's payment can be significantly different from the revenue of sellers [5]. In a competitive power market, there are three net surpluses: ISO, LSEs, and generation companies (GenCos) net surpluses. In [6], all the three surpluses are determined based on the auction basics in a competitive market [7], in which both seller and

buyer offer the biding respectively until they settle at a certain price. Seller surplus indicates that at a certain quantity, the price's difference between seller's receiving and reservation values. Similarly, the buyer surplus can be considered as the price's divergence between buyer's payment and reservation values. Intuitively, in the biding scheme, both seller and buyer are willing to maximize their surplus and market efficiency. The total net surplus (TNS) is defined as summation of ISO, LSE, and GenCos net surpluses.

However, within the field of a competitive power market, most conventional studies are based on individually developed software tools without using existing power flow simulation tools, making a lot of powerful analytical and visualization functions available in the commercial software unable to be integrated with competitive power market studies. In [6], an AMES Wholesale Power Market Test bed is developed based on Java, and is used to investigate how ISO net surplus varies in response to changes in the price-sensitivity of demand in ISO-operated competitive power markets with congestion managed by LMP. In [8], a continuous LMP is proposed and is applied to a small five bus system. In [9], although a computer program PROCOSE is used for assessment of transmission congestion and LMP, the price sensitive loads and generations are not properly reflected in the program. Hence, developing an efficient computing system becomes an important issue that was specially emphasized and discussed during 2012 IEEE PES General Meeting in the Session of ISS Panel and TF on Agent-Based Modeling of Smart-Grid Market Operations [10].

2.2 Economic Dispatch Models with Nodal Prices

2.2.1. Competitive Electricity Market

A competitive electricity market exists when competing generators offer their electricity output to retailers. The retailers then re-price the electricity and take it to market. While

wholesale pricing used to be the exclusive domain of large retail suppliers, increasingly markets like New England are beginning to open up to end-users.

For an economically efficient electricity wholesale market to flourish it is essential that a number of criteria are met typically through a bid-based, security-constrained, economic dispatch with nodal pricing or locational marginal pricing (LMP) in North America [11]. The object of LMP is to adjust energy prices in a pool to reflect their locational value in the node, which must account for congestion and transmission losses. The method relies on the actions of the pool ISO: (i) receiving demand bids and supply offers, (ii) selecting the most efficient sources to satisfy prevailing constraints, and (iii) making financial transactions that involve payments from consumers and payments to suppliers [5]. The prices that govern these payments are based on the bids submitted by dispatched generators, and on an adjustment made by the ISO to reflect the locational value of suppliers in terms of their contribution to the system losses and transmission constraints. In general, the LMPs are higher at consumer locations than at source locations. The price differentials between a sending and a receiving node result in a net income or surplus to the ISO.

2.2.2. Demand bids and supply offers

For each day (d), the demand bid reported by LSE j for each hour (h) of the day-ahead market in day d+1 consists of a fixed demand bid and a price-sensitive demand bid. The fixed demand bid has a constant increment bidding rate $\gamma_j^F(h)$ for a fixed power demand $P_{Lj}^F(h)$. The price-sensitive demand bid has a variable increment bidding rate $\gamma_j^V(h,p)$ for an adjustable demand $P_{Lj}^S(h)$ that drops as power demand increases [5]

$$\gamma_j^V(h, P_{Lj}^S) = \alpha_j(h) - \beta_j(h) \cdot P_{Lj}^S(h) \quad (1)$$

The price-sensitive demand is defined over an interval of

$$0 \le P_{Lj}^{S}(h) \le P_{Lj\_\max}^{S} \tag{2}$$

For each day (d), the supply offer of GenCo i for each hour (h) of the day-ahead market in day d+1 consists of a reported increment cost function and a true increment cost function. The true increment cost $C_i^T(h)$ represents the actual power production cost of GenCo i per MWh as

$$C_i^T(h) = a_i^T(h) + b_i^T(h) \cdot P_{Gi}(h) \tag{3}$$

where $P_{Gi}(h)$ is defined over a maximum and minimum operating capacity interval

$$P_{Gi}^{Min} \le P_{Gi}(h) \le P_{Gi}^{Max} \tag{4}$$

In a competitive power market, the reported increment cost function $C_i^R(h)$ represents the minimum dollar amount that GenCo i is willing to accept per MWh and is always larger than the true increment cost $C_i^T(h)$. Thus, the coefficients of the reported increment cost function is different from (3) and is represented by

$$C_i^R(h) = a_i^R(h) + b_i^R(h) \cdot P_{Gi}(h) \tag{5}$$

2.2.3. Profits and Net Earnings

The profit of a wholesale power market consists of three parts: LSE profit, GenCo profit and ISO profit. The profit of LSE j as shown by (8) on day (d) and hour (h) is the difference of the revenue $Rev_{Lj}(h)$, corresponding to payments received from its customers as shown by (6), and payments $Pay_{Lj}(h)$, paid to ISO according to the LMP structure as shown by (7).

$$\begin{aligned} Rev_{Lj}(h) &= \gamma_j^F(h) \cdot P_{Lj}^F(h) + \int_0^{P_{Lj}^S(h)} \gamma_j^V(h,p) \cdot dp \\ &= \gamma_j^F(h) P_{Lj}^F(h) + \alpha_j(h) P_{Lj}^S(h) - \frac{1}{2}\beta_j(h)\left[P_{Lj}^S(h)\right]^2 \end{aligned} \tag{6}$$

$$Pay_{Lj}(h) = LMP_j(h) \cdot \left(P_{Lj}^F(h) + P_{Lj}^S(h)\right) \tag{7}$$

$$LSENet_j(h) = Rev_{Lj}(h) - Pay_{Lj}(h) \quad (8)$$

The profit of GenCo *j* as shown by (11) on day (*d*) and hour (*h*) is the difference of the revenue $Rev_{Gi}(h)$, paid by ISO according to the LMP structure as shown by (9), and GenCo expense $Exp_{Gi}(h)$, obtained based on the true cost function as shown by (10)

$$Rev_{Gi}(h) = LMP_i(h) \cdot P_{Gi}(h) \quad (9)$$

$$Cst_{Gi}(h) = \int_0^{P_{Gi}} C_i^T(h, p) \cdot dp \quad (10)$$

$$GenNet_i(h) = Rev_{Gi}(h) - Cost_{Gi}(h) \quad (11)$$

The profit of the ISO on day (*d*) and hour (*h*) is the difference of payments received from all the LSEs and GenCos as shown by

$$ISONet(h) = \sum_j Pay_{Lj}(h) - \sum_i Rev_{Gi}(h) \quad (12)$$

2.2.4. Optimal Dispatch with Nodal Prices

For each day (d) and hour (h), the optimal dispatch for a competitive power market is to find power supply by individual GenCos, power demand by each LSE, and system LMP levels so as to maximize the total net surplus involving all the three parties. At the same time, the power balance constraint at each bus, GenCo power generation capacity, price-sensitive demand capacity, and power capacity of transmission lines should not be exceeded. This results in a quadratic programming strategy [12] as shown below

Maximize:

$$TNS(h) = \sum_j LSENet_j(h) + \sum_i GenNet_i(h) + ISONet(h) \quad (13)$$

Subject to:

$$\sum_{\substack{m=1 \\ m\neq k}}^{N} \frac{\delta_k(h)-\delta_m(h)}{x_{km}} + P_{Lk}^{F}(h) + P_{Lk}^{S}(h) = P_k(h),\ k = 1,\cdots,N \tag{14}$$

$$P_{Gi}^{Min} \le P_{Gi}(h) \le P_{Gi}^{Max} \tag{15}$$

$$0 \le P_{Lj}^{S}(h) \le P_{Lj\_\max}^{S} \tag{16}$$

$$P_{km}^{Min} \le \frac{\delta_k(h)-\delta_m(h)}{x_{km}} \le P_{km}^{Max} \tag{17}$$

where P_k is the active power of the generator injected into the network at bus k, and x_{km} is the branch reactance between buses k and m, and $\delta_k(h)$ is the voltage angles at bus k. Note that $GenNet_i(h)$ in (13) is computed by using the reported increment cost function rather than the true increment cost function. This is a little bit different from Eqs. (10) and (11). For a large power system, it is very complex and time consuming to develop a program to solve the optimal dispatch problem. Hence, most conventional studies use dc power flow approximation (Eqs. (13)-(17)). This would cause errors compared to AC power flow computation. In addition, to accurately capture changes and solve the optimization problem throughout a day, calculations must be repeated hour by hour using practical system data.

2.3 Optimal Power Dispatch for Competitive Power Market Using PowerWorld

PowerWorld Simulator is an interactive power systems simulation package designed to simulate power system operation on a time frame ranging from several minutes to several days. The software contains a highly effective power flow analysis package capable of efficiently

solving systems with up to 100,000 buses [13]. Theoretically, PowerWorld can be used for simulation study of any practical time frame, such as few hours to one week ahead.

2.3.1 Optimal Power Dispatch using PowerWorld

The first step for the optimal power flow evaluation using PowerWorld is to develop a single-line diagram. The program reads in impedance data of each line and the length of the line and then automatically transfers the impedance of each line into per unit. For each line, the MVA limit, representing the constraint of a line, is specified too.

The next step is to define generation units. This includes maximum and minimum power generation and increment cost function of each unit. The generator capacity, i.e., Max_MW, Min_MW, Max_Mvars and Min_Mvars values of a generator, are specified except for the slack bus generator. These parameters represent maximum and minimum active and reactive power constraints of a generator, respectively. Note: the actual generation of a generator is obtained through optimal power flow computation. The coefficients of the cost models associated with the generators are specified using one of the following two options defined in PowerWorld: cubic model option and piecewise linear model option. Actually a cubic cost model is converted into a default piecewise linear model automatically for the optimal power flow computation in PowerWorld. But, the piecewise linear model option makes it more convenient to define a user specified piecewise linear model [14]. The reported increment cost function is used for each generation unit.

The final step is to create a special technique so that the fixed and price-sensitive loads can be properly implemented in the PowerWorld simulator. For fixed loads, only the fixed power demands need to be specified because these loads do not participate the open market bidding process. These loads can be represented by the conventional load model defined in PowerWorld.

But, the price-sensitive loads will participate in the wholesale power market auction so that both power demands and variable increment bidding rates must be specified. Hence, the conventional load model defined in PowerWorld is not suitable to a price-sensitive load. To overcome the challenge, we use a specially developed strategy to model a price-sensitive load based on the conventional generator model defined in PowerWorld. The strategy requires: 1) the power generated by the generator is negative instead of positive, and 2) an increment bidding rate function $\gamma_{PW\_j}^{V}(h,p)$ that is different from Eq. (1) as shown by

$$\gamma_{PW\_j}^{V}(h, P_{Lj}^{S}) = \alpha_j(h) + \beta_j(h) \cdot P_{PW\_Lj}^{S}(h). \tag{18}$$

where instead of a negative sign, a positive sign is applied to $\beta_j(h)$ coefficient because a negative price-sensitive generation is used to model a price-sensitive load. The conversion from (1) to (18) for the increment bidding rate function of a price-sensitive load is based on a special mechanism that makes it possible to solve the optimal power dispatch problem (13) in PowerWorld as explained below.

PowerWorld uses linear programming [15] in its Optimal Power Flow Analysis Tool (OPF), an optional add-on to the base Simulator package. The OPF provides the ability to optimally dispatch the generation with the minimum overall cost in an area or group of areas while simultaneously enforcing the transmission line and interface constraints. PowerWorld OPF also calculates the marginal price (LMP) to supply electricity to a bus, while taking into account of transmission system congestion.

However, the objective of the PowerWorld OPF is to find a solution that minimizes the overall generation cost. This requirement is different from (13). Thus, to use PowerWorld OPF, (13) must be converted into the PowerWorld compatible format. By applying (8), (11), (12) to (13), it is obtained

$$TNS(h) = \sum_j \left(Rev_{Lj}(h) - Pay_{Lj}(h) \right) + \sum_i \left(Rev_{Gi}(h) - Cst_{Gi}(h) \right) + \sum_j Pay_{Lj}(h) - \sum_i Rev_{Gi}(h) \quad (19)$$

Also, maximizing $TNS(h)$ is equivalent to minimizing $-TNS(h)$ as shown below

$$-TNS(h) = \sum_i Cst_{Gi}(h) - \sum_j Rev_{Lj}(h) . \quad (20)$$

Considering Eq. (6) and a price-sensitive load that is represented in PowerWorld by a negative power generation $P_{PW\_Lj}^S(h)$, i.e., $P_{Lj}^S(h) = -P_{PW\_Lj}^S(h)$, Eq. (20) then becomes

$$-TNS(h) = \sum_i Cst_{Gi}(h) + \sum_j \left(\alpha_j(h) P_{PW\_Lj}^S(h) + \frac{1}{2} \beta_j(h) \left[P_{PW\_Lj}^S(h) \right]^2 \right) - \sum_j \gamma_j^F(h) P_{Lj}^F(h) \quad (21)$$

Note: the fixed demand component in (21) is constant. Thus, removing the constant loads from the objective function (21) does not affect the optimal solution. Then, the optimal power dispatch problem can be represented by (22), in which $Cst_{PW\_Lj}^S(h)$ stands for the equivalent generator cost associated with the price-sensitive load $P_{Lj}^S(h)$ and the corresponding increment bidding rate function is (18). According to (22), the optimal power dispatch problem becomes to minimize the overall generation cost of all the positive and negative generators.

Minimize: $$-TNS(h) = \sum_i Cst_{Gi}(h) + \sum_j Cst_{PW\_Lj}^S(h) \quad (22)$$

By this way, we can use PowerWorld OPF to solve the optimal power dispatch problem for a competitive power market, in which a generator model is used to represent a price-sensitive load. However, the active power of the "generator" must be negative (absorbing) while the reactive power can be both negative and positive. This means that when using the PowerWorld generator model, the Min_MW value of the "generator" is negative while the Max_MW value of the "generator" is zero. Max_Mvars and Min_Mvars values of the "generator" can be selected to represent the generating and absorbing reactive power constraints of the price-sensitive load. For

price-sensitive load *j*, coefficients of α_j and β_j associated with the variable bidding rate (Eq. (1)) of the load need to be specified. However, different from (1), both α_j and β_j must be positive according to (18).

2.3.2 Comparison and Validation

We used Matlab optimization toolbox [16] for the validation. The optimization toolbox provides widely used algorithms for standard and large-scale optimization. The toolbox includes functions for linear programming, quadratic programming, binary integer programming, nonlinear optimization, nonlinear least squares, multi objective optimization, and systems of nonlinear equations [16].

The comparison and validation is conducted for several small power systems. The comparison focused on the following three aspects: 1) whether an optimal solution obtained by using PowerWorld is consistent with the results obtained by using Matlab, 2) how the piecewise linear simplification in PowerWorld affects the accuracy, and 3) how much difference is between the results generated by using DC and AC OPFs [17]. In general, the comparison shows that the results generated by using Matlab and PowerWorld are very close, demonstrating the effectiveness of using PowerWorld to solve the optimal power dispatch problem for a competitive power market. For small power systems, the results generated by using AC and DC OPFs are close.

2.4 Using PowerWorld for Optimal Power Dispatch Investigation

With the successful validation of optimal power distich study for small scale competitive power markets, this section presents an extensive optimal power dispatch study for more practical systems by using PowerWorld.

2.4.1 An 8-Bus System

The 8-bus system has six generators located on Bus 1, 3, 4, 5, 6 and 7, respectively. Bus 1 is the slack bus. Five fixed loads, as shown in Figure 1, are located on Bus 2, 3, 4, 6, and 8, respectively. The cost coefficients and capacities of generators are given in Table 2.1. The transmission line parameters and capacities are provided in [20]. The study focuses mainly on 1) how much difference between ac and dc OPFs is, 2) what impact the price-sensitive loads and capacities of transmission lines and generators can cause, and 3) how variable loads affect optimal power dispatch of a competitive power market.

Bus	Generator cost coefficients			P_{min} (MW)	P_{max} (MW)
	a ($/MW^{2}h)	*b* ($/MWh)	*F* ($/h)		
1	0.0060	18.00	100	5	20
3	0.0041	17.02	145	5	70
4	0.0039	12.00	112	10	70
5	0.0040	10.10	110	10	90
6	0.0040	30.00	180	10	70
7	0.0035	9.30	100	20	200

Table 2.1 Generator cost coefficients and capacities

For the 8-bus system, the LMP difference between AC and DC OPFs is small. In general, results generated by DC OPF do not have line losses, and the bus voltages on all buses are 1pu; while results generated by AC OPF contain line losses because line resistance is included and the bus voltages on PQ buses could be lower than 1pu. Due to the line losses, the LMP on each bus is normally higher for AC OPF than DC OPF. Table 2.2 shows the comparison of LMPs generated by using AC and DC OPFs as well as the LMP decomposition into Energy price (i.e., LMP at reference bus), Congestion price and Loss price generated by the PowerWorld [8]. As it can be seen from the table, the main difference between AC and DC OPFs is the LMP decomposition in line loss price.

The impact of price-sensitive loads and capacities of transmission lines and generators to the optimal power dispatch solution is very convenient to study using the PowerWorld. For the 8-bus system shown by Figure 2.1, each load bus could include a price-sensitive load. The increment bidding rate coefficients are set as α=32\$/MWh and β=0.03\$/MW^{2}h. By connecting or disconnecting a price-sensitive load and changing capacities of transmission lines or generators, the optimal power dispatch solutions can be easily evaluated and visualized. For any change of system conditions, the difference between the two adjacent system changes can be demonstrated by using the Difference Flows function in the PowerWorld as shown by Figure 2.2 .In general, the following observations are obtained:

1) The line capacity and location and size of loads are primary factors to affect the congestion. When congestion appears on a line, the LMP of a bus associated with that line could be much higher than the LMPs of other buses.

2) To reduce the congestion of a line, either the capacity of generators close to a large load area or the capacities of the lines supplying the same load area need to be strengthened. However, the offered costs of generators are also an important factor to affect congestion.

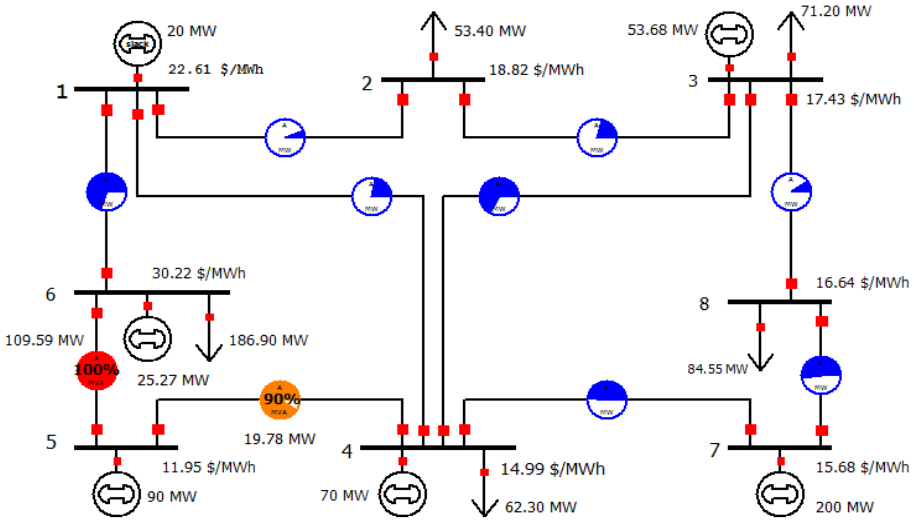

Figure 2.1 AC OPF difference between two adjacent system condition changes

Bus	LMP $/MWh		Energy $/MWh		Congestion $/MWh		Losses $/MWh	
	DC	AC	DC	AC	DC	AC	DC	AC
1	22.61	22.61	22.61	22.61	0	0	0	0
2	18.82	18.83	22.61	22.61	-3.79	-3.79	0	0.01
3	17.43	17.43	22.61	22.61	-5.18	-5.18	0	0
4	14.98	14.95	22.61	22.61	-7.63	-7.62	0	-0.04
5	11.94	11.91	22.61	22.61	-10.67	-10.66	0	-0.04
6	30.22	30.26	22.61	22.61	7.61	7.61	0	0.04
7	15.65	15.59	22.61	22.61	-6.96	-6.93	0	-0.09
8	16.63	16.62	22.61	22.61	-5.98	-5.97	0	-0.02

Table 2.2 LMP's decomposition from PowerWorld's OPF

3) The inclusion of the price-sensitive loads causes the LMPs to drop and a reduction of the overall surplus of GenCos, ISO and LSEs. The larger percentage of the price-sensitive loads over fixed loads, the smaller the net surpluses of all the involved three entities are.

4) As the percentage of price-sensitive loads over fixed loads increases, the net surplus of some expensive generators could become negative if the LMP is lower than the generator true cost.

To evaluate the optimal power dispatch for variable loads over time, the load profiles are first created by using other software tools (such as Excel) and then loaded into the PowerWorld simulator. For the 8-bus system, three different types of variable loads are considered as shown by Figure 2.3. Type 1 loads are located on Bus 2 and 8, Type 2 load is located on Bus 6, and Type 3 loads are located on Bus 3 and 4. The power factor is 0.85 lagging for Type 1 load and 0.9 for Type 2 and 3 ones. The Time-Step simulation option is chosen for the optimal power dispatch study. For the 8-bus system, the difference between AC and DC OPFs is again very small. Using AC OPF, the ISO net surplus is slightly smaller than that calculated based on the DC OPF due to the losses caused by line resistance. Under variable load conditions, the LMP on each bus and average LMP change with the change of the loads. The LMP curves could be quite

different depending on the congestion condition of the lines connecting a bus (Figure 4a). For example, LMP at Bus 4 is much higher than other buses due to the congestion of the line between Bus 5 and 6. The two exceptions are peak and low load conditions. During a low load condition, there is no congestion in the system so that LMPs at all the buses are the same. During the peak load, when the capacities of all cheap generators have reached their limits, any additional MW power production must be supplied by the expensive generator, making the LMPs very close on all the buses in another way (Figure 2.4).

The surplus of each generator is calculated by using the generator true cost (Eq. (11)) and is affected by the cost and capacity of generator on Bus 7 supplies most of the power, making its net surplus higher than other generators, especially at peak load conditions. The surplus of a generator could be the generator.

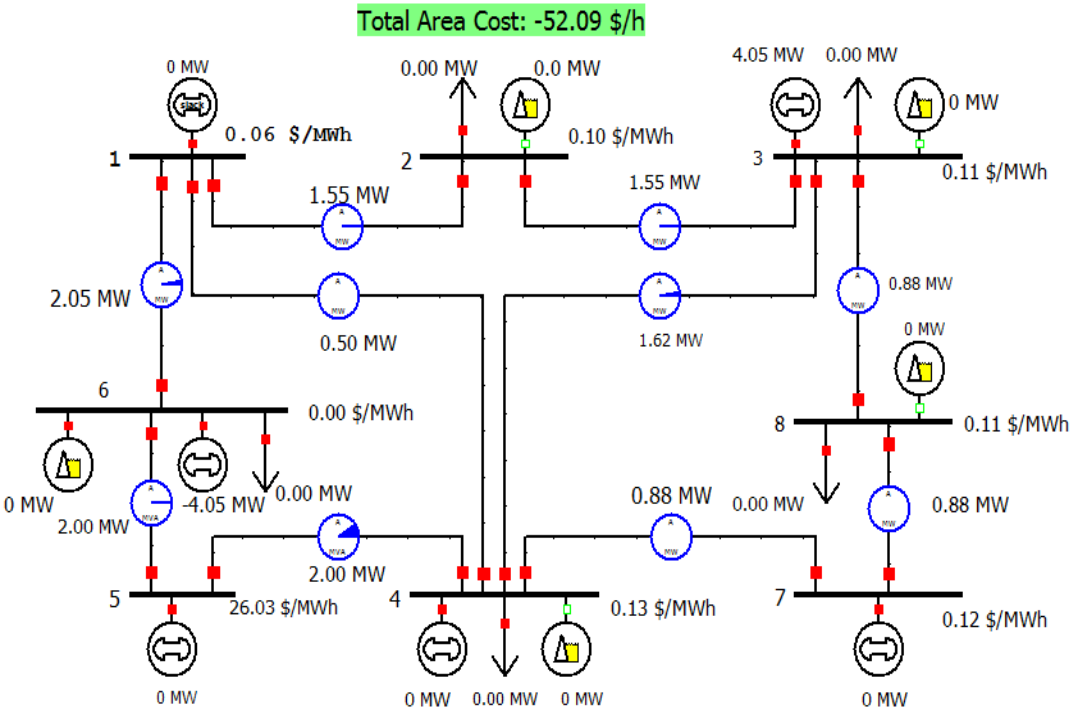

Figure 2.2 AC OPF difference between two adjacent system condition changes

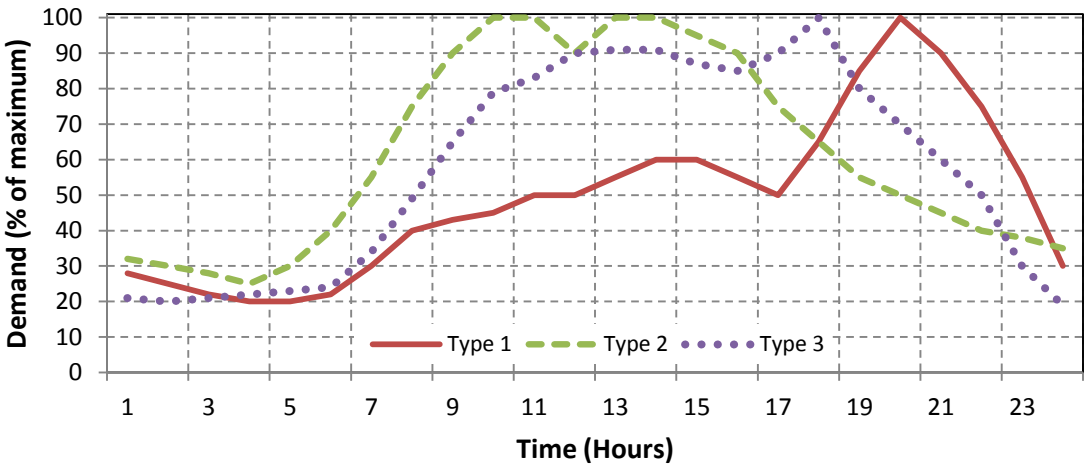

Figure 2.3 Daily load curves of the three feeders

For example, the cheap and high capacity negative under a light load (Figure 2.5). The primary cause for this is the low LMP at a low load as well as the minimum amount of generation that a generator must supply. Thus, for the expensive generator at Bus 6, if the generator cost is higher than the LMP at the Bus, the surplus of the generator could be trivial or negative especially at a low load condition when the generator supplies the minimum amount of generation.

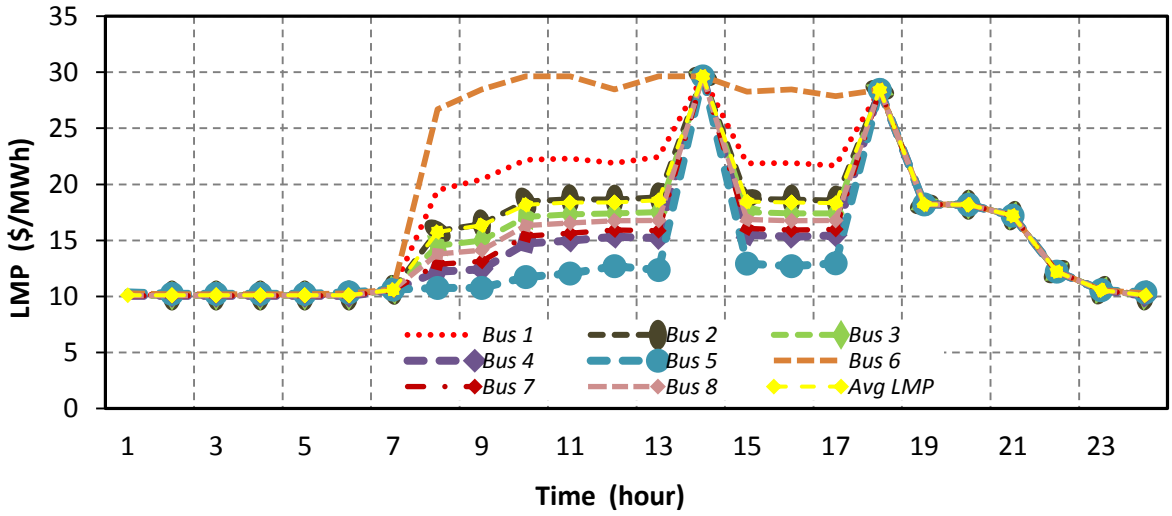

Figure 2.4 LMP at each load bus and average LMP

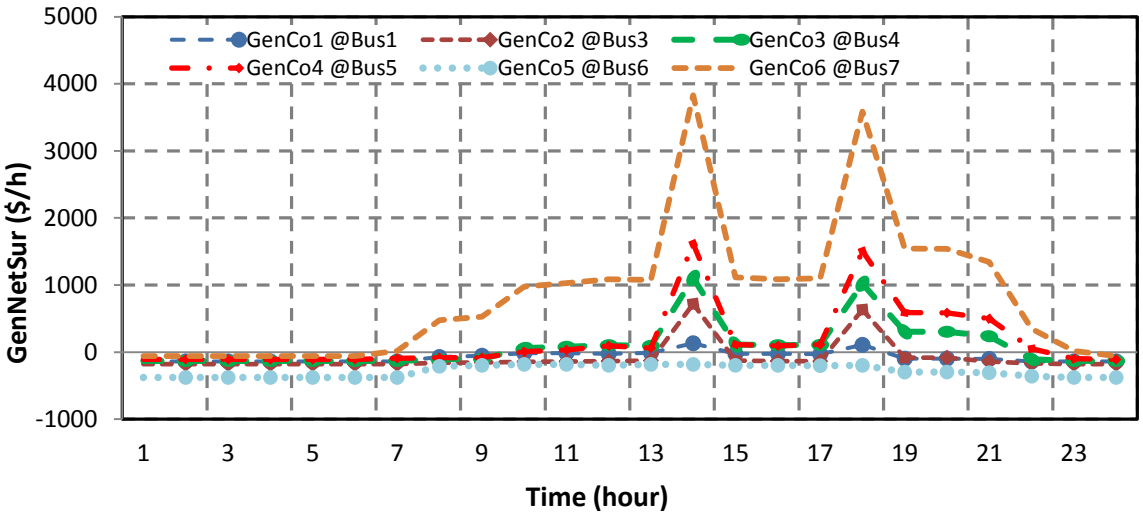

Figure 2.5 generator surpluses at each generator bus

The ISO net surplus is determined by the payments received from LSEs and payments given to generators by ISO, both of which are calculated based on LMPs. Therefore, if the LMPs at all the buses are close or the same, the net surplus of ISO could be very low or even negative due to the line losses that are not reflected in the LMP payment structure (Figure 2.7).

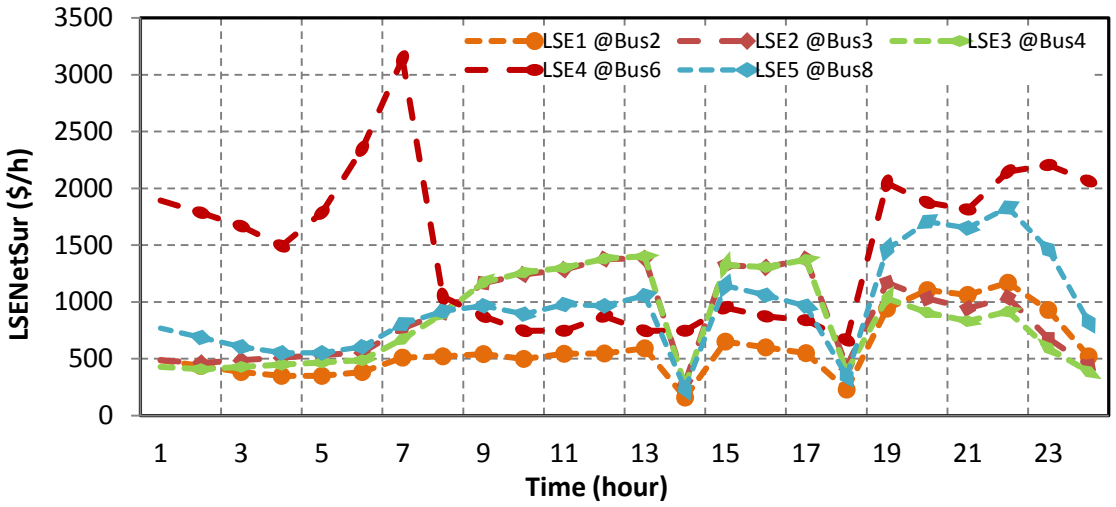

Figure 2.6 LSE surpluses at each load bus

The LSE gain depends strongly on the price structure of the LSE to sell the power to customers as shown by Eq. (6). An interesting issue shown in Figure 2.6 is a high LSE surplus

at Bus 6 for a low load condition between 1am to 7am. This is due to the fact that during that time period, the primary load is the Type 2 load at Bus 6. Since the LMPs are low at that time period, the LSE can gain a large profit if the LSE price structure is not modified during a low load period.

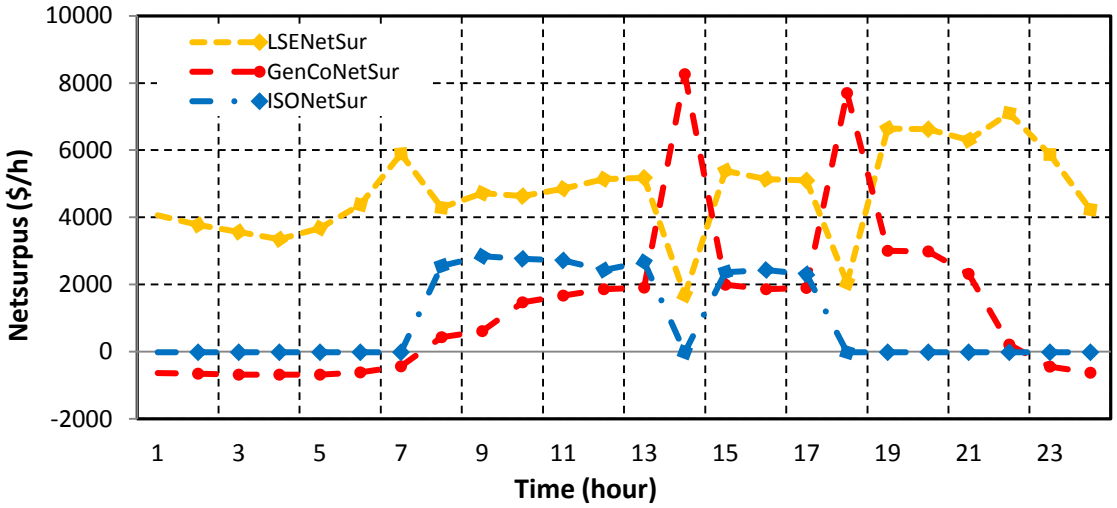

Figure 2.7 generator, ISO and LSE net surplus

2.4.2 IEEE 118-Bus System

The IEEE 118-bus system (Figure 2.8) has 3 zones, 54 generators, 186 branches, and 91 loads [21, 22]. Zone 2 is connected to Zone 1 and Zone 3 through several interconnection tie lines. Three major price-sensitive loads are located on Bus 18 in Zone 1, Bus 64 in Zone 2, and Bus 102 in Zone 3. The cost coefficients and capacities of generators, and transmission line parameters and capacities are provided in [21]. Similar to the 8-bus system, three different types of variable loads (Figure 2.3) are considered.

For the 118-bus system, the LMP difference between AC and DC OPFs is more evident than the 8-bus system as shown by Table 2.3. The energy decomposition of the LMP for the three zones is different. Again, the main LMP difference between AC and DC OPFs is the

Bus	LMP $/MWh		Energy $/MWh		Congestion $/MWh		Losses $/MWh	
	DC	AC	DC	AC	DC	AC	DC	AC
1	25.13	26.62	25.13	23.99	0.00	0.00	0	2.63
21	25.13	26.30	25.13	23.99	0.00	0.00	0	2.30
72	25.13	25.70	25.13	23.99	0.00	0.00	0	1.40
33	26.78	28.70	26.78	28.31	0.00	0.00	0	0.39
59	26.78	29.36	26.78	28.31	0.00	0.00	0	1.05
97	26.77	27.13	26.78	28.31	-0.01	-0.02	0	-1.17
83	18.23	18.35	18.12	19.67	0.11	-0.56	0	-0.75
88	18.30	17.02	18.12	19.67	0.17	-0.53	0	-2.11
106	18.42	19.54	18.12	19.67	0.30	-0.16	0	0.04

Table 2.3 LMP's decomposition from PowerWorld's OPF

decomposition in line loss price. Figure 6a shows the LMPs at eight selected buses in the three zones, as well as the overall average LMP. The figure shows that LMPs are very close in light load period but could be quite different during peak load period. The study indicates that for the 118-bus system, the congestion is a major factor to affect the LMPs when there is sufficient generator capacity to meet the load demand.

The generator net surplus is affected by the bus LMPs. For the same reported cost during 24 hours, the higher the LMPs, the more net surplus a generator obtains. The net surplus is also affected by the power generation of a generator, which is affected by the reported cost or the bid offered by a generator.

The LSE net surplus depends on 1) size of the load, 2) the LSE fixed and variable demand bid, and 3) LMP at the LSE bus. In general, when the LMP is high, the LSE net surplus could be low depending on how much difference between LSE demand bid and the LMP.

The ISO profit depends strongly on how much the LMPs within the system are different. When all LMPs are close, ISO basically does not gain any profit. The difference of net surplus of all the LSEs and generators depends on the demand and generation bids. Although the overall

LSE net surplus is high in Figure 6d, a change of the generator reported cost could affect the final LSE net surplus.

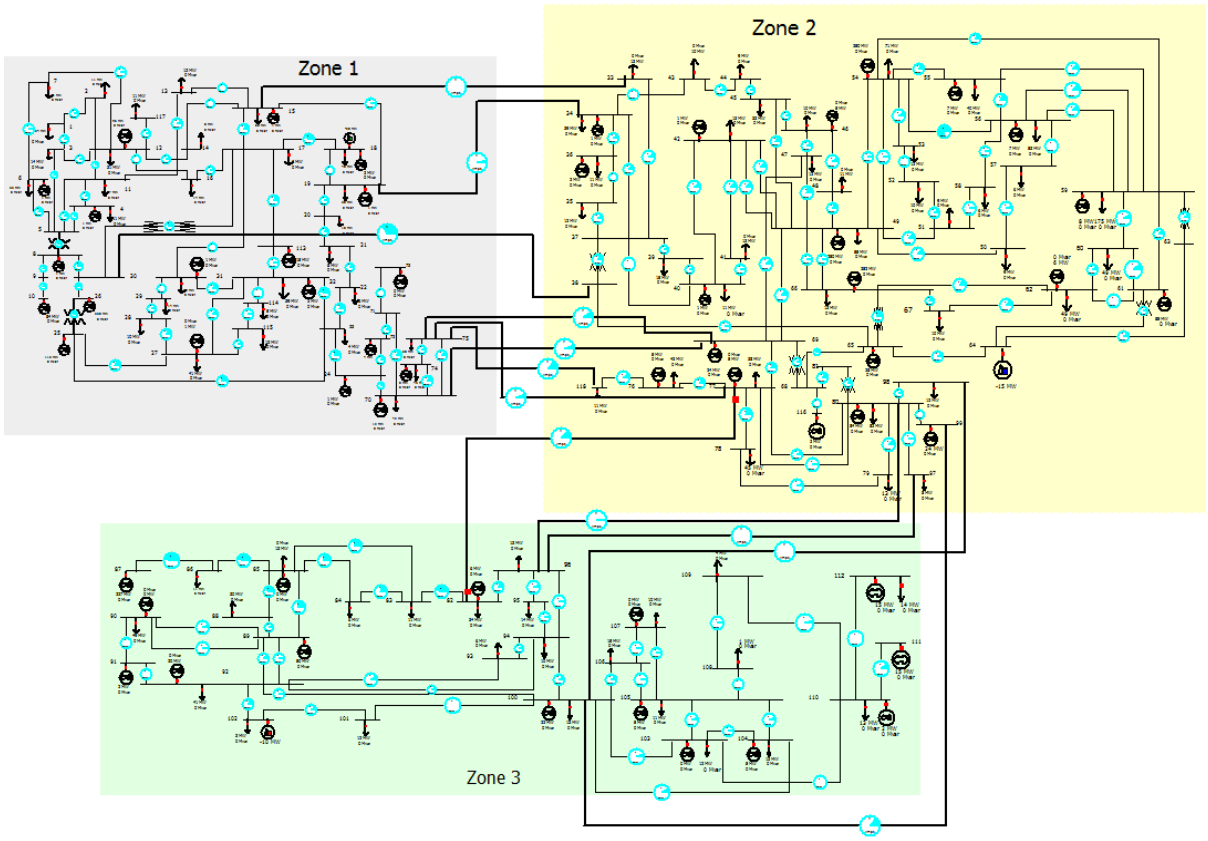

Figure 2.8 AC OPF difference between two adjacent system condition changes

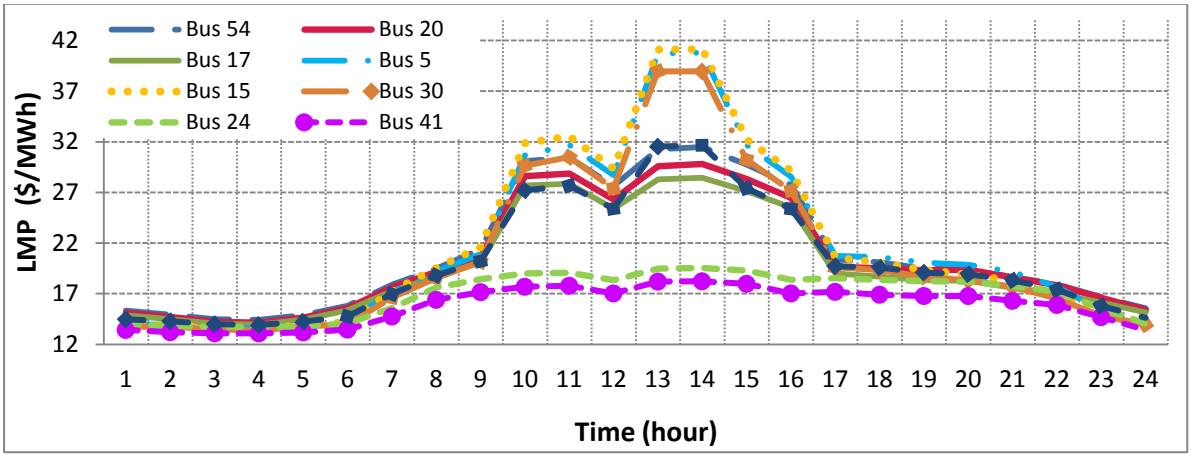

Figure 2.9 LMP at selected load buses and average LMP

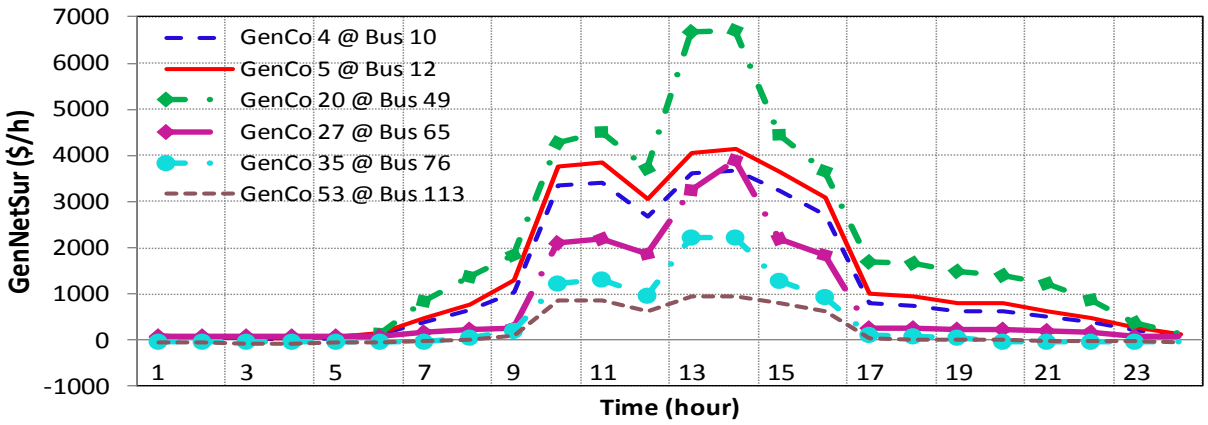

Figure 2.10 generator surplus at selected generator buses

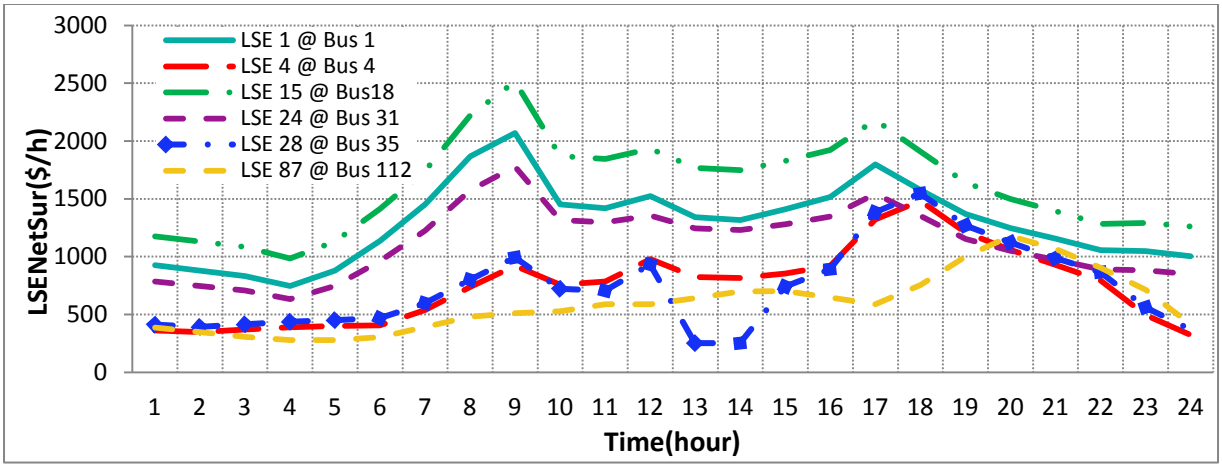

Figure 2.11 LSE surplus at selected load buses

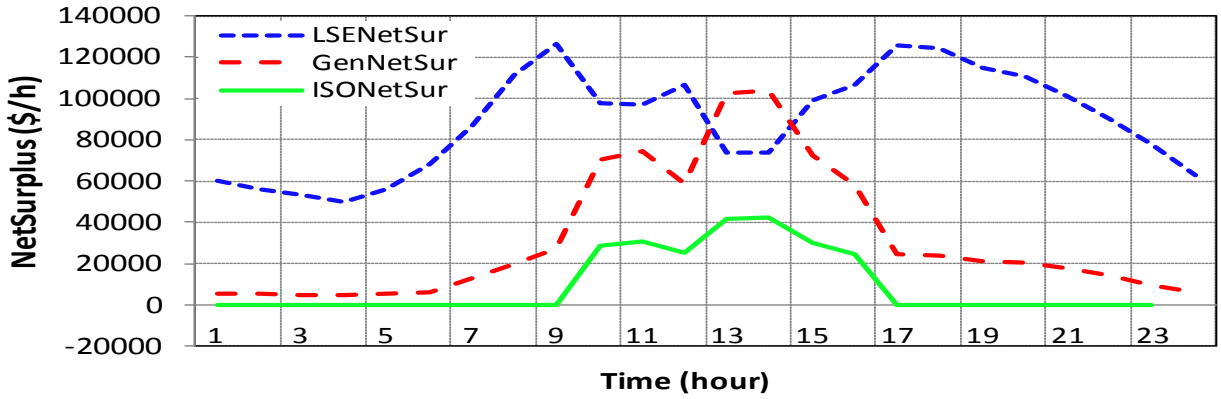

Figure 2.12 Generator, ISO and LSE net surplus

2.5 Integrating PowerWorld and Matlab for Optimal Dispatch and Unit Commitment Study of Competitive Wholesale Power Markets

A competitive power market is usually represented as a security-constrained unit commitment (SCUC) problem [21]. The unit commitment (UC) problem involves finding the best sets of available generation resources to meet the electrical load. It determines the optimal operational schedule of a set of generators by considering the operating fuel cost and transition cost to switch on and off a generator. However, the normal UC function is not available in PowerWorld. To overcome the weakness, we propose a mechanism by integrating Matlab and PowerWorld together for combined optimal power dispatch and SCUC study.

The basic idea of the integrated computational system is to use PowerWorld for optimal power dispatch computation and to use Matlab for UC evaluation. The two software programs are connected together through Simulator Automation Server (SimAuto). SimAuto provides a COM interface so that a user can extend the functionality of PowerWorld Simulator to any external program. By using SimAuto, we can launch and control PowerWorld from our Matlab-based program. Basically, we use Matlab to solve a UC problem based on a dynamic programming approach [22, 23] and use PowerWorld to do the optimal power flow computation. By this way, we are able to use the special power of both Matlab and PowerWorld for very fast formulation and computation of a large-scale competitive power market.

2.5.1 Backward and Forward Sweep Procedure

The integrated UC and optimal power flow computation consists of a backward and a forward sweep procedures as shown by Algorithm 1. For a day of 24 hours, for example, we first generate all possible generator combinations for 24 hours in Matlab. Note: although we used 24 hours as an example here, the mechanism can be applied to simulation study of a competitive

Algorithm 1: Backward and Forward Sweep Procedure

Generate all generator combinations for 24 hours
$h \leftarrow 24$ {termination time}
$N \leftarrow$ total number of all generator combinations
{ Backward Sweep Procedure }
{Compute initial optimal cost at the termination time}
for i=1 to N **do**
  if combination i is feasible
    Pass combination i and loads for hour h from Matlab to PowerWorld by calling SimAuto.
    Optimal power flow computation in PowerWorld
    $c_i(h) \leftarrow$ Generator operating cost obtained from PowerWorld OPF is transferred to MaltLab
    $F_i(h) \leftarrow c_i(h)$
  end if
end for
{Compute optimal cost for the rest hours}
for h=23 to 1 **do**
  for i=1 to N **do**
    if combination i is feasible
      Pass combination i and loads for hour h from Matlab to PowerWorld by calling SimAuto.
      Optimal power flow computation in PowerWorld
      $c_i(h) \leftarrow$ Generator operating cost obtained from PowerWorld OPF is transferred to MaltLab
    end if
    {include accumulated cost at hour $h+1$}
    for j=1 to N **do**
      if combination j is feasible
        $F_{ij}(h) \leftarrow c_i(h) + t_{ij}(h) + F_j(h+1)$
      end if
    end for
    $F_i(h) \leftarrow \min_j F_{ij}(h)$; $j_i^*(h+1) \leftarrow j$ {record the combination associated with $\min_j F_{ij}(h)$ }
  end for
end for
{ Forward Sweep Procedure }
$F_{\min} \leftarrow \min_i F_i(1)$; $i^*(1) \leftarrow i_{\min}$ {record the combination associated with $\min_i F_i(1)$ }
for h=2 to 24 **do**
  $i^*(h) \leftarrow j^*_{i^*(h-1)}(h)$; **{**recall the best combination at hour h}
end for

power market with any practical time frame, such as few hours to one week ahead. In each hour, any unit can be considered either on (denoted by 1) or off (denoted by 0). For a power system with n generators, there are $N=2^n-1$ candidate combinations available. But, some combination may not be feasible due to various constraints. For instance, if the total capacity of the generating units is less than the total loads at an hour, that generator combination cannot be included.In the backward sweep, the dynamic programming and optimal power flow computation (limes 4 to 11) starts at the termination time (h=24) to get an initial cumulative costs for all the feasible combinations. We assume that there is no transition cost at the termination time. Therefore, the initial cumulative cost for a combination equals to the generator operational cost obtained from PowerWorld (lines 8 and 9). For a feasible combination i at hour h at a non-termination time, the minimum operational cost $c_i(h)$ is calculated in PowerWorld (lines 18 and 19 of Alg. 1) and then transferred back to Matlab, where the transition cost $t_{ij}(h)$ from the combination i at hour h to a combination j at hour $h+1$ is added to the minimum operational cost $c_i(h)$ at hour h plus the minimum cumulative cost of the combination j at hour h+1 to form the cumulative cost of the combination i at hour h (line 24 of Algorithm 1). After the computation of the cumulative costs of the combination i at hour h to all the combinations j at hour h+1, only the minimum one of the cumulative costs is saved (line 27) for the cumulative cost computation at hour h-1 and the combination j^* at hour h+1 associated with this minimum cumulative cost is saved for the forward sweep computation.

In the forward sweep, the computation starts at the beginning time (h=1) by finding the minimum cumulative cost and the associated combination (line 31 in Algorithm 1). Then, through a forward recursive process, the program recalls the combination j^* at previous hour until the termination time (lines 32 to 34 of Algorithm 1). At the end of the forward sweep

procedure, the most efficient generator combinations as well as the optimal power dispatch solution at all the time segments is available.

2.5.2 Using PowerWorld and Matlab for Unit Commitment Investigation

With the development of the integrated computational system, this section presents an extensive optimal power dispatch and UC study for a 37-bus system by using Matlab and PowerWorld [24]. The system has nine generators, among which four generators are always online while the other five generators participate SCUC scheduling. Bus 31 is the slack bus. The system has twenty-five fixed loads and two price-sensitive loads. The maximum capacities of the two price-sensitive loads are 40MW and 70MW, respectively.

The cost coefficients and capacities of generators are given in Table 2.4, where *F* represents the fixed price of a generator. The transmission line parameters and capacities are specified in PowerWorld for each line. Three different types of variable loads are considered as shown by Figure 3. The power factor is 0.85 lagging for Type 1 load and 0.9 for Type 2 and 3 ones. The load profiles are first created by using other software (such as Excel) and then loaded

Bus	Generator cost coefficients			P_{min} (MW)	P_{max} (MW)
	a ($/MW^{2}h)	b ($/MWh)	F ($/h)		
1	0.0050	36.00	410	14	140
2	0.0082	15.2	420	5	200
3	0.0097	14.5	390	35	100
4	0.0123	14.3	530	31	150
5	0.0260	25	450	44	180
6	0.0050	28	390	48	150
7	0.030	22	410	50	170
8	0.025	16.3	400	53	200
9	0.023	20	420	54	150

Table 2.4 Generator cost coefficients and capacities

into PowerWorld simulator from Matlab at each simulation interval. The study focuses mainly on 1) UC scheduling, 2) how much difference between AC and DC OPFs is [25], 3) what impact

the price-sensitive loads and capacities of transmission lines and generators can cause, and 4) how variable loads affect optimal power dispatch and unit commitment of a competitive power market.

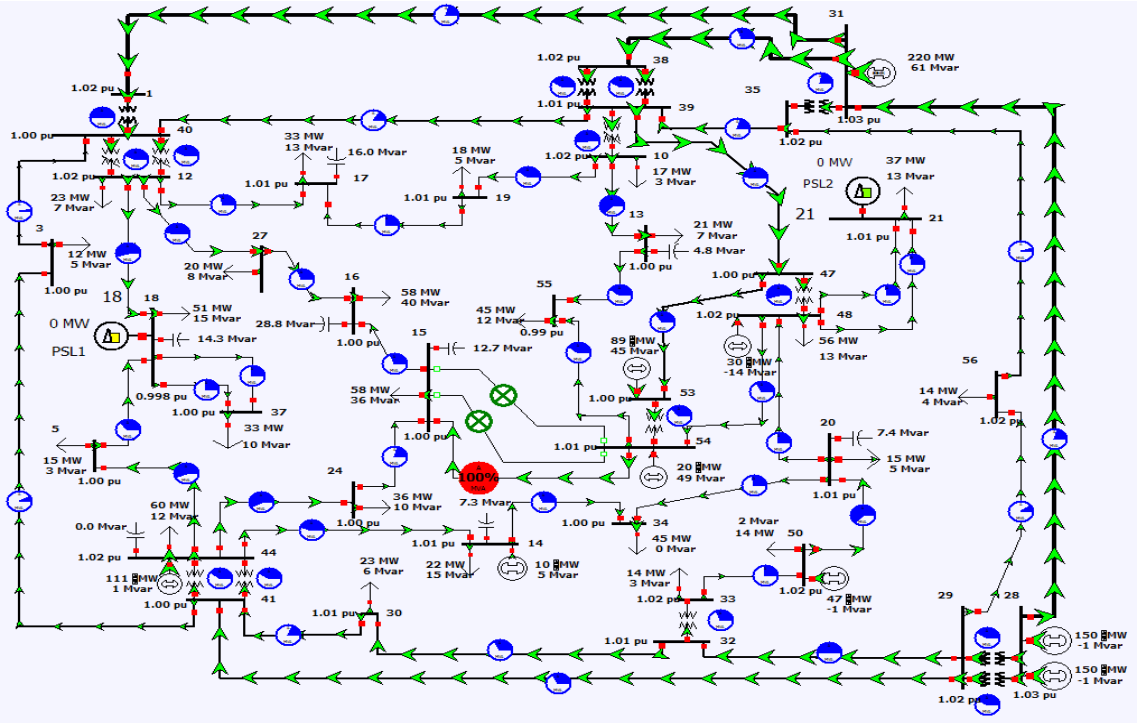

Figure 2.13 AC OPF difference between two adjacent system condition changes [24]

2.5.3 Optimal Power Dispatch Based on AC and DC OPFs

For the 37-bus system, the difference between AC and DC OPFs is evident. In general, the LMP on each bus is normally higher for AC OPF than DC OPF. Tables 2.3 and 2.4 show the comparison of UC scheduling generated by using AC and DC OPFs as well as the total daily operational cost. As it can be seen from the tables, the UC scheduling is clearly different between AC and DC OPFs. Compared to DC OPF, AC OPF requires more generator units to be online at a certain hour, and the total operational cost obtained from AC OPF is higher than that of DC OPF, demonstrating the importance of using AC OPF for accurate UC scheduling and optimal power dispatch evaluation in a competitive power market.

Daily operational cost: $396139.0																									
U	Hours (0-24)																								
1	1	1	1	1	1	1	1	1	1	1	1	1	1	1	1	1	1	1	1	1	1	1	1	1	1
2	1	1	1	1	1	1	1	1	1	1	1	1	1	1	1	1	1	1	1	1	1	1	1	1	1
3	1	1	1	1	1	1	1	1	1	1	1	1	1	1	1	1	1	1	1	1	1	1	1	1	1
4	1	1	1	1	1	1	1	1	1	1	1	1	1	1	1	1	1	1	1	1	1	1	1	1	1
5	0	0	0	0	0	0	0	1	1	1	1	1	1	1	1	1	1	1	0	0	0	0	0	0	
6	0	0	0	0	0	0	0	0	0	0	0	0	0	0	0	0	0	0	0	0	0	0	0	0	0
7	0	0	0	0	0	0	0	1	1	1	1	1	1	1	1	1	1	1	1	1	1	1	1	1	1
8	1	1	1	1	1	1	1	1	1	1	1	1	1	1	1	1	1	1	1	1	1	1	1	1	1
9	1	1	1	1	1	1	1	1	1	1	1	1	1	1	1	1	1	1	1	1	1	1	1	1	1

Table 2.5 UC based on AC OPF using PowerWorld

Daily operational cost: $306466.0																									
U	Hours (0-24)																								
1	1	1	1	1	1	1	1	1	1	1	1	1	1	1	1	1	1	1	1	1	1	1	1	1	1
2	1	1	1	1	1	1	1	1	1	1	1	1	1	1	1	1	1	1	1	1	1	1	1	1	1
3	1	1	1	1	1	1	1	1	1	1	1	1	1	1	1	1	1	1	1	1	1	1	1	1	1
4	0	0	0	0	0	0	1	1	1	1	1	1	1	1	1	1	1	1	1	1	1	1	1	0	0
5	0	0	0	0	0	0	0	0	1	1	1	1	1	1	1	1	0	0	0	0	0	0	0	0	0
6	0	0	0	0	0	0	0	0	0	0	0	0	0	0	0	0	0	0	0	0	0	0	0	0	0
7	0	0	0	0	0	0	0	0	0	0	0	0	0	0	0	0	0	0	0	0	0	0	0	0	0
8	1	1	1	1	1	1	1	1	1	1	1	1	1	1	1	1	1	1	1	1	1	1	1	1	1
9	1	1	1	1	1	1	1	1	1	1	1	1	1	1	1	1	1	1	1	1	1	1	1	1	1

Table 2.6 UC based on DC OPF using PowerWorld

2.5.4 Impact of Price-sensitive Loads and Capacities of Transmission Lines and Generators

The impact of price-sensitive loads and capacities of transmission lines and generators to the optimal power dispatch and UC scheduling is very convenient to study by using PowerWorld and Matlab. For the 37-bus system shown by Figure 2.13, it is convenient to assign a price-sensitive load to each bus. By connecting/disconnecting a price-sensitive load or changing capacities of transmission lines or generators, the optimal power dispatch and UC scheduling can be easily evaluated and visualized. For any change of system conditions, the difference between

the two adjacent condition changes of the power system can be demonstrated by using the Difference Flows function in PowerWorld. The following observations are obtained:

1) The line capacity and location and size of loads are primary factors to affect the congestion. When the congestion appears on a line, the LMP of a bus associated with that line could be much higher than the LMPs of other buses.

2) To reduce the congestion of a line, either the capacity of generators close to a large load area or the capacities of the lines supplying the same load area need to be strengthened. However, the offered costs of generators are also an important factor to affect congestion.

3) The inclusion of the price-sensitive loads causes the LMPs to drop and a reduction of the overall surpluses of GenCos, ISO and LSEs. The larger percentage of the price-sensitive loads over fixed loads, the smaller the net surpluses of all the involved three entities are.

2.5.5 Optimal Power Dispatch and UC Scheduling Over Time

Under the conditions of variable loads over time, the LMP on each bus and average LMP vary as the loads change. The LMP curves could be quite different depending on the congestion of the lines connecting a bus (Figure 2.14). For example, LMP at Bus 15 is much higher than other buses due to the congestion of the line between Buses 15 and 54. One exception is the low load condition. During a low load condition, there is no congestion in the system so that LMPs on all the buses are the same.

The surplus of each generator is calculated by using the generator true cost (Eq. (11)) but also is affected by the reported cost, capacity, and unit transition cost of the generator. For example, the cheap and high capacity generator on Bus 17 supplies most of the power, making

its net surplus higher than other generators, especially at a peak load condition. The surplus of a generator could be negative under a light load or on/off transition (Figure 2.15). The primary cause of the negative surplus at a light load condition is the low LMP as well as the minimum amount of generation that a generator must supply. Thus, for the expensive generator 7 at Bus 33, the surplus of the generator could be trivial or negative when the generator supplies the minimum amount of generation with a low LMP.

The ISO net surplus is determined by the payments received from LSEs and payments given to generators by ISO, both of which are calculated based on LMPs. Therefore, if the LMPs at all the buses are close or the same, the net surplus of ISO could be very low or even negative due to the line losses that are not reflected in the LMP payment structure (Figure 2.17).

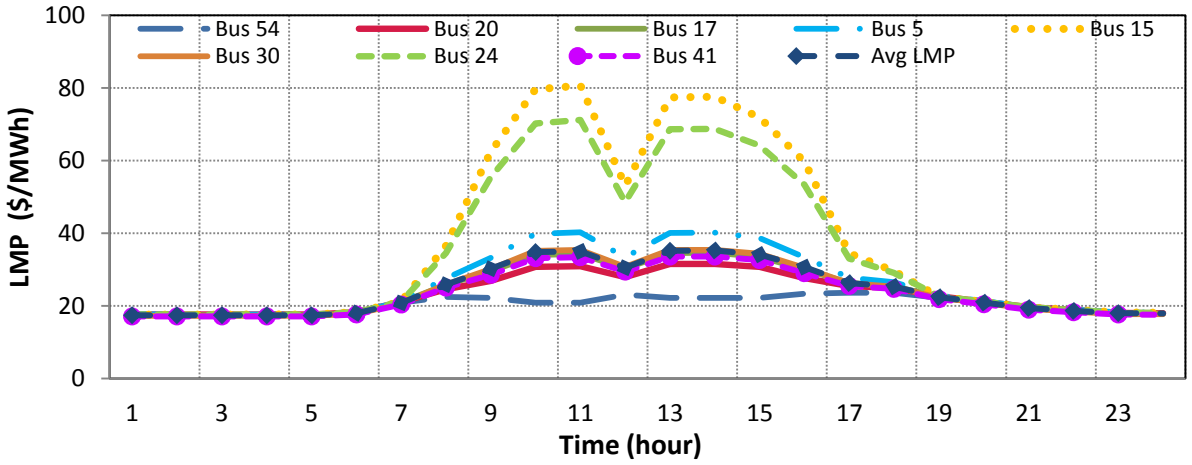

Figure 2.14 LMP at each load bus and average LMP

The LSE gain depends strongly on the price structure of a LSE as shown by Eq. (6), the LPM price at the bus connecting the LSE, and the load capacity associated with the LSE customers. An interesting issue shown in Figure 2.16 is a low surplus for some LSEs at peak load conditions around 10am and 2pm. This is due to the fact that during that time period, LMP prices at most buses are high due to the congestion so that the LSE surplus drops according to

Eq. (6). If there is no congestion at a LSE bus, the LSE surplus could be high especially when the load on that bus is large as shown by LSE 23 at Bus 32.

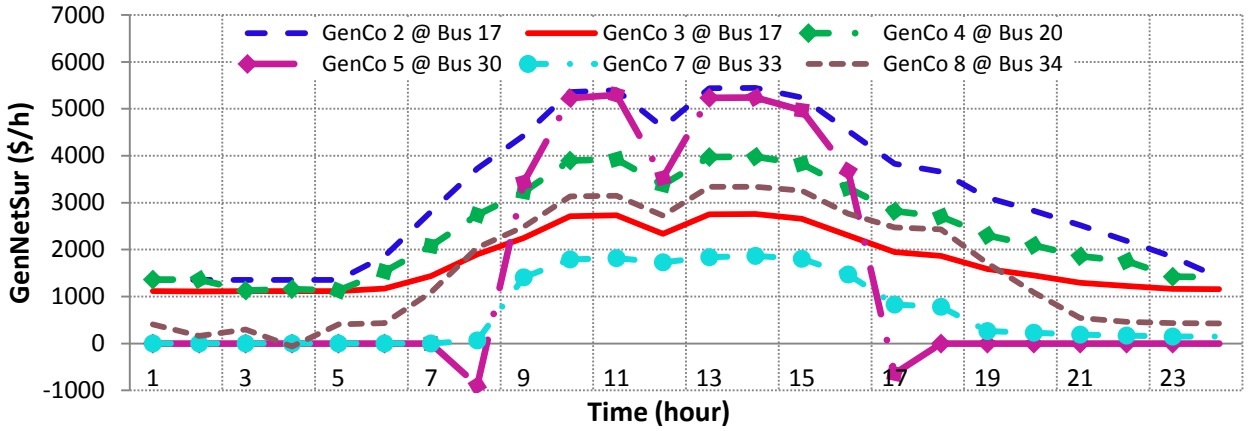

Figure 2.15 generator surpluses at each generator bus

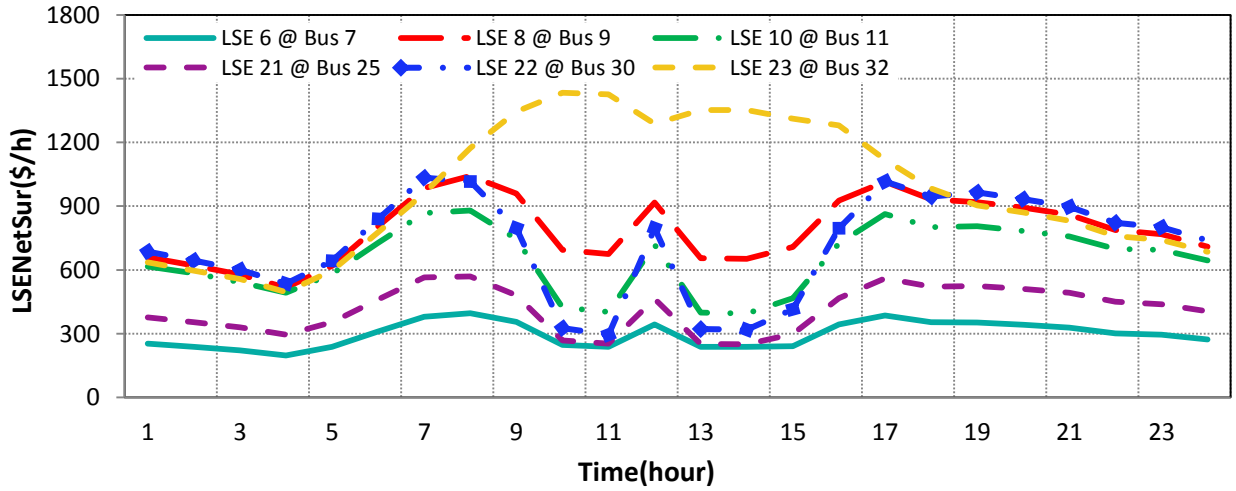

Figure 2.16 LSE surpluses at each load bus

2.6 Conclusion

With the transition to competitive wholesale and retail markets for electric utilities around the world, it is urgently needed to have efficient computing tools for design, analysis, evaluation, and visualization of a competitive wholesale power market. This paper investigates mathematical models associated with a competitive wholesale power market and how these models can be converted and transformed in such a way that makes it possible to use the

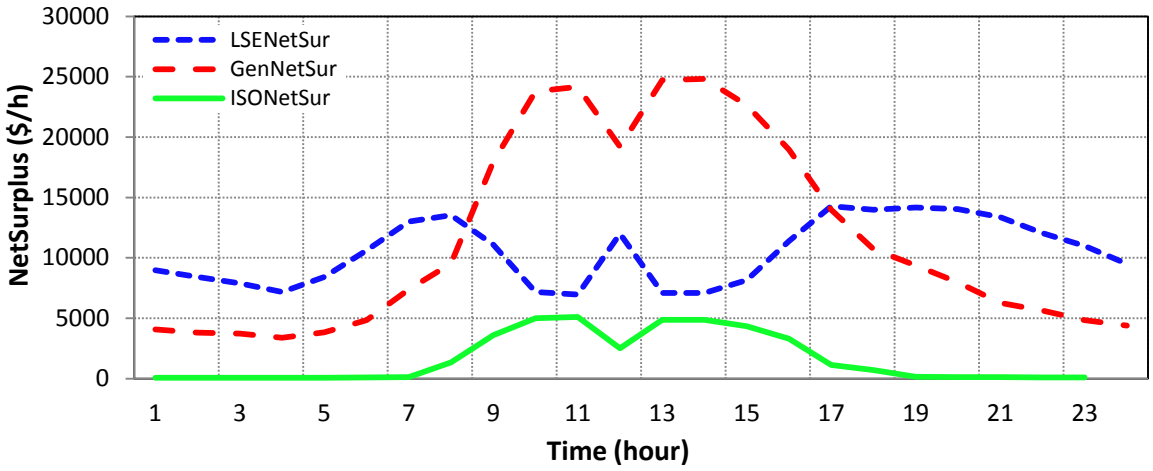

Figure 2.17 Generator, ISO and LSE net surplus

PowerWorld for the optimal power dispatch computation. The paper demonstrates that with proper conversion mathematically, the optimization problem can be solved effectively by using the PowerWorld.

The optimal dispatch using the PowerWorld is validated through Matlab. It is found that the results generated by using the piecewise linear models for generator cost functions and price-sensitive load bidding rate functions in PowerWorld are very close to the results generated by using the accurate cubic models for the generators and price-sensitive loads in Matlab. In PowerWorld, it is very convenient to build a large power system for optimal power dispatch study and to select either DC or AC OPF. The comparison shows that the difference between the DC and AC OPFs is very small. Using PowerWorld, the system study for a competitive wholesale power market becomes very easy due to powerful analytical and visualization tools available in the PowerWorld.

For variable loads over time, the load profiles can be first created by using other software tools (such as Excel) and then loaded into the PowerWorld simulator. Then, the Time-Step simulation option can used for the optimal power dispatch study. Under variable load conditions,

the LMP curves could be quite different depending on the congestion condition of the lines connecting a bus. If the LMPs at all the buses are close or the same, the net surplus of ISO could be very low or even negative due to the line losses. The surplus of each generator is affected by the cost and capacity of the generator. The LSE gain depends strongly on the price structure of the LSE.

2.7 References

[1] Paul L.Joskow, "Markets for Power in the United States: An Interim Assessment," The Energy Journal, Vol. 27, No. 1 2006.

[2] California ISO, "Market Redesign and Technology Upgrade: Locational Marginal Pricing (LMP) Study 3C," Nov. 2005.

[3] Hongyan. Li, Junjie. Sun, and L. Tesfatsion, "Dynamic LMP response under alternative price-cap and price-sensitive demand scenarios," 2008 IEEE Power and Energy Society General Meeting, 20-24 July 2008, Pittsburgh, PA, USA.

[4] W.W. Hogan, "Electricity Market Reform: Market Design and Resource Adequacy," Harvard University, Cambridge, Massachusetts, June 2011.

[5] Hongyan. Li, and L. Tesfatsion, "ISO Net Surplus Collection and Allocation in Wholesale Power Markets under LMP," IEEE Transactions on Power Systems, vol.26, no.2, pp.627-641, May.2011.

[6] Hongyan. Li, and Tesfation. L, "The AMES wholesale power market test bed: A computational laboratory for research, teaching, and training," 2009 IEEE PES Power & Energy Society General Meeting, 26-30 July 2009, Calgary, AB, CA.

[7] L. Tesfatsion, "Auction basics for wholesale power markets: Objectives and pricing rules," 2009 IEEE Power & Energy Society General Meeting, July 26-30, 2009, Calgary, Canada.

[8] F. Li, "Continuous Locational Marginal Pricing (CLMP)," IEEE Transactions on Power Systems, vol.22, no.4, pp.1638-1646, Nov. 2007.

[9] G. Hamoud, "Assessment of transmission congestion cost and locational marginal pricing in a competitive electricity market," IEEE Transactions on Power Systems, vol.19, no.2, pp. 769 - 775, May 2004.

[10] L. Tesfatsion, "ISS Panel and TF on Agent-Based Modeling of Smart-Grid Market Operations," 2012 IEEE PES Power & Energy Society General Meeting, July 26, 2012,

San Diego, CA.

[11] F. Li, "DCOPF-Based LMP Simulation: Algorithm, Comparison with ACOPF, and Sensitivity," IEEE Transactions on Power Systems, Vol. 22, No. 4, pp.1475-1485, Nov. 2007.

[12] D. Bertsekas, "Convex Analysis and Optimization," ISBN-13: 978-1886529458, April 2003.

[13] PowerWorld, " PowerWorld Simulator Overview," available at http://www.PowerWorld.com/products/simulator/overview.

[14] E.D. Sontag, "Nonlinear Regulation: The Piecewise Linear Approach," IEEE Transactions on Automatic control, Vol. 26, No. 2, pp 346-358, Apr.1981.

[15] P.R. Thie and G.E. Keough, "An Introduction to Linear Programming and Game Theory", 3rd Ed., Wiley, ISBN: 978-0-470-23286-6, Aug. 2008.

[16] Mathwork, "MATLAB Optimization Toolbox User's Guide," The MathWorks, Inc., Natick, MA, 2012.

[17] Rui. Bo, and Fangxing. Li, "Comparison of LMP simulation using two DCOPF algorithms and the ACOPF algorithm," Third International Conference on Electric Utility Deregulation and Restructuring and Power Technologies, April 2008, Nanjuing, China.

[18] R. Azami, M.S. Javadi, and G. Hematipour, "Economic Load Dispatch and DC-Optimal, Power Flow Problem- PSO versus LR," International Journal of Multidisciplinary Sciences and Engineering, vol. 2, no. 9, pp. 8-13, Dec. 2011.

[19] V. Sarkar and S.A. Khaparde, "Optimal LMP Decomposition for the ACOPF Calculation," IEEE Transactions on power systems, vol. 26, no. 3, pp 1714-1723, Aug.2011.

[20] Z. Li and H. Daneshi, "Some Observations on Market Clearing Price and Locational Marginal Price," 2005 IEEE Power Engineering Society General Meeting, June 12 - 16, 2005.

[21] H. Pinto, F. Magnago, S. Brignone, O. Alsac, B, Stott: "Security Constrained Unit Commitment: Network Modeling and Solution Issues", PSCE 2006, Atlanta, 2006.

[22] Singhal. Prateek Kumar, and Sharma.R. Naresh, "Dynamic programming approach for solving power generating unit commitment problem," 2011 2nd International Conference on Computer and Communication Technology, Sept 15 - 17, 2011.

[23] Snyder. Walter L. Jr, Powell. H. David. Jr, and Rayburn. John C, "Dynamic Programming Approach to Unit Commitment," IEEE Transactions on power systems, vol. 2, no. 2, pp 339-348, May.1987.

[24] J.D. Glover, M.S. Sarma, and T. Overbye, "Power System Analysis and Design 6th ed," 200 First Stanford Place, Suite 400 Stanford, CT 06092 USA, CENGAGE Learning, 2012.

[25] Rui. Bo, and Fangxing. Li, "Comparison of LMP simulation using two DCOPF algorithms and the ACOPF algorithm," Third International Conference on Electric Utility Deregulation and Restructuring and Power Technologies, April 2008, Nanjuing, China.

3. INTEGRATING POWERWORLD AND MATLAB FOR AGENT-BASED MODELING AND SIMULATION OF COMPETITIVE ELECTRIC POWER MARKETS

3.1 Introduction

Electric utility systems around the world continue to evolve from regulated, vertically integrated monopoly structures to open markets that promote competition among suppliers and provide consumers with a choice of services. This business trend is called "deregulation of the electricity market." Standard Market Design was proposed by the US Federal Energy Regulatory Commission (FERC) in 2002 [1, 2] by using locational marginal pricing (LMP), load serving entities (LSEs), and an independent system operator (ISO). As a result, fully functioning markets are distinguished by the presence of a large number of companies and players that are in direct competition. Each market participant has its own, unique business strategy, risk preference, and decision model. Agent-based decision-making is one of the key features of the new deregulated markets.

Many of the modeling tools for power systems analysis that were developed over the last two decades are based on the implicit assumption of a centralized decision-making process. Although these tools are very detailed and complex and will continue to provide many useful insights into power systems operation (Conzelmann et al., 1999; Koritarov et al., 1999, Harza, 2001), they are limited in their ability to adequately analyze the intricate web of interactions among all the market forces prevalent in the new markets. Generally speaking, classical power system models and tools are no longer valid because they were not designed to fit to the new agent-based market context. Similarly, standard analytical economic approaches, based on game

theory models, are usually limited to stylized market situations without proper consideration of economic and technological constraints of an electric power system.

At present, most conventional studies for an agent-based competitive wholesale power market are based on individually developed software packages without using existing power system simulation tools, making a lot of powerful analytical and visualization functions available in the commercial software unable to be integrated with a competitive power market study. In [4], an AMES Agent-Based Wholesale Power Market Test bed is developed based on Java, and is used to investigate how ISO net surplus varies in response to changes in the price-sensitivity of demand in ISO-operated wholesale power markets with congestion managed by LMP. In [5], a continuous LMP is proposed and is applied to a small five bus system. In [6], although a computer program PROCOSE is used for assessment of transmission congestion and LMP, the price sensitive loads and generations are not properly reflected in the program. Therefore, developing an efficient computing system becomes an important issue that was specially emphasized and discussed in several sessions and panels during 2012 IEEE Power & Energy Society General Meeting hold in San Diego, USA [9, 10].

3.2 Agent-Based Electricity Market

An agent-based system is a system that contains autonomous agents. There are three basic elements in an agent-based system: agents, environment, and rules. From the electric power market standpoint, an agent should have the following features [13]:

1) Autonomy: an agent is an independent entity of the underlying system. It communicates and interacts with other agents, but makes its decision without external control by its peers or administrative agents.

2) Heterogeneity: every agent could be different and maintains its own characteristics. For instance, while the agents of generation companies serve the same role of electricity generation in electricity market, each generation company has its own features such as production capacity and production cost.

3) Adaptation: each agent should be adaptive to its underlying environment. In other words, an agent must make adaptive decision according to its current states and the changing conditions in its environment.

Social ability: agents should have the ability to communicate and exchange information. For a competitive power market, the ISO, GenCos and LSEs are considered as agents in this paper. We focus primarily on how GenCo and LSE agents formulate their prices in an agent-based electricity market. In general, the competitive power market is represented as a stochastic game with multiplayer, where each player (GenCo or LSE) tries to maximize their individual benefit (GenCo or LSE net surplus). Due to the dynamic nature of the competitive power market, such as load fluctuation, network topology changes, generation units status changes, ISO operation changes, it is critical for each GenCo or LSE to build its own bidding strategies profile to guarantee individual welfare and risk hedge. Each GenCo or LSE agent is invisible to other GenCos or LSEs except for ISO. The general rule is that each GenCo agent has the same number of bidding strategies but may select a distinct bidding strategy day by day. The same rule is applied to LSE agents.

The bidding strategy profiles for GenCo *i* and LSE *j* are represented by SP_{Gi} and SP_{Li}, respectively. The number of available bidding strategies within the strategy profile of each GenCo is the same and represented by M_G. The number of available bidding strategies within the

strategy profile of each LSE is also the same and represented by M_L. Thus, for the *m*th bidding strategy associated with GenCo *i* and the *k*th bidding strategy associated with LSE *j*, we have $S_{Gi}(m) \in SP_{Gi}, m \in M_G;\ S_{Lj}(k) \in SP_{Lj}, k \in M_L$.

An agent determines a bidding strategy through either an offline or online learning process as shown in Section V. Each bidding strategy has a relevant propensity value, changing during the agent learning process, to indicate the potential for the agent to choose a bidding strategy.

Algorithm 1: Agent Learning Algorithm for GenCo *i* at day *D*

1: {Update the propensity of each strategy }
2: **for** $m = 1$ to M_G **do**
3: **if** $S_{Gi}(m) = SS_{Gi}(D\text{-}1)$
4: $Reward = \gamma \cdot GenNet_i(D\text{-}1)$
5: **else**
6: $Reward = (1-\gamma) \cdot GenNet_i(D\text{-}1)$
7: **end if**
8: {Update the propensity of GenCo *i*}
9: $q_{G\_mi}(D) = (1-\eta) \cdot q_{G\_mi}(D-1) + Reward$
10: **end for**
11: {Calculate the possibility for each strategy}
12: **for** $m = 1$ to M_G **do**
13: $p_{G\_mi}(D) = q_{G\_mi}(D) \Big/ \sum_{m=1}^{M} q_{G\_mi}(D)$
14: **end for**
15: Select $SS_{Gi}(D)$ through a stochastic approach and based on $p_{mi}(D)$, $m \in M_G$
16: {on exit, $SS_{Gi}(D)$ holds the bidding strategy for day *D*}

The Stochastic Reinforcement Learning (SRL) algorithm is used in this paper to help an agent to update its bidding strategy based on environmental information obtained from the agent-based system. Algorithm 1 gives the pseudo code of the learning process for the *i*th GenCo, in which SS_{Gi} stands for the selected strategy at a day, γ represents the discount factor, and η is the learning parameter [11]. The same code can be used for the *j*th LSE too. Basically, the algorithm is based on the selected bidding strategy and agent surplus from previous day *D-1* to determine

the reward (Line 4 or 6) and update the propensity (Line 9). Then, possibility associated with each strategy is calculated in Lines 12-14. In line 15, the bidding strategy for day *D* is obtained through a stochastic approach.

3.3 Integrating PowerWorld and Matlab for Agent-Based Modeling and Simulation of GenCo Learning

The interactions within an electricity market constitute a repeated game, whereby a process of experimentation and learning changes the behavior of GenCo and LSE agents in the market (Roth and Erev 1995). It is assumed that these agents are intelligent and adaptive, meaning that they can make operational and strategic decisions on the basis of the information available to them and the market's rules, and learn from past experiences (and mistakes) to improve their decision making and adapt to changes in environments. However, the normal agent-based modeling and simulation function is not available in PowerWorld. To overcome the weakness, we developed a mechanism by integrating PowerWorld and Matlab together for combined optimal power dispatch and agent-based learning and decision making.

The basic idea of the integrated computational system is to use PowerWorld for optimal power dispatch computation and to use Matlab for agent-based learning and bidding in a competitive electricity market. The two software programs are connected together through Simulator Automation Server (SimAuto). SimAuto provides a COM interface so that a user can extend the functionality of PowerWorld Simulator to any external program. By using SimAuto, we can launch and control PowerWorld from our Matlab-based program. By this way, we are able to use the special power of both Matlab and PowerWorld for very fast formulation and computation of a large-scale agent-based competitive power market.

Algorithm 2: Simulation of an agent-based competitive power market

1: **{*Initialization*}**
2: Generate GeoCo and LSE strategy profiles SP_*, where $S_{G\_mi} \in SP_{Gi}$, $m \in M_G$; $i \in N_G$; $S_{L\_kj} \in SP_{Lj}$, $k \in M_L$. $j \in N_L$
3: Set initial propensity values q_* for each strategy within SP_{Gi} and SP_{Lj}, where $q_{G\_mi} \leftrightarrow S_{G\_mi}$; $q_{L\_kj} \leftrightarrow S_{L\_kj}$
4: **{*Day 1*}**
5: Random select a strategy S_{G_*i} for each GenCo i and a strategy S_{L_*j} for each LSE j, and formulate GenCo and LSE reported cost models in Matlab
6: PowerWorld ← GenCo and LSE cost models in Matlab
7: Optimal power flow for Day 1 in PowerWorld
8: MaltLab ← Optimal power flow results
9: Calculate: GenNet_i, $i \in N_G$; $LSENet_j$, $j \in N_L$
10: **{*Offline learning*}**
11: **for** D=2 to *Num_of_days* **do** {This loop is removed for online agent-based learning}
12: Call Alg. 3
13: **end for**
14: **{*Online learning and updating*}**
15: $D \leftarrow D+1$
16: Call Alg. 3
17: **Goto** Line 15

Algorithm 3: Learning and updating procedures for a day

1: **for** i=1 to N_G **do** {GenCo learning}
2: Call Alg. 1 for GenCo i;
3: **end for**
4: **for** j=1 to N_L **do** {LSE learning}
5: Call Alg. 1 for GenCo j;
6: **end for**
7: Formulate GenCo and LSE reported cost models based on $SS_{Gi}(D)$ $i \in N_G$ and $SS_{Lj}(D)$, $j \in N_L$
8: PowerWorld ← GenCo and LSE cost models
9: Optimal power flow for Day D in PowerWorld
10: MaltLab ← Optimal power flow results
11: Calculate: GenNet_i, $i \in N_G$; $LSENet_j$, $j \in N_L$

Algorithm 2 gives the pseudo code for the agent-based simulation of a competitive electric power market, in which N_G N_L represent the total numbers of GenCos and LSEs, respectively, and Algorithm 3 represents the learning and updating procedures for a specific day. The algorithm starts with an initiation of bidding strategy profiles for GenCos and LSEs, with each strategy profile containing the same number of strategies for each GenCos and LSEs,

respectively. For Day 1, a strategy for each GenCo and LSE is randomly selected and then passed from Matlab to PowerWorld for optimal power flow computation. The proposed method can be used for either offline- or online-based agent learning. For offline-based agent learning, GenCo and LSE agents learn to improve their bidding strategies from history data based on the SRL algorithm .Then, the learned result is used for actual operation of the agent-based competitive power market, which involves continuous learning and updating as the daily operation continues. For online-based agent learning, without execution of lines 10 to 13, GenCo and LSE agents learn to improve their bidding strategies immediately based on the real-time data obtained as the daily operation of the system continues. Compared to the offline learning approach, the GenCo and LSE agents may begin with their bidding strategies that may be not economical to them for many days.

3.4 Using PowerWorld and Matlab for Agent-Based Simulation of Competitive Power Market

With the development of the integrative computational system, this section presents an extensive study of agent-based competitive power market for an 8-bus system. The system has six generators located on Bus 1, 3, 4, 5, 6 and 7, respectively. Bus 1 is the slack bus. Five fixed loads, as shown in Figure 1, are located on Bus 2, 3, 4, 6, and 8, respectively. Each load bus could include a price-sensitive load. The transmission line parameters and capacities are provided in [9]. The capacities and true cost coefficients of generators are given in Table 1, where *F* represents the fixed price of a generator. The generator bidding cost coefficients, different from the true cost coefficients, are generated before the simulation with the following rules: 1) bidding cost coefficients should be always larger than the true cost coefficients and 2) the increment bidding rate function (5) should be an increasing function with the generator

power production [12]. Three different types of variable loads are considered as shown by Figure 3. The power factor is 0.85 lagging for Type 1 load and 0.9 for Type 2 and 3 ones. The load profiles are first created by using other software (such as Excel) and then loaded into PowerWorld simulator from MATAB at each simulation interval. The study focuses mainly on 1) how the agent-based learning can change the gain or loss of GenCos and LSEs, 2) bidding strategies, and 3) number of days involved for training.

The impact of the agent-based learning is very convenient to study using the integrative computational system. For the 8-bus system as shown by Figure 1, each load bus could include a price-sensitive load. The increment bidding rate coefficients for price-sensitive loads are set as α=32\$/MWh and β=0.03\$/MW^{2}h. The GenCo learning study is conducted in two ways, i.e., online learning and testing, and offline learning and online testing. For online learning, an agent starts learning and bidding process immediately after receiving new data. For offline learning, an agent first learns from historical data and starts its repeating real-time learning and bidding process for the pre-learning (training).

GenCo	Average GenCo Net Surplus			
	1 strategy	4 strategies	8 strategies	12 strategies
1	4258367	4281974	4272849	4272088
2	2522090	2567114	2558235	2556093
3	2532764	2595355	2573370	2574376
4	3261685	3360390	3319969	3317626
5	2509565	2558818	2543946	2548754
6	7250768	7475250	7393719	7371158

Table 3.1 online learning: Average GenCo Net Surplus under different strategies

GenCo performs GenCo learning to generate the bid or reported cost. The bid will be sent to PowerWorld simulator as the generator cost for the optimal power flow evaluation in lines 9 and 10. GenCos will continue learning and update when new data is available. By connecting or

disconnecting a price-sensitive load and changing capacities of transmission lines or generators, the optimal power dispatch solutions can be easily evaluated and visualized. For any change of system conditions, the difference between the two adjacent system changes can be demonstrated by using the Difference Flows.

GenCo	Average GenCo Net Surplus				
	Online	30days	100 days	200days	300 days
1	3558251	3560778	3578108	3580123	3590012
2	2585324	2597431	2642824	2652103	2662304
3	2587523	2597634	2660669	2684520	2692513
4	3362423	3365339	3421376	3442356	3452025
5	2581235	2584759	2599380	2602158	2605625
6	7488526	7492434	7610116	7620325	7622035

Table 3.2 offline learning: Average GenCo Net Surplus under different days

3.4.1 Online Learning

For the online learning, 1000 days' loads data was used into the simulation including both real and reactive power demands. All the GenCos have the same number of bidding strategies and use the identical method [11] to generate their bidding strategies (Figure 3.1) based on their true marginal costs. In order to investigate the impact of the number of bidding strategies of each GenCo, in table 2, four different scenarios, 1 strategy (no Learning), 4 strategies , 8 strategies, and 12 strategies were evaluated. In general, using GenCo Learning has larger average Gen Net Surplus than without using GenCo Learning (only report their true marginal cost). In Figure 3b, after learning, GenCo3 doesn't have a dominated strategy. Therefore, even some strategies have relative lower possibilities to be chosen, they will not extinguish. Also, all GenCos will have very different mixed strategy distributions (Figure 3.2 and Figure 3.3) due to the various bidding strategies and generator's physical properties. Each

GenCo will keep plays their mixed strategy profile in the day ahead market in order to be better adapt any market's changes in the future. However, table 2 shows that the increasing number of strategies will lead the mean of average GenCo Net surplus to drop. Eventually, in the 8 (Figure 3.4) and 12 (Figure 3.5) strategies situation, each GenCo will have less possibility to choose the strategies which can contribute more net surplus than other strategies.

3.4.2 Offline Learning

For offline learning, we considered how the amount of the training data affects the agent performance. Each GenCo has 4 bidding strategies and use 30, 100, 200, and 300 days' load data for offline pre-learning (training) respectively. After certain runs, each GenCo's mixed strategy profile is able to converge to a stable distribution of bidding strategies under different pre-learning scenarios. Further, all the agents (GenCos) will perform online learning in a testing data set, (a whole year load's data). Table 3 shows that, by increasing the amount of training data, the average GenCo net surpluses of all GenCos will increase. Since the larger data set will provide more market information to each agent to find out better distribution of its own bidding strategies. In addition, to compare the offline learning and online learning, the above testing data was used. Generally, using offline learning , the net surplus of each GenCo is larger than using online learning.

3.5 Conclusions

With the transition to competitive wholesale and retail markets for electric utilities around the world, it is urgently needed to have efficient computing tools for design, analysis, evaluation, and visualization of a competitive wholesale power market. By exchanging data between Matlab program and PowerWorld simulator via SimAuto, the GenCo learning can be easily applied into any scale power system. This paper investigates both online and offline agent-

based GenCo learning and compares the results of these two algorithm. The paper also proposes a mechanism to integrate PowerWorld and Matlab for combined optimal power dispatch and agent-base learning.

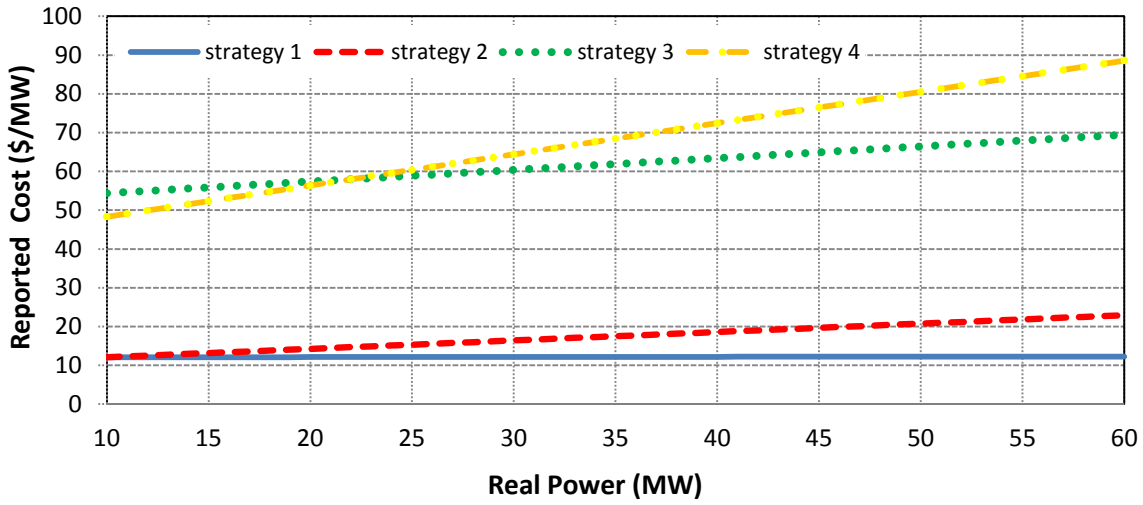

Figure 3.1 bidding strategies of GenCo 3 (Strategy 1 is the true marginal cost)

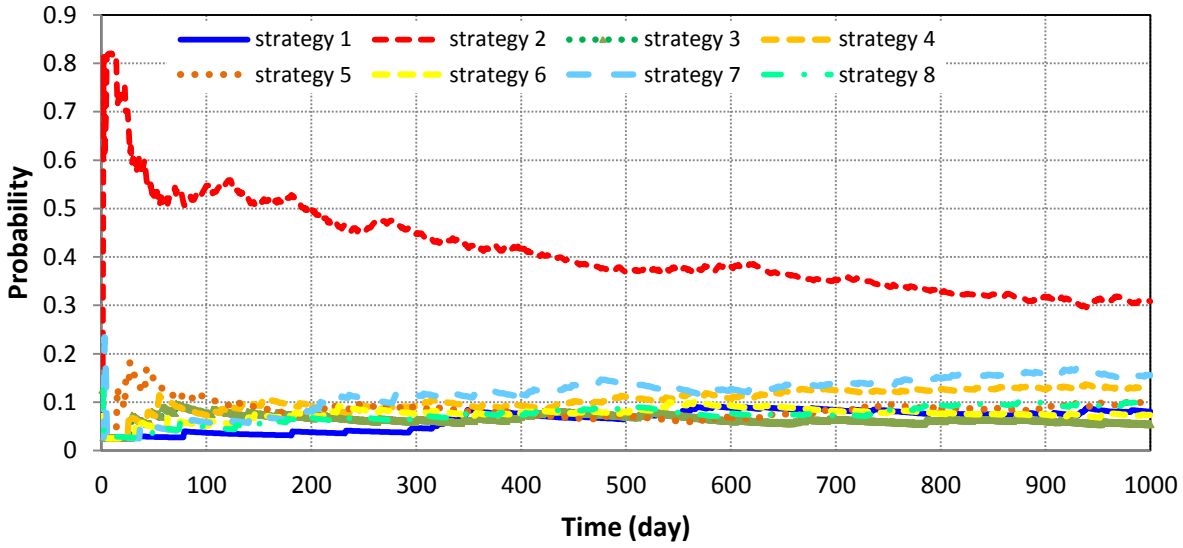

Figure 3.2 GenCo6 mixed strategy profile (4 strategies)

In the day ahead competitive power market, all GenCos aim to maximize their net surplus by making rational bids. By using GenCo learning, each GenCo are able to adjust the probability of each bidding strategy based on the changes of the electricity market daily. For the online

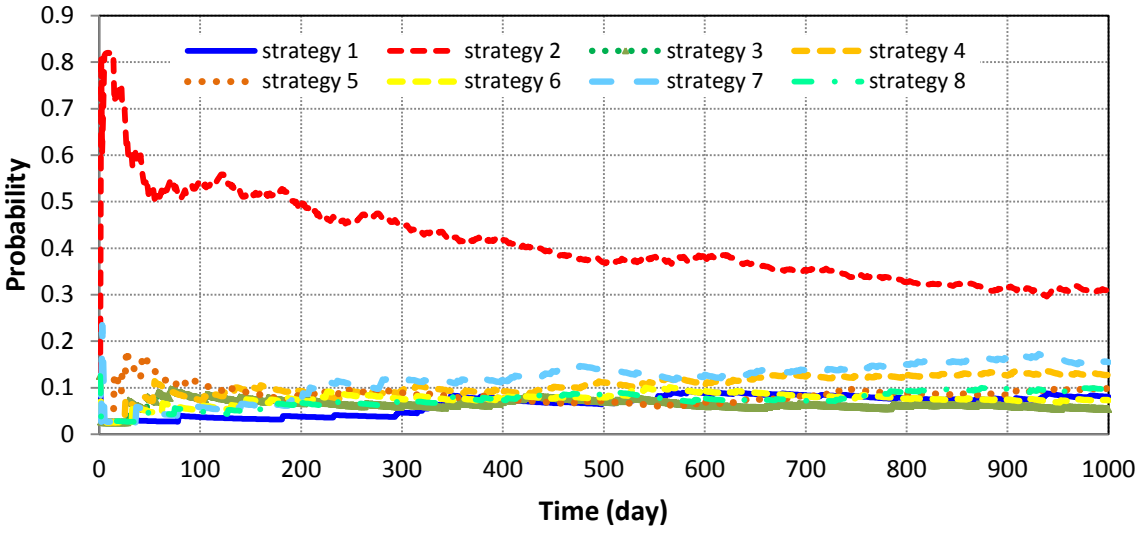

Figure 3.3 GenCo3 mixed strategy profile (8 strategies)

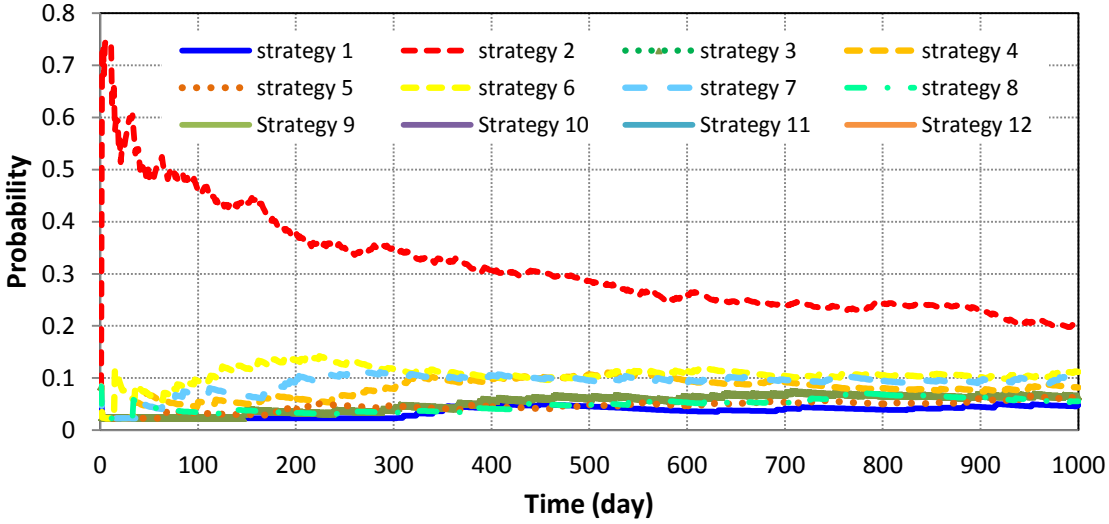

Figure 3.4 GenCo3 mixed strategy profile (12 strategies)

learning , GenCos will perform learning and biding based on the data stream. For the offline learning, GenCos will learn their mixed strategy's distribution by using the historical data, and then issue a bid in each day. Different number of bidding strategies will affect the overall net surplus directly. In some situations, more strategies will have negative impact on the net surplus of each GenCo, since the possibilities for choosing the valuable strategies will be lower. For the offline learning, the size of training data can also influence the outcome of the net surplus for each GenCo. By learning from a larger amount of training data, the GenCos are able to gain more benefits in the testing data, because the bidding strategies are more adaptable to the pattern of the electricity power market.

3.6 References

[1] Paul L.Joskow, "Markets for Power in the United States: An Interim Assessment," The Energy Journal, Vol. 27, No. 1 2006.

[2] California ISO, "Market Redesign and Technology Upgrade: Locational Marginal Pricing (LMP) Study 3C," Nov. 2005.

[3] Hongyan. Li, and L. Tesfatsion, "ISO Net Surplus Collection and Allocation in Wholesale Power Markets Under LMP," IEEE Transactions on Power Systems, vol.26, no.2, pp.627-641,May.2011.

[4] Hongyan. Li, and Tesfation. L, "The AMES wholesale power market test bed: A computational laboratory for research, teaching, and training," 2009 IEEE PES Power & Energy Society General Meeting, 26-30 July 2009, Calgary, AB, CA.

[5] F. Li, "Continuous Locational Marginal Pricing (CLMP)," IEEE Transactions on Power Systems, vol.22, no.4, pp.1638-1646, Nov. 2007.

[6] G. Hamoud, "Assessment of transmission congestion cost and locational marginal pricing in a competitive electricity market," IEEE Transactions on Power Systems, vol.19, no.2, pp. 769 - 775, May 2004.

[7] F. Li, "DCOPF-Based LMP Simulation: Algorithm, Comparison with ACOPF, and Sensitivity," IEEE Transactions on Power Systems, Vol. 22, No. 4, pp.1475-1485, Nov. 2007.

[8] H. Liu, L. Tesfatsion, and A. A. Chowdhury, "Derivation of locational marginal prices for restructured wholesale power markets," *J. Energy Markets*, vol. 2, no. 1, pp. 3–27, 2009.

[9] PowerWorld, "PowerWorld Simulator Overview," available at http://www.PowerWorld.com/products/simulator/overview.

[10] Snyder. Walter L. Jr, Powell. H. David. Jr, and Rayburn. John C, "Dynamic Programming Approach to Unit Commitment," IEEE Transactions on power systems, vol. 2, no. 2, pp 339-348, May.1987.

[11] Alvin E. Roth and Ido. Erev. "Learning in Extensive – Form Games: Experimental Data and Simple Dynamic Models in the intermediate Term," Games and Economic Behavior, 8, pp 164-212, 1995.

[12] J. Sun and L. Tesfatsion, "Dynamic testing of wholesale power market designs: An open-source agent-based framework," *Computational Economics*, Vol. 30, pp. 291-327, 2007.

[13] SuFang. Chen, "Automation power dispatch sheet system based multi-agent," International Conference on Apperceiving Computing and Intelligence Analysis, Oct 2009.

4 OPTIMAL MICROGRID CONTROL AND POWER FLOW STUDY WITH DIFFERENT BIDDING POLICIES BY USING POWER WORLD SIMULATOR

4.1 Introduction

A microgrid (MG) reflects a new way of designing and building future smart grids [1]. The MG approach focuses on creating a design and plan for local energy delivery that meets the needs of the constituents being served. It is expected that the development of MGs has the potential to bring a number of benefits into the system in terms of: 1) enabling development of sustainable and green electricity, 2) enabling larger public participation in the investment of small scale generation, 3) reduction in marginal central power plants, 4) improved security of supply, 5) reduction of losses, and 6) enabling better network congestion management [2, 3].

However, a technical challenge for operation of MGs is how to find a rational method to manage distributed energy resources (DERs) and loads [4, 5]. There are many differences in energy management requirements between MGs and traditional power systems because of the following reasons. (i) A MG is an autonomy system with DERs to satisfy different load requirements. (ii) The types of generators, loads and market participation strategies are different from traditional power systems. (iii) Scalability can allow DERs and loads to connect and disconnect into the MG independently [6].

At present, MG market and operation studies are primarily based on individually developed software without using existing power system simulation tools [7-9], making a lot of powerful analytical and visualization functions available in the commercial software unable to be used for MG power market research. This is due to the fact that the objective function for a MG

power market varies from cases to cases. Therefore, it is impossible to fit all different situations in a commercial software design. Regarding user-designed computer programs for a MG, many simplified conditions are usually assumed and a lot of studies do not consider special characteristics of power converters, causing actual MG operating conditions unable to be reflected in a user program properly. Hence, developing an efficient computing system for MG research becomes an important issue that was specially discussed in several sessions and panels during 2012 IEEE Power & Energy Society General Meeting hold in San Diego, USA [10, 11].

4.2 Operating Strategies of microgrid DERs

A microgrid mainly consists of three parts: a low-voltage distribution network, DERs, and controllable and uncontrollable loads [2, 3]. Typical DERs include solar photovoltaic, wind turbines, fuel cells, micro turbines and energy storage units [2, 12]. In order to convert the energy into grid compatible ac power, those DER units require power electronic converters for grid interfaces (Figure 4.1).

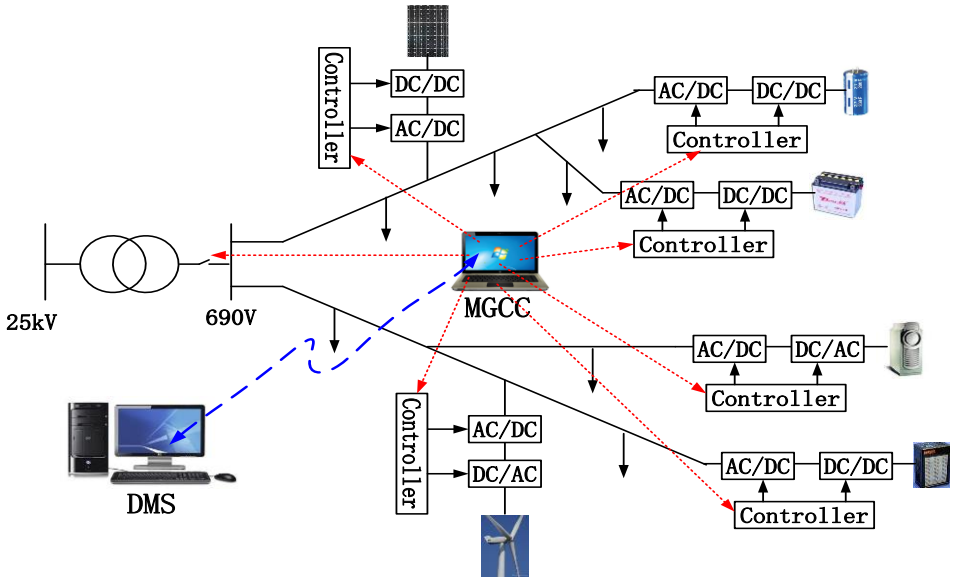

Figure 4.1 Typical configuration of a microgrid

The MG control and management system typically has three levels: device level at individual DERs, MG central control (MGCC) level, and distribution management system (DMS) level [13]. At the DER level, the energy is either captured from a renewable resource or generated from other micro-generation sources and then sent to the MG based on MGCC control demands. At the MGCC level, the power production and distribution of a MG is determined according to optimal overall cost or profit to operate DERs and loads of the MG. The MGCC sends out power references to DERs and controllable loads, while each individual DER or load control system ensures that the power reference from the MGCC is reached. At the DMS level, the power production of MGs are managed to meet the overall grid requirements.

Unlike conventional electric power systems, most DERs are connected to the MG network through power converters. Typical converter configurations include1) a dc/dc/ac voltage source converter (VSC) for energy storage devices and solar photovoltaic[14, 15], and 2) an ac/dc/ac VSC for wind power generators and micro-turbines [16, 17].It is important that operating principles of DER power converters are considered properly in MG power flow and market studies.

4.2.1 Decoupled power converter structure

A DER device normally has a decoupled power converter configuration (Figure 4.1). For a renewable energy based DER, the VSC on the renewable energy source side implements the maximum power extraction function while the VSC connected to the grid side is necessary for grid integration. The operation of the grid-side VSC should assure that the active power captured from a renewable energy source is transferred to the grid while the reactive power generated by the VSC follows the MGCC control demand. At the same time, the rated current and PWM saturation constraints of the power converter cannot be exceeded.

4.2.2 Control of grid-side converter

The standard control strategy of the grid-side converter (GSC) has a nested-loop structure as shown by Figure 4.2, which consists of a faster inner current loop and a slower outer loop. The outer-loop controller generates d- and q-axis current references, i_d^* and i_q^*, to the inner current-loop controller while the inner current-loop controller generates d- and q-axis voltage reference signals, v_{d1}^* and v_{q1}^*, to implement the final control function [14-17]. Using the motor sign convention, the d- and q-axis current references, i_d^* and i_q^*, are related to the desired active and reactive power to the grid by

$$i_d^* = P_{ac}^* / V_d \,, \qquad i_q^* = -Q_{ac}^* / V_d \tag{1}$$

where V_d is the d-axis component of the grid voltage at the point of common coupling (PCC). In terms of the converter d- and q-axis output voltage, V_{d1}^* and V_{q1}^*, the desired active and reactive power follows the relationship below

$$P_{ac}^* = \frac{V_d \cdot V_{q1}^*}{X_L} \,, \quad Q_{ac}^* = \frac{V_d}{X_L}\left(V_{d1}^* - V_d\right) \tag{2}$$

where X_L stands for the grid filter reactance.

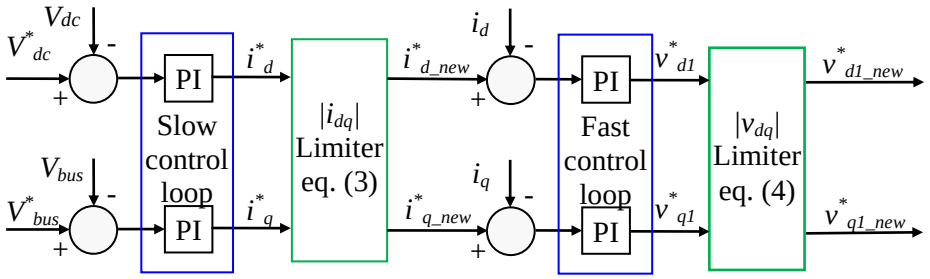

Figure 4.2 Nested-loop control configuration of GSCs

4.2.3 DER inverter constraints

In reality, the rated power and PWM saturation constraints of a GSC cannot be exceeded [18]. When it is jeopardized for the system to operate beyond these constraints, the GSC should meet the active power or dc-link voltage control demand first while minimizing the difference between the reference and actual reactive power as much as possible [18]. This results in a control strategy as shown below, where I_{rated} is the rated phase *rms* current of the converter.

Minimize: $\left|Q_{ac} - Q_{ac}^{*}\right|$

Subject to: $V_{dc} = V_{dc}^{*}$

$$\sqrt{\left(i_d^2 + i_q^2\right)/3} \le I_{rated}, \quad \sqrt{\left(v_{d1}^2 + v_{q1}^2\right)/3} \le V_{dc}/\left(2\sqrt{2}\right)$$

According to (1) and (2), the control mechanism is implemented in the following way [18]. If $|i_{dq}^{*}|$ generated by the dc-link voltage and reactive power control loops exceeds the rated current limit, i_d^{*} and i_q^{*} are modified by (3). If $|v_{dq}^{*}|$ generated by the current control loops exceeds the PWM saturation limit, v_{d1}^{*} and v_{q1}^{*} are modified by (4).

$$i_{d\_new}^{*} = i_d^{*} \quad i_{q\_new}^{*} = \operatorname{sign}\left(i_q^{*}\right) \cdot \sqrt{\left(i_{dq\_\max}^{*}\right)^2 - \left(i_d^{*}\right)^2} \tag{3}$$

$$v_{d1\_new}^{*} = \operatorname{sign}\left(v_{d1}^{*}\right) \cdot \sqrt{\left(v_{dq1\_\max}^{*}\right)^2 - \left(v_{q1}^{*}\right)^2} \quad v_{q1\_new}^{*} = v_{q1}^{*} \tag{4}$$

where $v^{*}_{dq1\_max}$ represents the maximum acceptable dq voltage of the DER inverter. Typical strategies to operate a DER inverter in a MG include PQ and PV inverters [19, 20].

4.2.4 PQ-inverter DER

A PQ-inverter DER operates by injecting active and reactive power into a MG. The active power of the DER is normally controlled according to a maximum power extraction rule

for a renewable source or according to a demand from the MGCC. The reactive power is controlled either locally for the unity power factor or centrally according a command from the MGCC. Due to the rated power constraint (eq. (3)), the maximum acceptable reactive power cannot exceed

$$Q_{\max} = \sqrt{S_{rated}^2 - P_w^2} \tag{5}$$

On the other hand, from the consideration of the PWM saturation constraint (eq. (4)), the maximum acceptable reactive power cannot surpass

$$\begin{cases} V_{q1}^* = P_{ac} X_L / V_d, \quad V_{d1}^* = \sqrt{3V_{dc}^2/8 - \left(V_{q1}^*\right)^2} \\ Q_{\max} = V_d \left(V_{d1}^* - V_d\right) / X_L \end{cases} \tag{6}$$

Therefore, the maximum reactive power of a DER under PQ-inverter mode should take the smaller value of the two boundary reactive powers calculated from (5) and (6).

4.2.5 PV-inverter DER

A PV-inverter DER operates by injecting active power into a MG and, at the same time, maintaining the PCC voltage at a desired value. The active power is usually controlled in the same way as that used in a PQ-inverter DER but the reactive power is controlled according to the error signal between the desired and actual PCC voltage to which the inverter is connected. For any voltage support control condition, the maximum reactive power supplied by a DER cannot exceed the smaller value of the two boundary reactive powers calculated from (5) and (6).

4.3 Market Model for microgrid Management

For the market of electricity transaction to exist, there has to be a compelling business model for sellers and incentive for buyers. The selling and buying of energy is usually managed

by the MGCC through a bidding process. During the islanded mode, the MGCC control strategies should also coordinate secondary load-frequency control to assure stable and secure operation of the MG.

4.3.1 Bidding in an open MG market

In an open MG market, at the first *m*-minute interval (such as a 15-minute interval) of an hour, there is a bidding process regarding the energy production by DERs and load demands of customers for the next hour. In order to make a rational bid, DER owners should consider both the operating costs of their DER units and the payoff for selling the energy.

For a customer or USER, the bidding procedure is more complex because it normally involves two different options: shift and curtailment. In the shift option, customers place two different bids for their high- and low-priority loads for next operating hour. In the curtailment option, customers may choose to shed low-priority loads.

In each *m*-minute bidding interval, both DER owners and customers will send their bids to the MGCC. The MGCC is responsible for i) informing DER owners and customers about the open market price, ii) accepting DER and USER bids, iii) running optimal routines, and iv) sending the optimization results to DERs and USERs. The optimization results are typically obtained by using one of the following two market policies: 1) minimum operational cost policy or 2) maximum overall profit policy [13].

4.3.2 Minimum operational cost policy

The main goal of this policy is to minimize the overall MG operational cost for the next hour [13]. The objective function in the every bidding period is

$$Cost = \sum_{i=1}^{N} DER\_bid(x_i) + AX + \sum_{j=1}^{M} User\_bid(y_j) \tag{7}$$

where *DER_bid*(x_i) denotes the bid from the *i*th DER, $x_i$is the active power anticipated to produce by the *i*th DER for the next hour, *A* is the open market price, *N* is the number of DERs, *X* is the amount of the active power bought by the MGCC from the grid, y_j is the *j*th USER bid for USER's load shedding, and *User_bid*(y_j) is the compensation cost that a USER will receive from the MGCC for the load shedding. Thus, the following optimization strategy will result.

Minimize:

$$Cost = \sum_{i=1}^{N} DER\_bid(x_i) + AX + \sum_{j=1}^{M} User\_bid(y_j) \tag{8}$$

Subject to:

$$X + \sum_{i=1}^{N} x_i = Total\_Demand - \sum_{j=1}^{M} y_j \tag{9}$$

$$X_i^{Min} \le x_i \le X_i^{Max} \tag{10}$$

$$0 \le y_j \le Y_j^{Max} \tag{11}$$

$$0 \le S_{mn}(h) \le S_{mn}^{Max} \tag{12}$$

Where *Total_Demand* is the total planned MG active power demand, (9) represents the active power balance constraint in the MG, X_i^{Min} and X_i^{Max} are minimum and maximum limits of the active power of the *i*th DER, Y_j^{Max} is the maximum limit of load y_j that can be curtailed, and S_{mn} is the power constraint of the line between nodes *m* and *n*. In addition, depending on PQ- or PV-inverter DERs, DER reactive power and/or PCC bus voltage constraints should be included.

4.3.3 Maximum overall profit policy

The goal of this policy is to maximize the overall MGCC profit [13]. The MGCC sells the power to the MG users in the open market price. If the production of DERs cannot satisfy the

local loads or the cost of DERs is too high, the MGCC needs to buy the power X from the main grid. Hence, the MGCC "Revenue" obtained by selling the power is give

$$\text{Revenue} = AX + A\sum_{i=1}^{N} x_i \tag{12}$$

The MGCC "Expenses" include payments for buying power from DERs and the grid as well as payments to USERs for compensation of load shedding. Therefore, the MGCC "Expenses" is described by

$$\text{Expenses} = \sum_{i=1}^{N} DER\_bid(x_i) + AX + \sum_{j=1}^{M} User\_bid(y_j) \tag{14}$$

The overall MGCC profit equals to the "Revenue" (13) minus "Expenses" (14) as shown by

$$\text{Profit} = A\sum_{i=1}^{N} x_i - \sum_{i=1}^{N} DER\_bid(x_i) - \sum_{j=1}^{M} User\_bid(y_j) \tag{15}$$

which is the objective function associated with the maximum profit policy while the constraints are the same as shown in Section III-B.

4.3.4 DER and USER Bids

A DER bid is the operational cost for a distributed energy source, which include payback and investment or depreciation of the DER. A DER bid can be described as [13]

$$DER\_bid(x_i) = b_i x_i + c_i \tag{16}$$

where b_i represents the fuel cost and c_i denotes the hourly profit. For renewable energy sources, b_i stands for the annual depreciation for generating each kWh of active power.

A User bid is the bid offered by a customer for the load shedding. In compensation, the MGCC will pay back the user for the load shedding at a certain percentage of the open market price. Thus, a User bid is given by

$$User\_bid(y_j) = \lambda_j A \cdot y_j \quad (17)$$

where λ_j is the ratio of the MGCC's compensation price with the utility open market price.

4.3.5 Load-generation balance in islanded mode

In MG islanded operation, the power purchased from the grid *X* is zero and the MGCC must coordinate secondary load-frequency control, which is crucial for the proper operation of the MG. The two objectives of the secondary control are [4, 21]: (a) to hold the system frequency at or close to the nominal system frequency from transient time scale stand point at the DER level, and (b) to maintain the load-generation balance at the MGCC level from steady-state time scale perspective. This paper focuses on how to gain load-generation balance that can assure load-frequency control at the MGCC system level in the most economical way. This economic dispatch problem can still be solved according to the above discussion by using either the minimum operational cost policy or the maximum overall profit policy. The primary difference is that in the islanded mode the grid power *X* is zero and a large amount of load curtailment is necessary.

4.4 MG Optimal Power Dispatch by using PowerWorld

PowerWorld Simulator is an interactive power systems simulation package designed to simulate power systems operation on a time frame ranging from several minutes to several days. The software contains a highly effective power flow analysis package capable of efficiently solving systems with up to 100,000 buses [22]. It is necessary to point out that although this paper uses PowerWorld as an example, the proposed strategy should be easily applied to other commercial power system simulators too.

4.4.1 Optimal power dispatch in grid-tied mode

The first step in solving an optimal power dispatch problem using PowerWorld is to develop a single-line diagram. The simulation program can read in impedance data of each line and the length of the line and then automatically convert the impedance of each line into per unit. For each line, the MVA limit of a line is specified. The grid is represented by a slack bus generator.

The next step is to define DERs. This includes specifying maximum and minimum power generation of each DER unit and the bid associated with a DER. The DER capacity, i.e., Max_MW, Min_MW, Max_Mvars and Min_Mvars values of a DER, are specified based on the procedures shown in Sections II-D and II-E. These parameters represent maximum and minimum active and reactive power constraints of a DER, respectively. A DER bid is defined through the cubic cost model in PowerWorld. However, to reflect the DER bid as shown by (16), only the linear and the constant coefficients of the cubic cost model are used.

The final step is to create a special technique so that curtail loads associated with USER bids can be properly implemented in PowerWorld. These loads are variable loads from 0kW to a maximum value representing the maximum amount of loads that can be curtailed. Bidding rates must be specified for those loads so that the conventional load model defined in PowerWorldis unsuitable to a curtail load. We developed a special mechanism to model a curtail load based on the conventional generator model defined in PowerWorld. The strategy requires: 1) the power generated by the "generator" to be negative instead of positive, and 2) a constant bidding rate as shown by (17) for those special "generators". The other loads that cannot be shed are defined by using the normal load models in PowerWorld.

To solve the optimal power dispatch for a MG policy presented in Section III-B or III-C, the PowerWorld Optimal Power Flow Analysis Tool (OPF) [22] is used. The OPF provides the ability to optimally dispatch the generation with the minimum overall cost in an area or group of areas while simultaneously enforcing the transmission line and interface limits. However, the objective of the PowerWorld OPF is to find a solution that minimizes the overall generation cost. This requirement is different from (8) and (15) for a MG. Thus, to use PowerWorld OPF, (8) and (15) must be converted into PowerWorld compatible formats.

For both the minimum operational cost policy (8) and the maximum overall profit policy (15), there is a difference between the curtail load y_j in (8), (9), (11) and (15) and the curtail load y_{pw_j} defined in PowerWorld. In general, y_j represents the amount of the load to be curtailed while y_{pw_j} represents the remaining load after the curtailment. Hence, considering y_{pw_j} has to be negative, then,

$$y_j = Y_j^{Max} + y_{pw\_j} \tag{18}$$

By applying (17) and (18) to (8), it is obtained

$$Cost = \sum_{i=1}^{N} DER\_bid(x_i) + AX + \sum_{j=1}^{M} \lambda_j A\left(Y_j^{Max} + y_{pw\_j}\right) \tag{19}$$

Since Y_j^{Max} is a constant number at a given bidding interval, removing the constant loads from the objective function (19) does not affect the optimal solution. Hence, the formulation for the Minimum Cost Policy is represented by

Minimize:

$$Cost = \sum_{i=1}^{N} DER\_bid(x_i) + AX + \sum_{j=1}^{M} \lambda_j A y_{pw\_j} \tag{20}$$

Subject to:

$$X + \sum_{i=1}^{N} x_i = Y_{fixed} - \sum_{j=1}^{M} y_{pw\_j} \tag{21}$$

$$X_i^{Min} \le x_i \le X_i^{Max} \tag{22}$$

$$-Y_j^{Max} \le y_{pw\_j} \le 0 \tag{23}$$

$$0 \le S_{mn}(h) \le S_{mn}^{Max} \tag{24}$$

where Y_{fixed} represents the total fixed demand. According to the above formulation, the optimal MG power dispatch problem becomes to minimize the overall generation cost of all the positive and negative generators. By this way, we can use PowerWorld OPF to solve the optimal power dispatch problem for a competitive MG market, in which a negative generator model is used to represent a curtail load.

For the Maximum Overall Profit Policy, considering the curtail load y_{pw_j} defined in PowerWorld and DER and USER bids of equations. (16) and (17), we can express (15) as

$$\text{Profit} = A\sum_{i=1}^{N} x_i - \sum_{i=1}^{N}\left(b_i x_i + c_i\right) - \sum_{j=1}^{M} \lambda_j A\left(Y_j^{Max} + y_{pw\_j}\right). \tag{21}$$

Also, maximizing the profit can be interpreted as minimizing the negative profit. Similarly, since Y_j^{Max} is a constant number at a given bidding interval, the objective function for the maximum overall profit policy can be represented by

Minimize:

$$\text{-Profit} = \sum_{i=1}^{N}\left[\left(b_i - A\right)x_i + c_i\right] + \sum_{j=1}^{M} \lambda_j A y_{pw\_j}. \tag{22}$$

By this way, the optimal power dispatch problem becomes to minimize the overall generation cost of all the positive and negative generators, in which the cost for the positive

generators (DERs) is $(b_i - A)x_i + c_i$ and the cost for the negative generators (curtail loads) is $\lambda_j A y_{pw\_j}$.

4.4.2 Optimal power dispatch in islanded mode

In the islanded mode, the MG is disconnected from the main grid. Hence, a DER within the MG network is specified as the slack bus generator. This DER unit should have a stronger power capacity than other DERs to support the operation of the MG. Different from the grid-tied mode, there is a power constraint for the slack bus generator and a cost function associated with the generator.

The objective function for the minimum cost policy is similar to Section IV-A except that the grid power X is zero. For the maximum profit policy, the MGCC revenue is calculated according to

$$\text{Revenue} = R \cdot \sum_{i=1}^{N} x_i \tag{23}$$

where *R* is a reference price that is formulated by considering the costs of all DERs. This is due to the fact that in the islanded mode, the MG is disconnected from the main grid so that it is improper to calculate the MGCC revenue by using the open market price. Therefore, the objective function for the maximum profit policy is a little bit different as shown by

Minimize:

$$\text{-Profit} = \sum_{i=1}^{N}\left[(b_i - R)x_i + c_i\right] + \sum_{j=1}^{M}\lambda_j A y_{pw\_j}. \tag{24}$$

4.4.3 Comparison and validation

We used Matlab optimization toolbox [23] for the validation. The validation is made for several simple MG networks. The procedure includes: 1) defining a MG optimization problem,

2) building the optimization problem using Matlab and the method presented in Section III, 3)building the optimization problem using PowerWorld and the method presented in Section IV, 4) running the simulation in PowerWorld and Matlab, and 5) comparing results. The comparison shows that the results generated by using Matlab and PowerWorld are very close for both the minimum cost and maximum profit policies, demonstrating the effectiveness of using PowerWorld to solve the optimal power dispatch problem for a MG market.

4.5 Optimal Power Dispatch Study in Grid-Tied Mode

This section presents an optimal power dispatch study for a typical benchmark MG network by using PowerWorld (Figure 4.3). The synchronous machine connected to bus 1 signifies the grid. Bus 2 stands for the LV bus of the transformer. The network consists of three feeders with the first feeder supplying residential loads, the second feeder supplying an industrial load, and the third feeder supplying commercial loads [21]. The DERs are located in the first feeder domain, which forms a microgrid by itself. The MG is supplied through the LV feeder to serve a suburban residential area with a limited number of consumers connected along its length and consists of DERs from all currently important technologies, such as solar photovoltaic, micro turbines, wind turbines and fuel cells. No DERs are connected to the second and third feeders. However, inclusion of the two feeders would benefit more extended system study. Of the two feeders, one is a dedicated underground cable line, serving a workshop, whereas the other one is an overhead line serving a small commercial district. The DERs are connected to the following buses: solar on buses 6 and 7, wind on bus 6, micro turbine on bus 5, fuel cell on bus 8 and battery on bus 4.

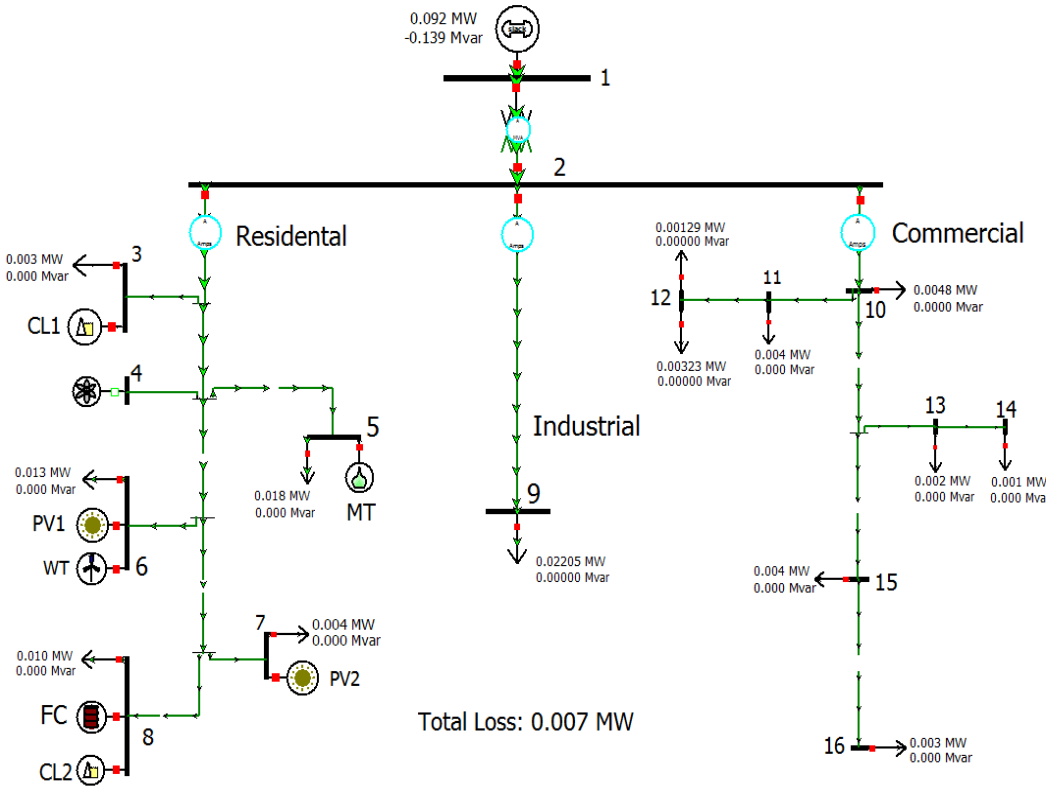

Figure 4.3 a benchmark LV network for microgrid study

The installed capacities of DERs and impedance data for various line types used in the network are given in [24, 25]. Daily load curves for the three load types of the benchmark network are shown in Figure 4.4. It is assumed that each residential load on the first feeder has the similar load pattern and the same condition is applicable to each commercial load on the third feeder. The power factor is 0.85 lagging for residential and commercial consumers and 0.9 for the industrial ones. Two loads in the first feeder domain, CL_1 and CL_2, are curtailable loads. Without curtailment, load CL_2 is about twice larger than load CL_1.Thus, the benchmark network maintains important technical characteristics of real life utility distribution systems, while dispensing with the complexity of actual MG networks, to permit efficient modeling and simulation study of the MG operation.

The maximum power captured by wind and solar generators are shown by Figure 4.4. Note that this paper only considers long-term variability impact of solar and wind to MGCC management and planning. In other words, it is assumed that the short-term variability is handled by using energy storage, such as battery and supercapcitor, with proper control at local DER level, and the MGCC only handles the long-term variability of the power delivered from an integrated DER and energy storage system.

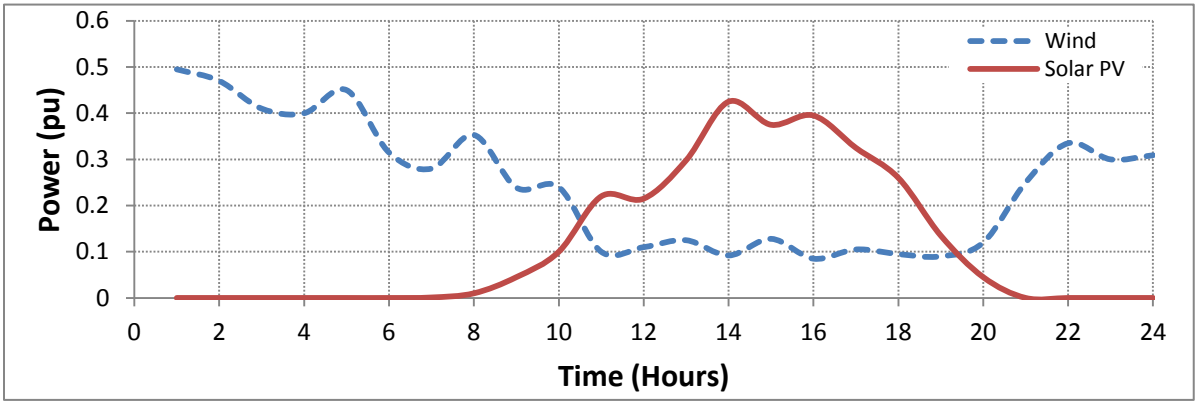

Figure 4.4 Daily power generation from wind and solar

To investigate the behavior of the MG network under variable load and variable generation conditions, Time Step Simulation function of PowerWorld is utilized. The load and generation profiles are first created by using other software tools and then loaded into PowerWorld. These include maximum DER generation and maximum amount of loads that can be curtailed. For wind and solar, the power generation limit at any time interval is the average maximum power captured by each unit in that time period. The battery does not participate in the bidding competition; it charges during night time and discharges during grid peak price interval. For all DER inverters, the dc-link voltage is 700V, the reactance of the grid filter is 2mH, and the rated power of the inverter is twice of the rated active power production of each DER unit. The grid real-time price is shown by Figure 6. The b_i and c_i values are ¢6.83/kWh and \$0/h for wind,

¢7.61/kWh and $0/h for solar PV1 and PV2, ¢3.6/kWh and $3.26/h for fuel cell, and ¢5.58/kWh and $1.08/h for micro turbine [13].Selection of b_i and c_i values for solar and wind has considered some power purchase agreement features[26].For example, the solar owner or developer should sell power to the MGCC at a rate that in average is lower than the open market price. This lower electricity price serves to offset the MGCC's purchase of electricity from the grid while the developer receives the income from the sales of electricity as well as any tax credits and other incentives generated from the system.

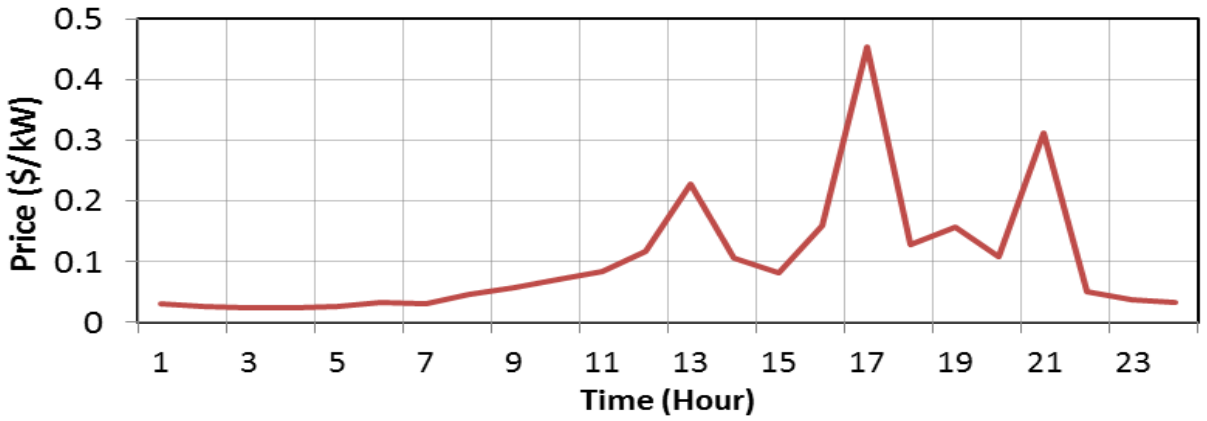

Figure 4.5 Grid electricity price during a day

4.5.1 Minimum operational cost policy

Figure 4.6 and 4.7 show the grid and DER powers for a case study based on the minimum cost policy by using AC OPF, in which it is assumed that all DERs use PQ-inverters with a unity power factor. According to Figure 4.6 and 4.7, solar and wind only produces a small amount of power due to its low rating. The fuel cell is cheaper than the micro turbine. Hence, when the grid price is high, it is the first to generate full power while the micro turbine starts to generate full power at a higher grid price. Both the fuel cell and micro turbine have minimum power generation constraints so that both produce a small amount of power during the night although the price is low during that time period. The price to curtail load CL_1at Bus 3 is more expensive

than DER bids and grid price while the price to curtail load CL_2at Bus 8 is cheaper than DER bids and grid price. As a result, load CL_2 is completely shed while CL_1 is not curtailed. This is consistent with (8). For example, curtailment of CL_2increases the cost by the last term in (8) but reduces the grid cost by the second term in (8). Since the cost to curtail CL_2 is cheaper than the grid cost, completely shedding of CL_2would minimize the overall cost.

4.5.2 Maximum overall profit policy

For the same MG condition, the result obtained by using the maximum profit policy (Figure 4.9) is a little bit different. The primary difference is the curtail loads. For the maximum profit policy, the remaining loads for both CL_1 and CL_2 are the same as the two loads without any curtailment, implying that there is no load shedding with the maximum profit policy. This indicates that the load shedding is not encouraged for this policy. This is consistent with (15) because for any load shedding the last term in (15) always has a negative contribution to the overall profit.

4.5.3 Normal power flow

For normal power flow without using economic dispatch, the active power output of solar photovoltaic sand wind turbine is variable depending on the weather conditions. It is assumed that both wind and solar operate in maximum power extraction mode. Therefore, the active power of wind turbine and solar photovoltaic represents the average maximum power captured from the wind or the Sun in every bidding period and is not affected by the power flow study.

For the micro turbine and fuel cell, it is assumed that there are sufficient resources for both DERs to participate in the automatic generation control of the network. Hence, the maximum active power of the DERs is the capacity specified by Max MW in PowerWorld while

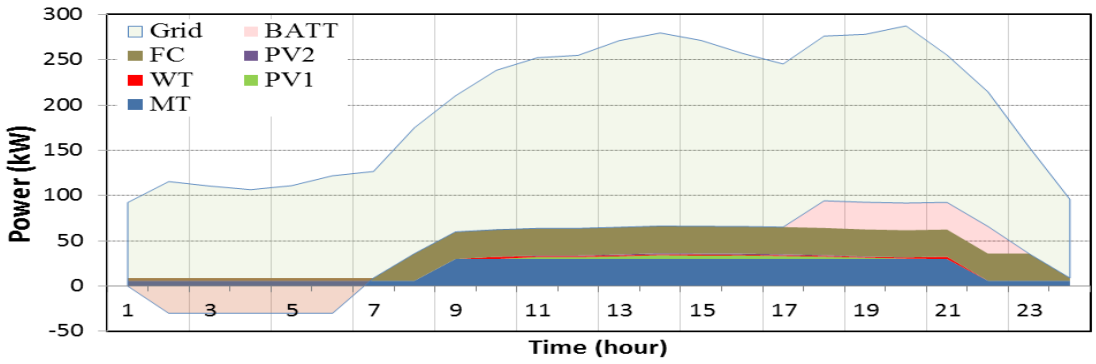

Figure 4.6 Grid and DER power

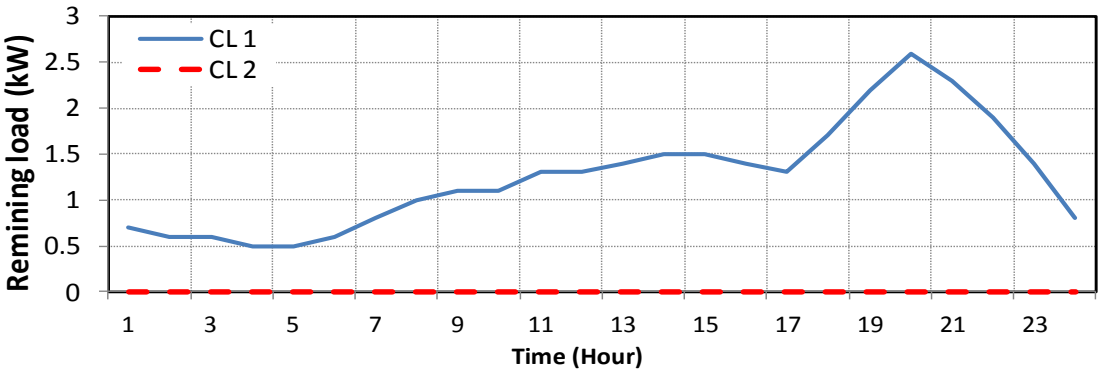

Figure 4.7 Remaining load after curtailment

the actual active power is determined by the power flow computation. The reactive power of all the DERs depends on PV or PQ operating mode of a DER inverter and is constrained by the rated power and PWM saturation limit of the DER inverter. The reactive power constraints are specified by Max Mvars and Min Mvars in PowerWorld and are calculated according to Section 4.3.4.

Table 4.1 compares results obtained by using minimum cost policy (Min Cost), maximum profit policy (Max Profit) and normal power flow without the market bidding competition (Power Flow). As it can be seen, in terms of both overall cost and profit of the MG

network, the normal power flow has the lowest advantage among the three strategies. The difference between the minimum cost and maximum profit policies is shown by the table too.

	Min cost		Max Profit		Power Flow	
	DC	AC	DC	AC	DC	AC
Cost ($)	574.94	576.55	577.83	579.05	609.74	624.11
Profit ($)	183.81	182.63	188.33	186.77	160.56	160.38

Table 4.1 Comparison of MG cost and profit for different policies

Figure 4.10 to 4.14 compare the voltage of buses 4, 5 and 8, power losses, and power supplied by the grid to the benchmark network for the following four scenarios: i) minimum cost policy, ii) maximum profit policy, iii) normal power flow without any market policy, and iv) normal power flow without any DERs. All DER converters are in PQ control mode with zero reactive power. From the figure as well as other results, the following remarks are obtained.

1) Among the four scenarios, the grid supplies the most power for scenario 4. Both minimum cost and maximum profit policies require more power from the grid than the normal power flow (Figure 4.14). In other words, without the economic dispatch consideration, DERs generate more power and cause less loss in the MG network (Figure 4.15). The loss reduction is particularly evident at the peak load period.

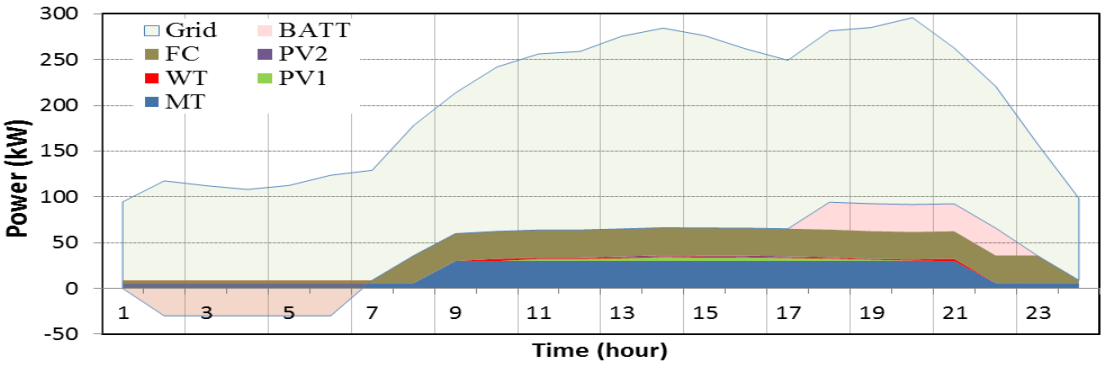

Figure 4.8 Grid and DER power

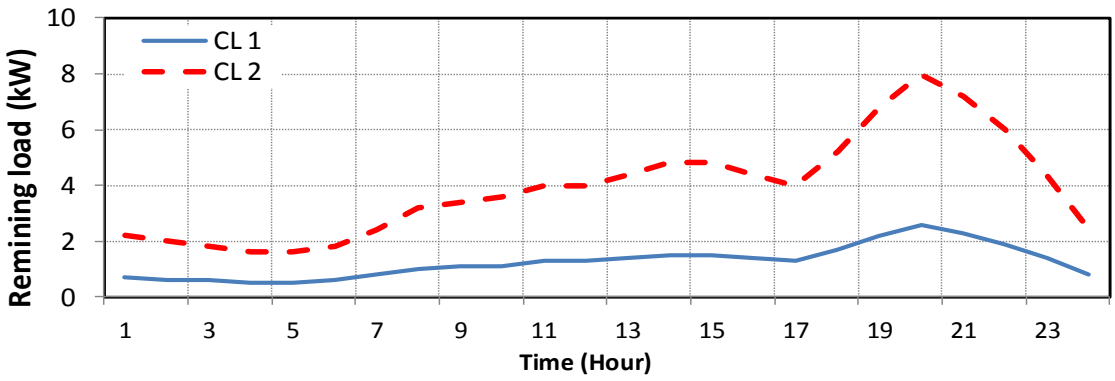

Figure 4.9 Remaining load after curtailment

2) There is some voltage improvement for all the buses along the residential feeder for the first three scenarios (Figures. 4.10-4.12). But, no bus voltage enhancement is found along the industrial and commercial feeders, showing that the voltage boast contributed by DERs is mainly limited to the buses within the MG network. The voltage boost is more evident if a DER is connected to the bus and supplies power into the MG network. For example, Bus #5 has more voltage boost than other buses because the microturbine connected to that bus generates more power than other DERs.

3) The battery reduces grid power during discharge mode (Figure 4.14). Similarly, the voltage boost is more evident at the bus which connects the battery (Figure 4.11). During the charge mode, the battery absorbs power and the bus voltage drops (Figures 4.11-4.14).

Figures 4.16-4.20 show the voltage of buses 4, 5 and 8, power losses, and power supplied by the grid to the benchmark network under the same scenarios when DER converters operate in the PV mode. The reference bus voltage is 1pu. However, the reactive power required to maintain the desired bus voltage at each DER cannot exceed the maximum allowable reactive power of the DER as presented in Section II-E. From the figure as well as other results, the following regularities are obtained.

1) In the PV inverter mode, the MG network voltage is improved. If no active power is generated by a DER, the bus voltage boost is achieved through reactive power production of GSCs. If a DER produces active power, additional bus voltage boost can be achieved. The bus voltage improvement reduces load current and hence the loss of the distribution network (Figure 4.20).

2) The ability of the bus voltage boost also depends on the rated power and converter PWM saturation constraint. As a result, desired bus voltage of 1pu may not be able to obtain, especially at peak load conditions.

3) Although the bus voltage boost reduces losses of the MG network, it is possible that the PV-controlled DERs may absorb reactive power from the grid under a light load condition, which results in more losses (Figure 4.20).

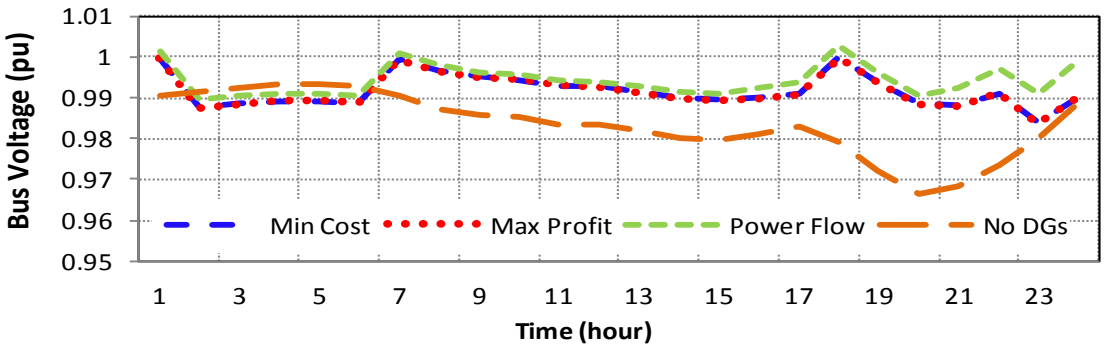

Figure 4.10 Per unit voltage of Bus #4

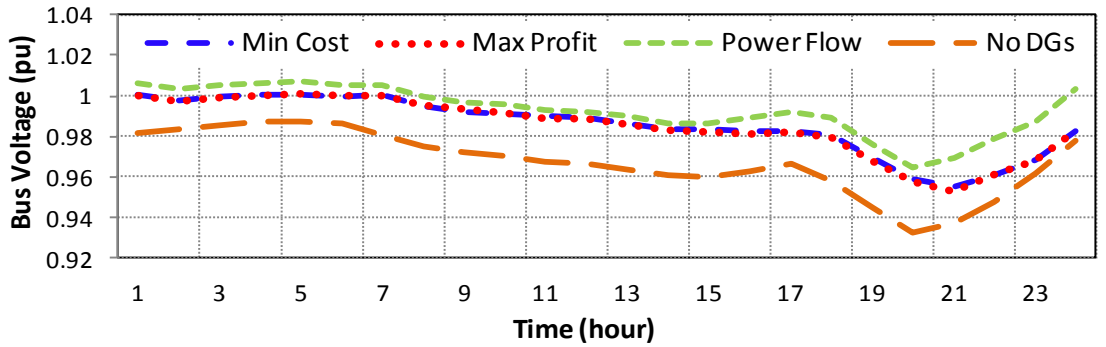

Figure 4.11 Per unit voltage of Bus #5

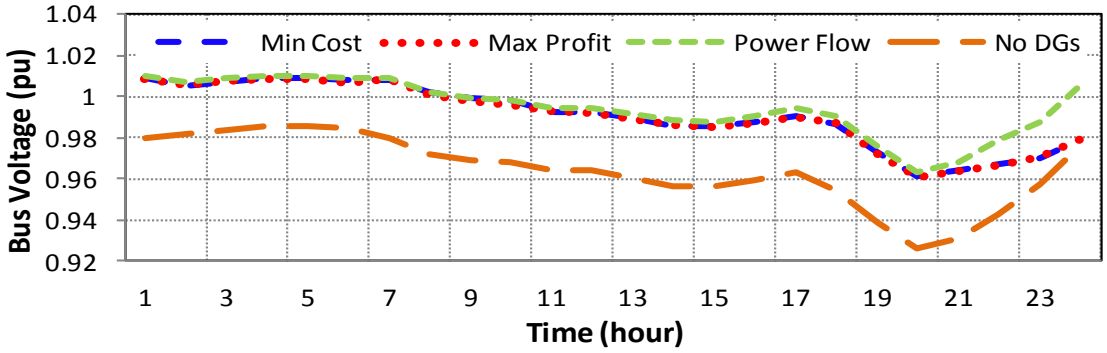

Figure 4.12 Per unit voltage of Bus #8

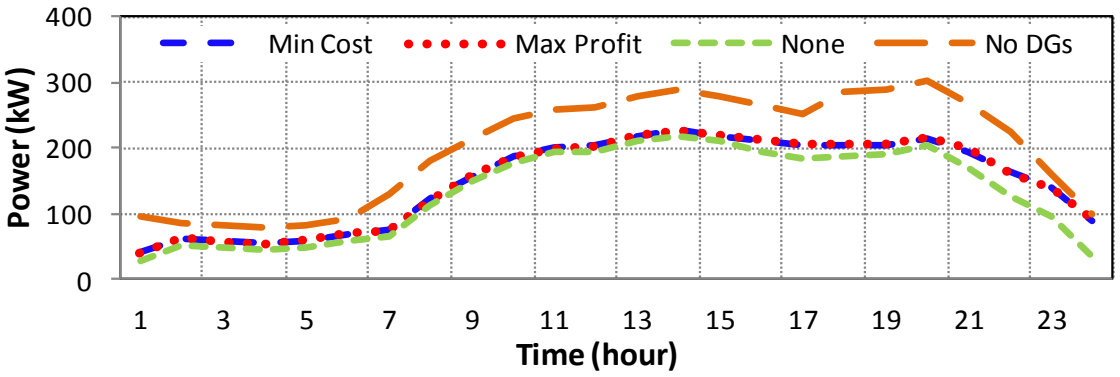

Figure 4.13 Grid power supplied to the network

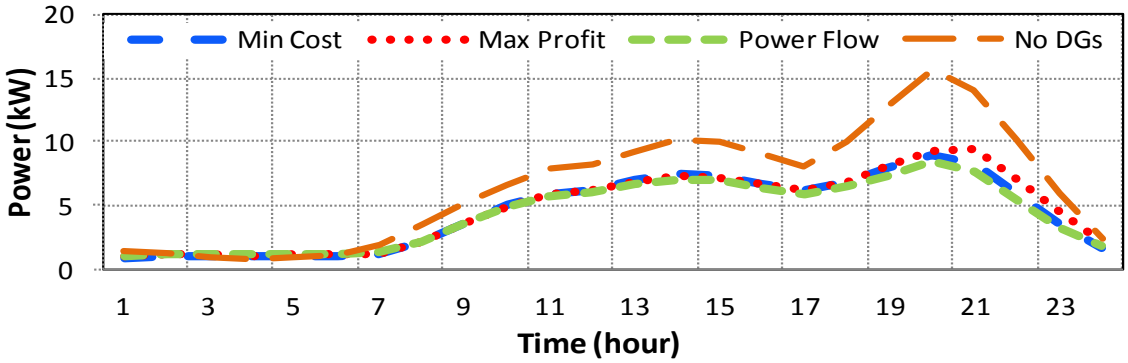

Figure 4.14 Losses of the network

4.6 Optimal Power Dispatch Study in Islanded Mode

In the islanded mode, the micro turbine is selected as the slack bus generator due to its stable and larger power availability compared other DERs. It is assumed that the islanding operation of the MG network is for short-term emergency condition only so that the battery operates only in discharge mode from 6pm and 10pm with the rated output power. Different from the grid-tied mode, all the loads except one critical load at Bus 5are set as curtail loads. The load pattern before the curtailment is the same as the residential load pattern shown in Figure 4.4. In the islanded mode, voltage control of the MG network is critical. Hence, only PV mode of DER inverters is considered in the following study.

Figures 4.20 and 4.22 show power provided by DERs and load curtailment in the islanded mode based on the minimum cost and maximum profit policies, in which DER cost functions are the same as those used in the grid-tied mode. Compared to the grid-tied mode, more power has to be generated by DERs especially during the peak load period. Even so, there may be insufficient power to supply all the loads. Thus, load curtailment is necessary.

For the minimum cost policy, loads at Buses 3 and 8 are completely curtailed because the price to curtail these loads is cheaper than the reference price *R*, and loads at Buses 6 and 7 are partially curtailed at the peak load period depending on the price to curtail each load.

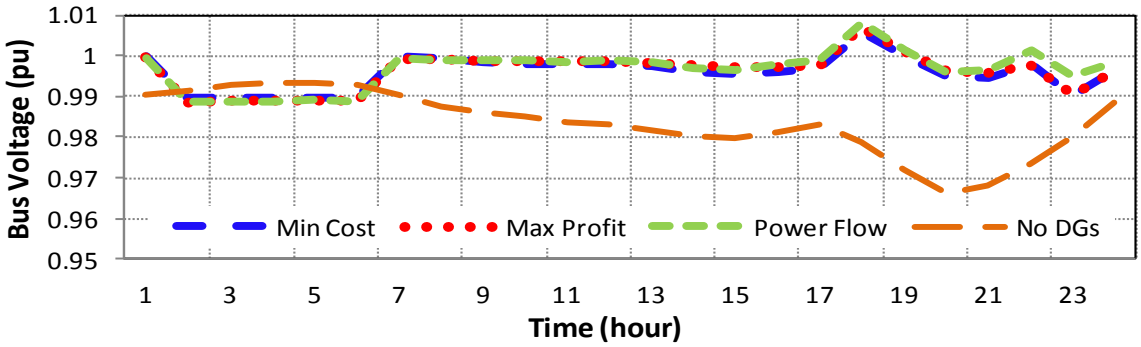

Figure 4.15 Per unit voltage of Bus #4

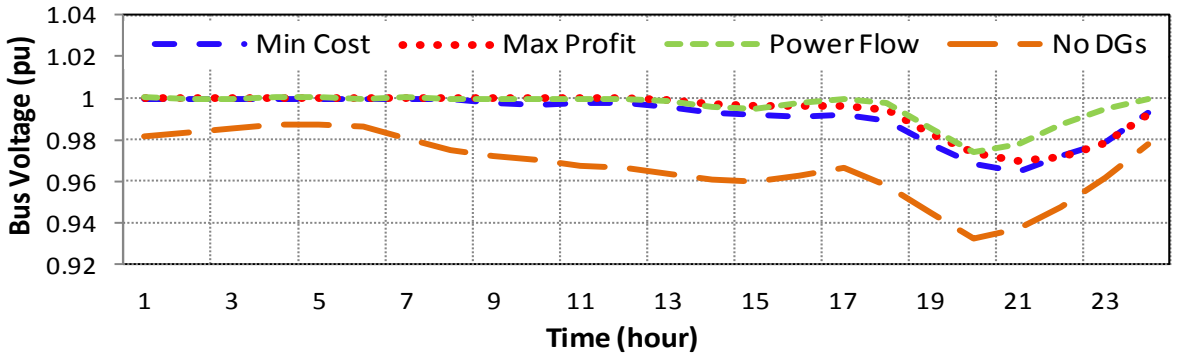

Figure 4.16 Per unit voltage of Bus #5

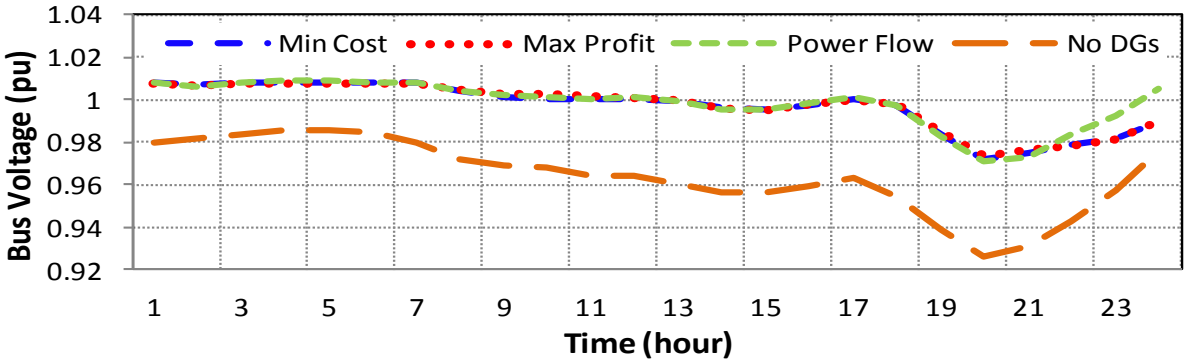

Figure 4.17 Per unit voltage of Bus #8

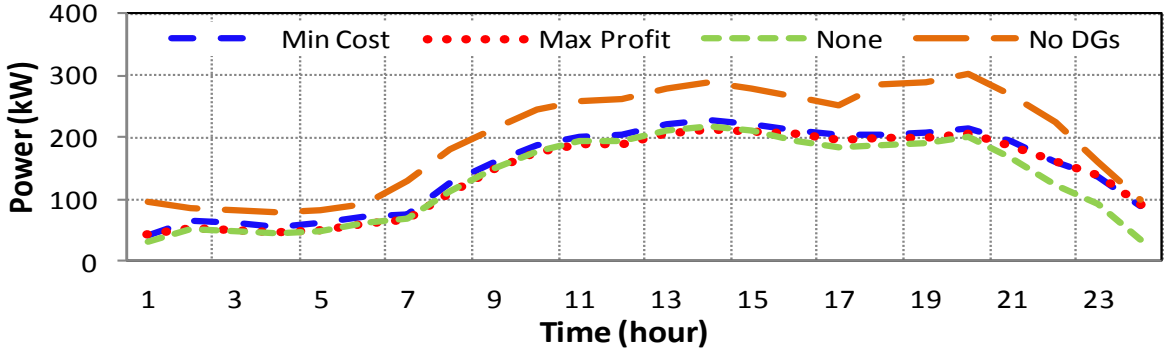

Figure 4.18 Grid power supplied to the network

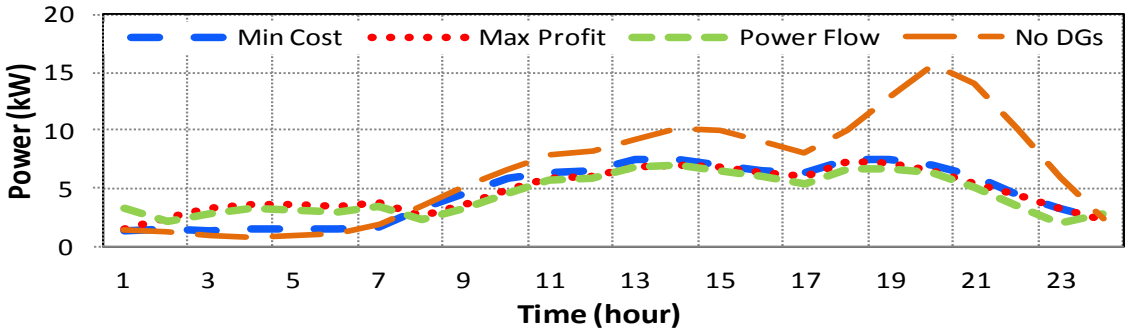

Figure 4.19 Losses of the network

For the maximum profit policy, the load curtailment reduces the profit gain according to Section 4.4.2. Similar to the grid-tied mode, the load curtailment is not encouraged if there is sufficient DER power to supply the loads. Hence, no load is curtailed during the light load period. However, during the peak period, load curtailment is required because of the limitation of available total DER power. The bus voltages can be maintained at adequate values after the curtailment as shown by Figures 4.25 and 4.26. Again, the voltage at a bus with a supplying DER power to the MG (Figure 4.26) is higher than the voltage at a load bus (Figure 4.25).

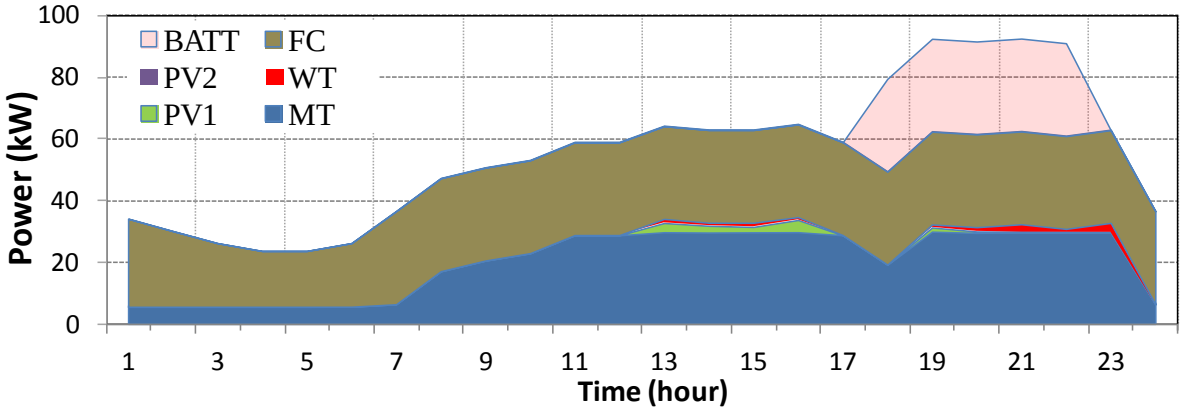

Figure 4.20 DER power under policy 1

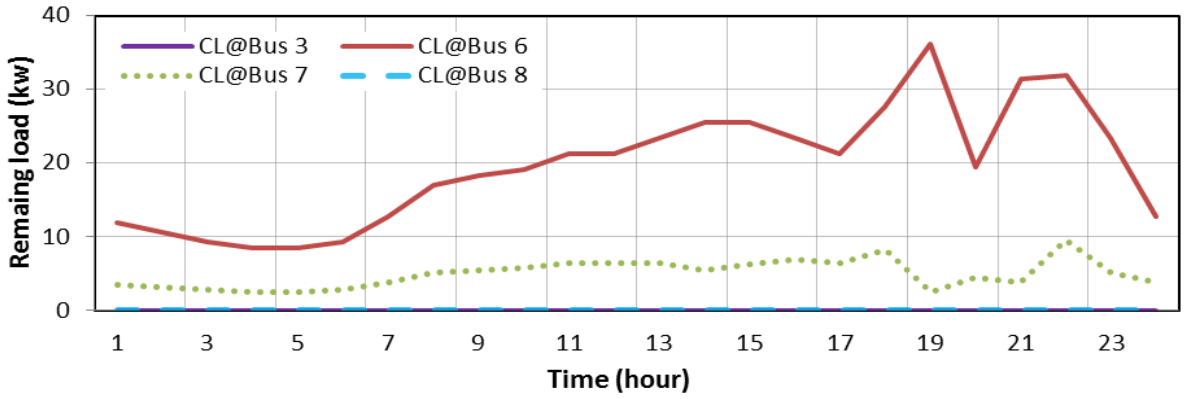

Figure 4.21 Remining load after curtailment under polciy 1

4.7 Conclusions

The optimal dispatch problem by using PowerWorld is validated through Matlab. Using the commercial power system software, the study for a competitive microgrid power market becomes a very easy task due to powerful analytical and visualization tools available in the software. In the grid-tied mode, the operation of the microgrid using the minimum cost or maximum profit policy has either the lowest cost or the highest profit compared to normal power flow solution. The difference is mainly caused by the shedding of curtail loads using the two

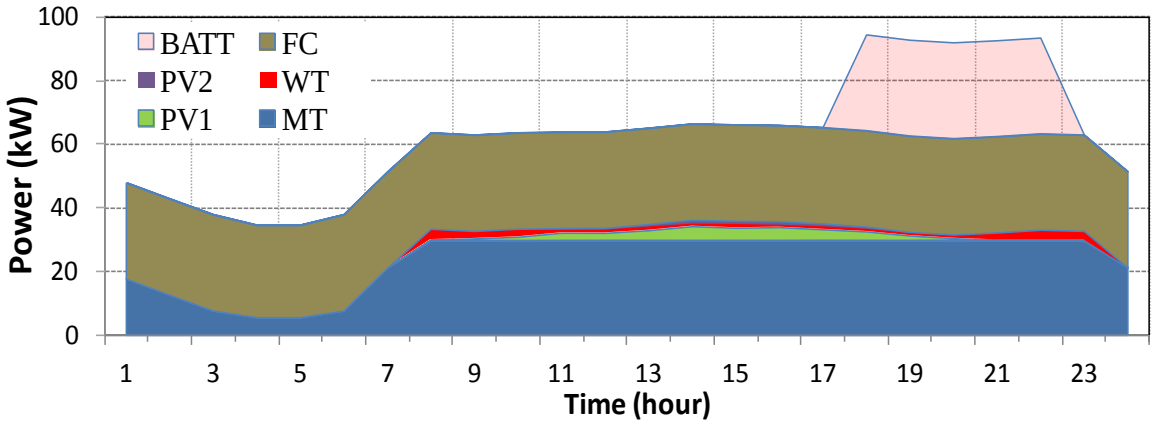

Figure 4.22 DER power under policy 2

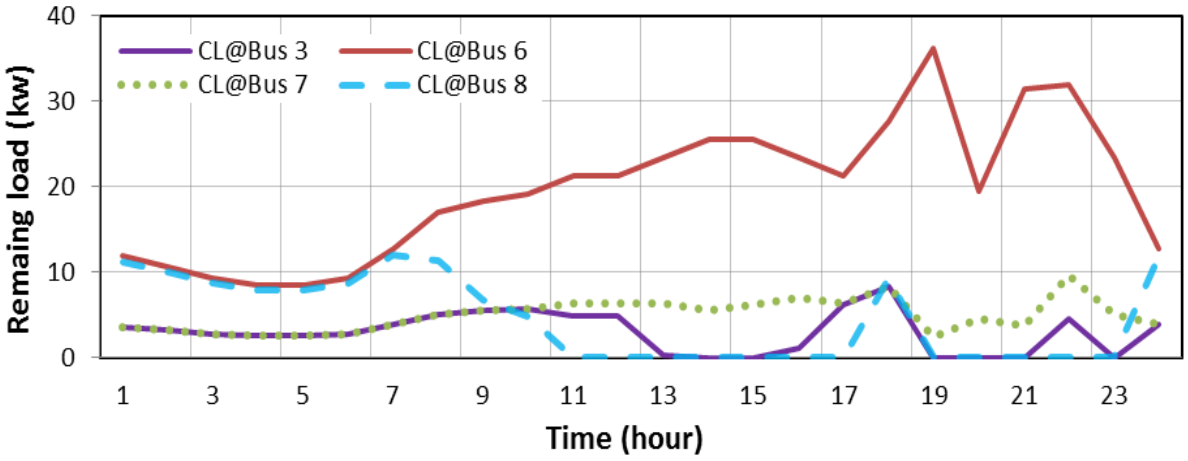

Figure 4.23 Remining load after curtailment under policy 2

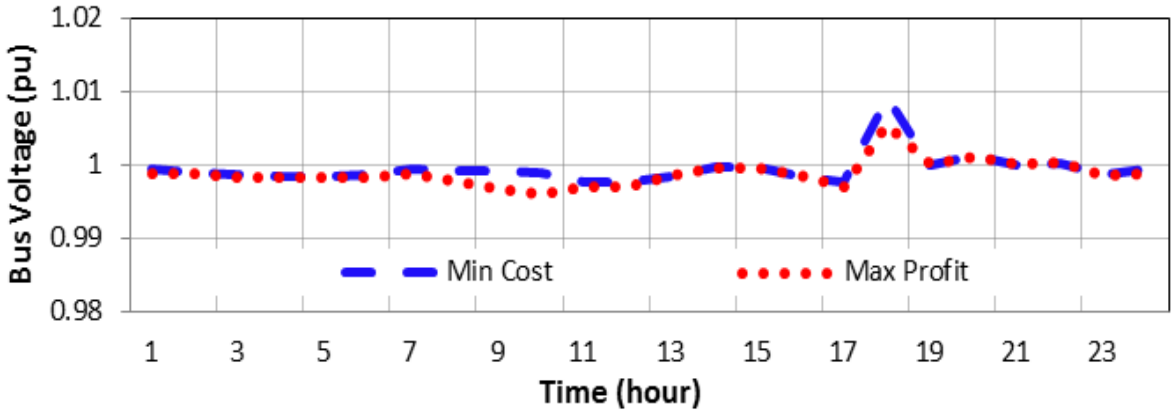

Figure 4.24 Per unit voltage of Bus #4

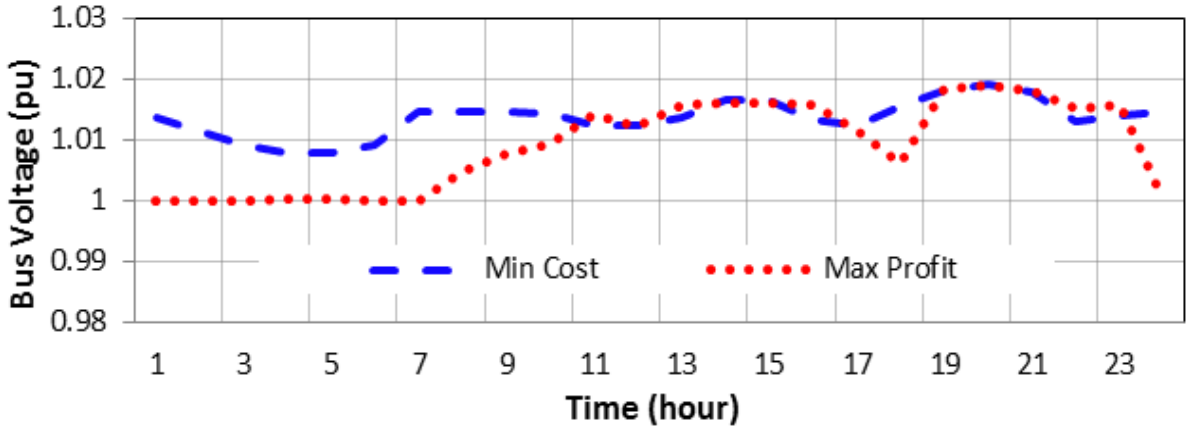

Figure 4.25 Per unit voltage of Bus #8

different policies. In terms of overall cost and profit of the microgrid network, the normal power flow has the lowest advantage among the three strategies. The microgrid network has better bus voltage and lower losses under PV inverter condition than PQ inverter condition. However, due to the rated power and converter PWM saturation constraints, the desired bus voltage may not be able to achieve especially at the peak load period.

In the islanded mode, the grid does not supply power to the microgrid so that large amount of load curtailment is necessary, and voltage control of the microgrid network becomes an important issue. The load curtailment depends on the market policies employed as well as the total available DER power of the microgrid. The bus voltages of the microgrid network can be maintained at adequate values after the load curtailment.

4.8 References

[1] H. Farhangi, "The Path of the Smart Grid," *IEEE Power & Energy Mag.*, Vol. 8, No. 1, January/February 2010.

[2] N. Hatziargyriou, H. Asano, R. Iravani, and C. Marnay, "Microgrids," IEEE Power and Energy Mag., Vol.5, No. 4, Jul/Aug 2007, pp.78-94.

[3] C. Schwaegerl, etc., "Advanced Architectures and Control Concepts for More Microgrids," *STREP project funded by the EC under 6FP, SES6-019864*, Dec. 30, 2009, Siemens AG, Germany.

[4] J.A. Peças Lopes, C.L. Moreira, and A.G. Madureira, "Defining Control Strategies for Microgrids Islanded Operation," *IEEE Trans. on Power Sys.*, Vol. 21, No. 2, May 2006, pp. 916-924.

[5] W. Yang, A. Xin, and G. Yang, "Micorgrid's operation-management containing distributed generation system," *IEEE Electric Utility Deregulation and Restructuring and Power Technologies (DRPT) Conf.*, July 6-9, 2011, Weihai, China.

[6] B. Kroposki, R. Lasseter, T. Ise, S. Morozumi, S. Papatlianassiou, N. Hatziargyriou, "Making Microgrids work," *IEEE Power and Energy Mag.*, Vol. 6, Issue 3, May-June 2008, pp. 40-53.

[7] H. Chen, J. Chen, D. Shi and X. Duan, "Power flow study and voltage stability analysis for distribution systems with distributed generation," 2006 *IEEE Power Engineering Society General Meeting*, June 18–22, 2006, Montreal, Canada.

[8] S.M. Moghaddas-Tafreshi and E. Mashhour, "Distributed generation modeling for power flow studies and a three-phase unbalanced power flow solution for radial distribution systems considering distributed generation," *Electric Power Sys. Research*, Vol. 79, Issue 4, April 2009, pp. 680-686

[9] Y. Zhu and K. Tomasovic, "Adaptive power flow method for distribution systems with dispersed generation," *IEEE Trans. on Power Del.,*17 (3) (2002), pp. 822–827.

[10] L. Tesfatsion, "ISS Panel and TF on Agent-Based Modeling of Smart-Grid Market Operations," *2012 IEEE Power & Energy Society General Meeting*, July 26, 2012, San Diego, CA.

[11] V. Romero,"Super Session 1: Opportunities and Challenges of Integrating Wind, Solar, and Other Distributed Generation and Energy Storage," *2012 IEEE Power & Energy Society General Meeting*, July 26, 2012, San Diego, CA, USA.4

[12] J. A. Peças Lopes, C. L. Moreira, and A. G. Madureira, "Defining Control Strategies for Microgrids Islanded Operation," *IEEE Trans. on Power Sys.*, Vol. 21, No. 2, May 2006, pp. 916-924.

[13] A.G. Tsikalakis and N.D. Hatziargyriou, "Centralized Control for Optimizing Microgrids Operation," *IEEE Trans. on Energy Convers.*, Vol. 23, No. 1, March 2008, pp. 241–248.

[14] E. Figueres, G. Garcera, J. Sandia, F. Gonzalez-Espin, and J.C. Rubio, "Sensitivity Study of the Dynamics of Three-Phase Photovoltaic Inverters With an LCL Grid Filter," *IEEE Trans. on Ind. Electron.*, Vol. 56, No. 3, March 2009, pp. 706-717.

[15] C. Wang, and M.H. Nehrir, "Short-Time Overloading Capability and Distributed Generation Applications of Solid Oxide Fuel Cells," *IEEE Trans. on Energy Convers.*, Vol. 22, No. 4, Nov. 2007, pp. 898-906.

[16] Z. Chen, J. M. Guerrero, and F. Blaabjerg, "A review of the state of the art of power electronics for wind turbines," *IEEE Trans. on Power Electron.*, vol. 24, no. 8, pp. 1859–1875, Aug. 2009.

[17] F. Pai and S. Huang, "Design and Operation of Power Converter for Microturbine Powered Distributed Generator with Capacity Expansion Capability," *IEEE Trans. on Energy Convers.*, Vol. 23, No. 1, March 2008, pp. 110–118.

[18] S. Li, T.A. Haskew, Y. Hong, and L. Xu, "Direct-Current Vector Control of Three-Phase

Grid-Connected Rectifier-Inverter," *Electric Power Sys. Research*, Vol. 81, Issue 2, February 2011, pp. 357-366.

[19] J. Rocabert, A. Luna, F. Blaabjerg, and P. Rodríguez, "Control of Power Converters in AC Microgrids," *IEEE Trans. on Power Electron.*, vol. 27, no.11, pp. 4734-4749, Nov. 2012.

[20] F. Katiraei, R. Iravani, N. Hatziargyriou, and A. Dimeas, "Microgrid Management," *IEEE Power and Energy Mag.*, Vol. 6, Issue 3, May-June 2008, pp. 54-65.

[21] A. Madureira, C. Moreira, and J.A.P. Lopes, "Secondary load-frequency control for Microgrids in islanded operation," *Proc. Int. Conf. Renewable Energy Power Quality*, Spain, 2005.

[22] PowerWorld, "PowerWorld Simulator Overview," available at http://www.PowerWorld.com/products/simulator/overview.

[23] Mathwork, "MATLAB Optimization Toolbox User's Guide," The MathWorks, Inc., Natick, MA, 2012.

[24] S. Papathanassiou, N.Hatziargyriou, and K. Strunz, "A Benchmark Low Voltage Microgrid Network", *Proc. CIGRE Symposium: Power Systems with Dispersed Generation*, April 2005, Athens, Greece.

[25] S. Li, J. Proano, and D. Zhang, "Microgrid power flow study in grid-connected and islanding modes under different converter control strategies," *2012 IEEE Power and Energy Society General Meeting*, July 22-26, 2012, San Diego, CA, USA.

[26] T.D. Bridenbaugh, "Request for proposals: Solar/Wind power purchase agreement," District of Columbia Department of General Service, May 8, 2013.

5 INTEGRATING HOME ENERGY SIMULATION AND DYNAMIC ELECTRICITY PRICE FOR DEMAND RESPONSE STUDY

5.1 Introduction

It is expected that the achievement of energy conservation can be significantly accelerated by integrating smart, energy-efficient appliances into a "smart" electricity grid [1]. In general, smart appliances will be no longer merely passive devices that drive energy productions but active participants in the electricity infrastructure for energy optimization for greater compatibility. A key requirement for the smart appliances within the smart grid framework is the demand response (DR). The North American Electric Reliability Corporation has defined demand response as [2, 3] "changes in electricity usage by end-use customers from their normal consumption patterns in response to changes in the price of electricity, or to incentive payments designed to induce lower electricity use at time of high wholesale market prices or when system reliability is jeopardized."

In general, DR includes all intentional modifications to consumption patterns of electricity of end-use customers that are intended to alter the timing of energy usage, level of instantaneous demand at critical times, or consumption patterns in response to market prices [4]. At the same time, DR is a component of smart energy management, which includes distributed renewable resources and electric vehicle charging. For example, a real-time central DR strategy is developed in [5] for primary frequency regulation to enhance renewable energy penetration within a microgrid; a distributed DR algorithm is developed in [6] with a special focus on charging management of plug-in hybrid electric vehicles.

Overall, there are two types of DR: controllable DR and price-responsive DR. In controllable DR, an end-use customer agrees to curtail under certain circumstances in response to dispatch by the load serving entity (LSE), aggregator, or the system operator [7]–[9], and the customer receives an explicit payment for curtailing load. In price-responsive DR, an end-use customer is exposed to time-varying (dynamic) rates and does not receive an explicit payment as a compensation for curtailing load [10]–[12], which is the focus of this paper.

For price-responsive DR, the technical literature includes a significant number of references dealing with the problem of a consumer sufficiently large to participate in the electricity markets to minimize its energy procurement costs [12]–[17]. For the time being, however, small residential consumers in the North America primarily engage in fixed-price contracts with a LSE or a utility company. The role of a LSE basically consists in purchasing energy from the electricity markets to resell it to their clients at a price as competitive as possible [18], [19]. Yet, with the development of smart grids, the interaction between a residential consumer and its LSE or utility company is expected to become more involved through the real-time pricing of electricity [20].

Nevertheless, great challenges in developing a price-responsive DR strategy for a residential consumer include how to accurately estimate the energy consumption of a house, and how to develop a DR algorithm in a dynamic price setting. In existing technologies, many DR techniques are developed based on the optimization principle by using simplified energy consumption models. In [21], Black proposed an optimal strategy to minimize the cost for electricity consumption, in which the energy consumption of a house is modeled based on simple conduction heat transfer equations. In [22], a simplified equivalent and thermal parameter (ETP) modeling approach is used in the GridLAB-D, a distribution system simulator, to estimate

thermal loads of a residential house based on first principles. In [23], a quasi-steady-state approach is adopted to estimate hourly building electricity demand, in which the building thermal model is built based on an equivalent resistance-capacitance network [24]. In [12], the hourly energy consumption is determined through an optimization strategy under the constraints of several predefined customer load levels which include maximum and minimum hourly demands, minimum daily consumption, and ramping up and down limits. In [25], a dynamic cost-minimizing method is proposed, in which the energy consumption of home appliances are divided into noninterruptible and interruptible tasks with each task requiring certain units of energy.

However, actual energy consumption of a residential house is much more complicated, which could be affected by the geographical location, design architectures, materials for insulations, arrangement of windows, occupants, etc. At present, one of the major difficulties that utilities are facing is the absence of emulating real world energy consumption capability of residential houses in a dynamic price framework that can allow them to develop, validate and qualify technologies, solutions, and applications for their DR programs [26].

This paper presents a mechanism to develop and evaluate a price-responsive DR strategy through a computational experiment approach. The novelties and contributions of the paper include:

- A mechanism to obtain energy consumption of a residential house by using professional building simulation software. Through this method, one can 'build' a simulated house that is equivalent to a practical one. The simulation uses standard commercial building materials defined in the software library and real-life weather data available at [27].

- An approach of using regression technique to model home energy consumption based on the energy consumption obtained from the home energy simulation software. Therefore, it is possible to model the energy consumption of a residential house more accurately for complicated energy usage and weather conditions.
- A method to develop optimal DR algorithms based on the regressed household energy consumption model and conventional optimization and particle swam techniques.
- An integrative computing platform that combines the home energy simulator and Matlab together for DR development and evaluation.
- A detailed comparison study focusing on characteristics and advantages and disadvantages of different DR policies for both real-time and day-ahead binding customers.

In the sections that follow, the paper first presents, in Section II, heat transfer issues and how to use a home energy simulator to obtain energy consumption of a residential house. Section III gives a computational experiment system that combines home energy simulation and dynamic electricity prices for DR evaluation. Section 5.4 illustrates how to use the computational experiment strategy to develop different DR policies based on optimization approach, particle swarm method, and a heuristic algorithm. The performance of different DR policies is evaluated in Section V. Finally, the paper concludes with the summary of the main points.

5.2 Home Energy Consumption Simulation

5.2.1 Heat Transfer of a Residential House

In modeling energy consumption of a residential house, the amount of energy consumed by the heating, ventilation, and air conditioning system (HVAC) is the most dominant part and is

related to heat transfer. The heat load that a HVAC must overcome is mainly generated in three ways: conduction, convection, and radiation (Figure 1) [28-30].

For a residential house, conduction heat transfer results from internal and ambient temperature differences, such as the conduction through exterior walls and the roof (Figure 5.1). Convective heat transfer occurs as wind blows over exterior walls, windows, and the roof and also through velocity induced by temperature differences between surfaces and the fluid [28, 29]. Both convection forms are present in regards to internal heat loads too. Heat radiation may include heat produced by internal loads, such as refrigeration, appliances, and people. Heat gain (and loss) also occurs through the introduction of outdoor air. Hence, for a practical house, computation of the heat loads in terms of the three heat transfer modes is very complicated. In addition, to accurately capture changes in temperature and solar loading throughout a day, calculations must be repeated hour by hour using practical weather and solar load data.

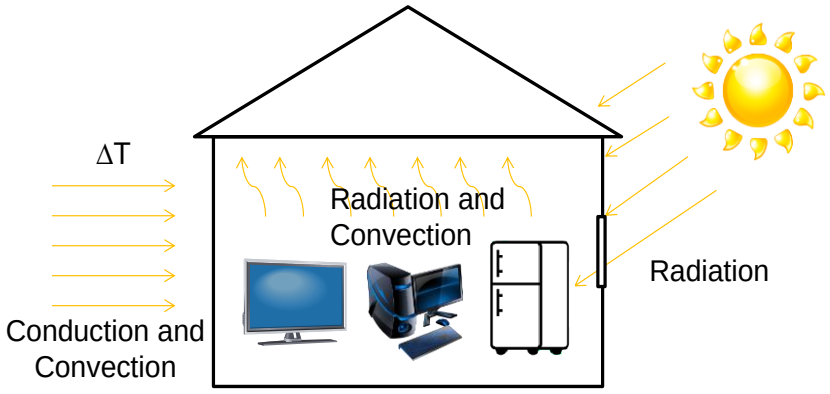

Figure 5.1 HVAC Heat Load Sources

5.2.2 Home Energy Consumption Simulation

In most conventional DR studies [21-24,31], the heat loads of a residential house is primarily computed based on 1) approximate heat transfer equations, 2) an equivalent rectangle

configuration for a residential house, and 3) a house model without detailed consideration of doors, windows, building materials and internal heat loads.

This paper uses building simulation software eQUEST as a virtual test bed to determine home energy consumption. The software is an up-to-date, unbiased simulation tool that predicts hourly energy use of a house over one year [32] given hourly weather information and a description of the house and its HVAC equipment [33]. It can use real-life weather and solar data for a specific geographic location [27]. Hence, one can estimate changes in the electrical load of a practical house throughout a year, certain days within the year, or certain time period of a day. The software is a steady-state simulation program having a large simulation time step, such as minutes, and does not consider short-term transient by assuming that a transition from one steady state to another can be achieved immediately. For home energy consumption simulation in minutes or hours, this is accurate and efficient.

For energy consumption simulation of a residential house, an architectural model of the house is created based on the blueprint and construction materials used to build the house. For the study in this paper, a generic floor plan for a two story, 2,500 square foot house is used. The exterior walls of the house are created by using standard 2 x 4 framing with R-13 batt insulation and a stucco finish. The roof is constructed by using standard built up roof construction. The roof is pitched at 25º and the attic has R-32 insulation. Doors and windows are added when appropriate. A garage is created, but is not air conditioned. Figure 2 shows the front view of the house. The location for the model is Springfield, IL.

The next step is to define internal loads. Two sources are used to define the internal loads. The first is a residential electricity survey conducted by the Department of Energy [34]. The survey shows the energy usage of a typical residential house by breaking down the energy

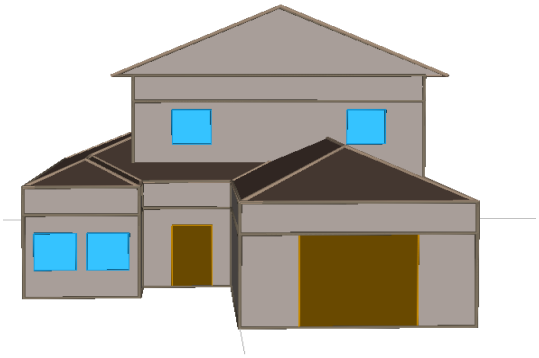

Figure 5.2 Building Model Facade using eQUEST

consumption of typical equipment such as washing machines, dryer, water heater, dishwasher, electric stove, refrigerator, microwave oven, lights for each room, occupants, etc. The second source shows the power draw of typical residential appliances [35]. After that, appropriate schedules are added to model these loads, such as when, how long, and how much of these loads are used each day.

The final step is creating the HVAC system. A heat pump is chosen to condition the house because of its relative efficiency [36]. In this paper, a three-ton unit is used to condition the first floor and a two-ton unit is used to condition the second floor. The energy efficiency ratio (EER) used for both units is 12. The supply fan flow rates are set to 2500ft^3/min and the outdoor air ratio (OAR) is set to 0.3 air changes per hour (ACPH). Details about how to build a simulated house can be found in [32].

5.3 Integrating Home Energy Simulation and Dynamic Price for demand Response Study

5.3.1 Dynamic Electricity Price

Electric utility companies typically use hourly real-time price (RTP) or day-ahead price (DAP) structure in their dynamic pricing programs. In North America, Ameren Focused Energy,

serving about 2.4 million electric customers in Illinois and Missouri, has very detailed RTP and DAP tariffs posted on their website since June 1, 2008 for both day-ahead and real-time markets [37]. The day-ahead market produces financially binding schedules for the production and consumption of electricity one day before the operating day. The real-time market reconciles any differences between the amounts of energy scheduled day-ahead and the real-time load, market participant re-offers, hourly self-schedules, self-curtailments and any changes in general, real-time system conditions. Figure 5.3 demonstrates Ameren's RTP and DAP in Summer 2011 for its residential customers as well as temperature associated with those days that the RTP or DAP prices occurred. The figure shows that: (1) a high price rate may occur at a moderate temperature day (Figures 5.4 and 5.5), (2) the electricity price of an extremely hot day does not mean a high electricity price day (Figures 5.6 and 5.7), and (3) real-time price fluctuates more than the day-ahead price.

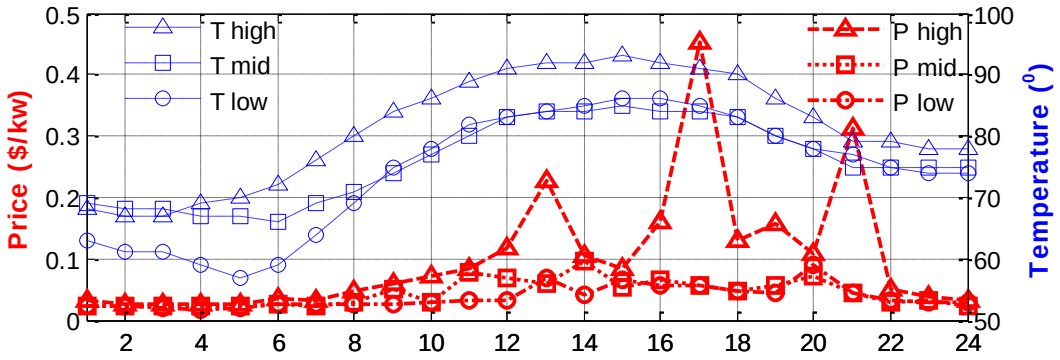

Figure 5.3 Real-time price for the highest, medium and low RTP days and corresponding temperature during those days

5.3.2 Integrated Computational Experiment System

The integrated computational experiment system consists of three parts: 1) home energy consumption simulation, 2) dynamic electricity price, and 3) demand response methods. The integrated system starts with a specification of home appliance usage strategy, which includes

thermostat setting of HVAC units and when to use dishwasher, dryer, electric stove, etc. Then, energy consumption of a residential house (Figure 5.1) is simulated for a practical weather pattern during a year or a day, including temperature, humidity, solar radiation, etc., at a location. The results generated by the home energy simulator are loaded into a MATLAB-based energy cost computation subsystem, based on which a new DR policy is generated. The updated DR policy is loaded into the home energy simulator and the process is repeated until an acceptable policy is reached. Figure 5.8 shows the flowchart of the computational experiment system.

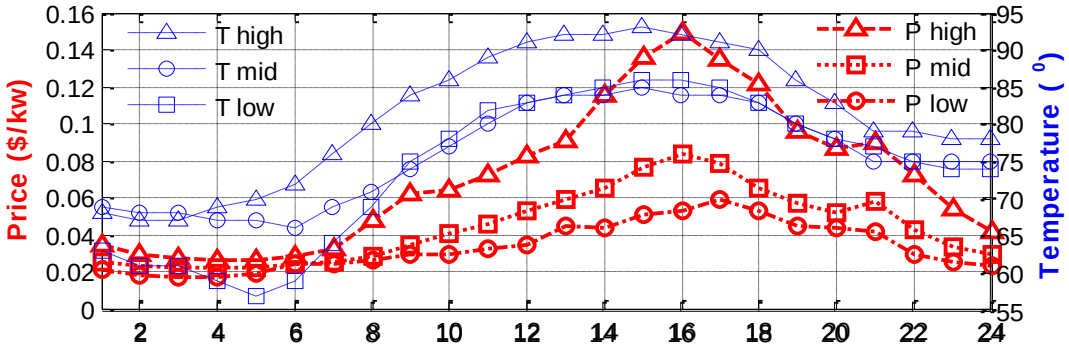

Figure 5.4 Day-ahead price for the highest, medium and low DAP days and corresponding temperature during those days

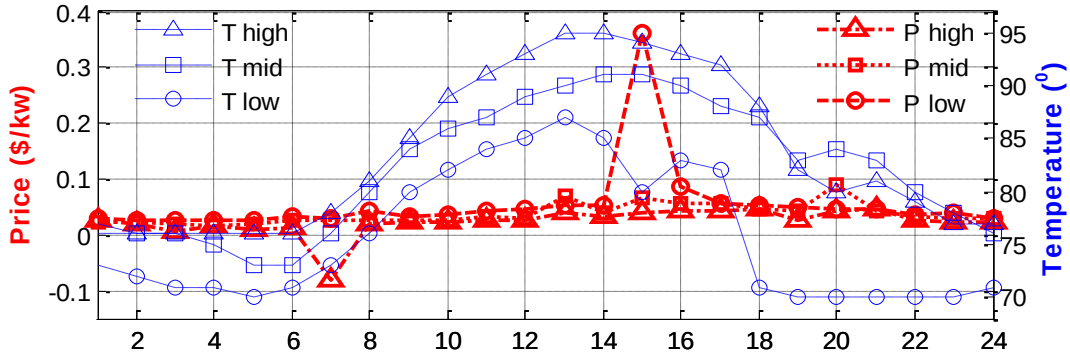

Figure 5.5 Real-time price for the hottest, medium and low temperature days and corresponding RTP during those days

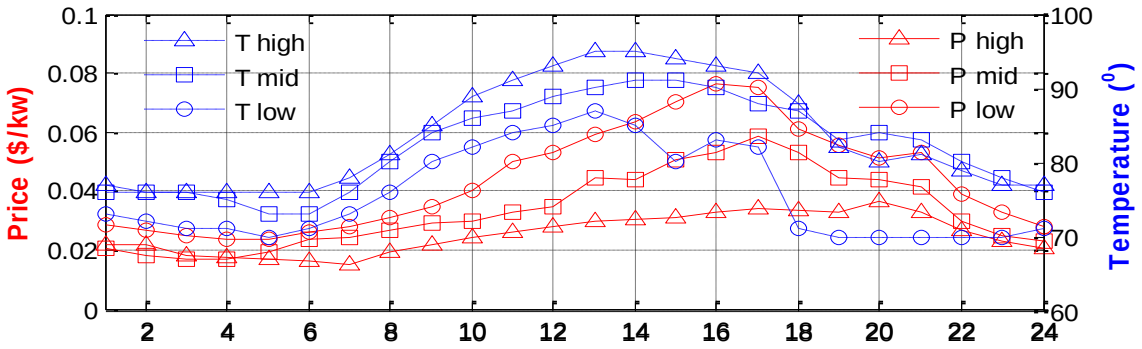

Figure 5.6 Real-time price for the hottest, medium and low temperature days and corresponding RTP during those days

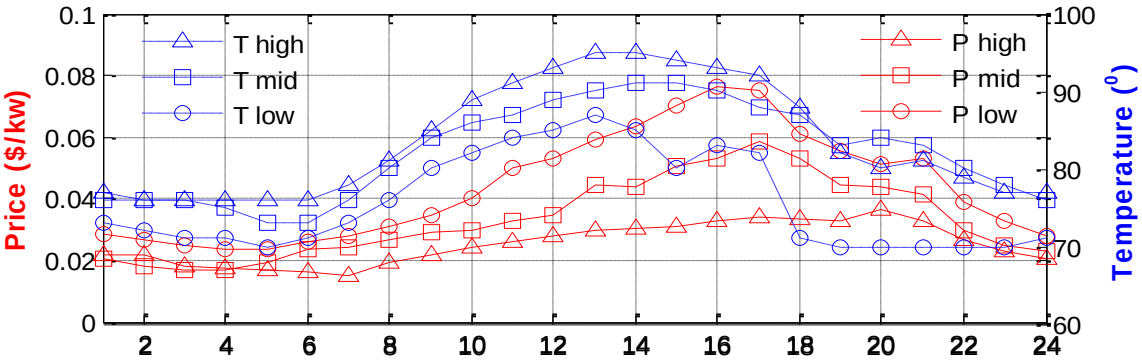

Figure 5.7 Day-ahead price for the hottest, medium and low temperature days and corresponding DAP during those days

5.4 Developing HVAC Demand Response Strategy

The development of a DR strategy is based on the energy usage natures of major home appliances, which are divided into two categories: 1) regulated energy usage allowable but delayed energy usage unacceptable and 2) delayed energy usage allowable. The first category may include HVAC and water heater. The second may contain dishwasher, dryers, and electric drive vehicles.

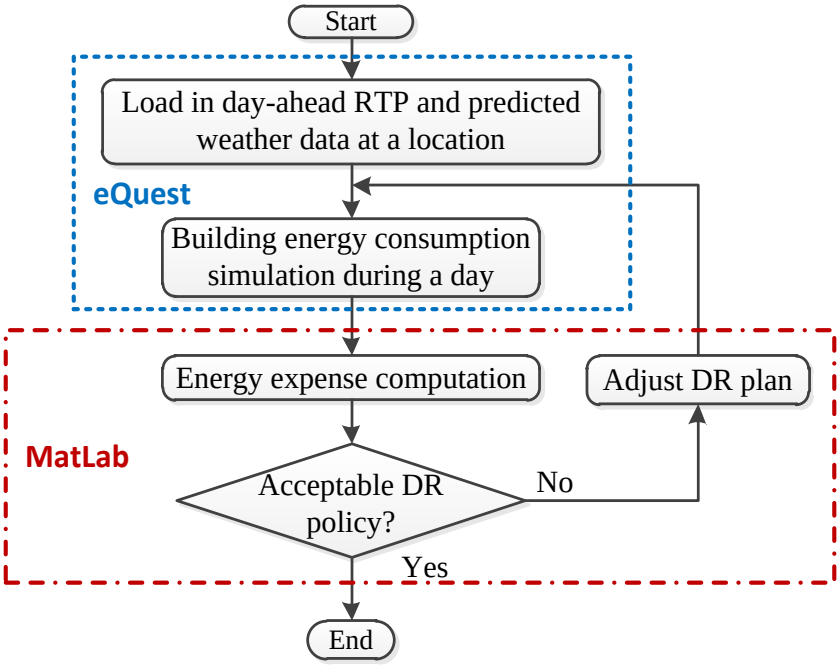

Figure 5.8 Integrative computational experiment system for DR study

For all the appliances, the most challenging one is a DR policy for a HVAC. Traditionally, the thermostat of a HVAC unit is set at 71° or 72° for a typical house in the United States. For a thermostat setting of 72°, for example, the HVAC unit normally starts to operate when the room temperature is 2° above the temperature setting and stops when the room temperature reaches 72°. Otherwise, the HVAC unit will constantly start and stop, which is not the way how a real-life HVAC operates. This operating condition is accurately programmed and simulated in the home energy simulator.

5.4.1 Optimal DR policy based on Simplified Model

To develop an optimal DR policy, a nonlinear programming formulation is needed as shown below,

Minimize:

$$C = \sum_i p_i \cdot Q_i \tag{1}$$

Subject to:

$$0 \le Q_i \le Q^{\max},\ T^{\min} \le T_i \le T^{\max} \tag{2}$$

where $T^{min} = T^{ideal} - d$, $T^{max} = T^{ideal} + d$,

d is the acceptable temperature deviation, i represents a time slot in one hour, T_i is the room temperature in hour i, C is the electricity cost during a day, p_i stands for the electricity price in hour i, Q_i signifies the energy consumed by the HVAC unit in hour i, and Q^{max} denotes the maximum energy that can be consumed by the HVAC unit. The energy consumed by the HVAC Q_i is modeled as a function of room temperature T_i and outside temperature T_i^o based on a simplified thermal model [21]

$$T_{i+1} = \varepsilon \cdot T_i + (1-\varepsilon)\left(T_i^o - \eta \cdot Q_i / A\right) \tag{3}$$

where η is the efficiency of the HVAC unit, ε is the system inertia, and A is the thermal conductivity. It is found that one problem associated with the simplified modeling approach is the difficulty to distinguish heating and cooling impacts to the energy cost and room temperature properly.

The solution of the DR during a day under a dynamic price tariff includes 1) the optimal operating room temperature T_i within T^{min} and T^{max} and 2) energy consumed by the HVAC unit Q_i, for i=1 to 24. It is necessary to point out that a real-life HVAC unit cannot operate at a given temperature as explained beforehand, which could affect the optimal DR policy developed by using the simplified model.

5.4.2 Optimal DR policy based on Regression Model

In reality, the relationship between indoor and outdoor temperatures and energy consumed by a HVAC unit is more complicated than Eq. (3). To overcome the challenge, this paper proposes a regression approach to model HVAC energy consumption based on the results

Algorithm 1: Regression Model based Optimal DR policy

1: $C \leftarrow 0$ {Clear HVAC energy cost}
2: Load an initial 24-hour thermostat setting T_i and obtain HVAC energy consumption Q_i (i=1, ..., 24) by solving the optimization problem in MATLAB.
3: **do**
4: $C_{buf} \leftarrow C$ {HVAC energy cost to buffer in MATLAB }
5: $C \leftarrow \sum_{i=1}^{24} p_i \cdot Q_i$ {Calculate new energy cost}
6: eQUEST $\Leftarrow T_i$ (i=1, ..., 24).
7: Obtain HVAC energy consumption Q_i (i=1, ..., 24) through simulation in eQUEST
8: MATLAB $\Leftarrow Q_i$ (i=1, ..., 24)
9: Polynomial regression approximation of HVAC energy consumption in MATLAB:
$$Q_i = q\left(T_{i+1}, T_i, T_i^o, \boldsymbol{\beta}\right) \quad i = 1, ..., 24$$
10: Solving the optimization problem based on HVAC energy model $Q_i = q\left(T_{i+1}, T_i, T_i^o, \boldsymbol{\beta}\right)$ in MATLAB
11: $T_i \leftarrow$ 24 hour thermostat setting obtained from line 10
$Q_i \leftarrow$ 24 hour HVAC energy consumption from line 10
12: **while** $\left|C_{buf} - C\right| > \varepsilon$

generated from the home energy simulator. Algorithm 1 presents the pseudo code that shows how a DR policy is developed by using the regressed HVAC modeling strategy and the computational experiment system. First, an initial optimal DR policy is generated (line 2) using a simplified energy consumption model (Eq. (3)). The DR policy is then loaded into the home energy simulator to obtain household energy consumption (lines 6 and 7), based on which more accurate energy model is built by using polynomial regression approximation (line 9). Then, a new optimal DR policy is obtained by using MATLAB Nonlinear Programming Toolbox (lines 10 and 11). The process is repeated until there is no significant error between two consecutive iterations.

Note that the initial energy cost is set to zero in line 1. Hence, for the first iteration, C_{buf} in line 4 is zero. The updated energy cost of the first iteration is calculated in line 5 based on the

energy consumption obtained from line 2. For the second iteration, C_{buf} in line 4 has the energy cost of the first iteration while the updated energy cost is calculated in line 5 based on the energy consumption obtained during the first iteration from line 11. The same rule follows for other iterations. It is necessary to point out that in reality, it is impossible to repeat the iteration several times. Even so, the proposed method builds an important foundation for the development of real-time DR strategies. This is one of our ongoing research activities in this area.

The polynomial linear regression model associated with the HVAC energy consumption is mathematically described by

$$Q_j = q\left(T_{j+1}, T_j, T_j^o, \boldsymbol{\beta}\right) \quad j = 1, ..., n \tag{2}$$

where $q(\bullet)$ is a 3rd order polynomial function of (T_{j+1}, T_j, T_j^o), n is the number of the observations obtained from the home energy simulator, Q_j is the jth HVAC energy consumption observation, (T_{j+1}, T_j, T_j^o) is the predictor variable vector consisting of indoor and outdoor temperatures related to observation Q_j, and $\boldsymbol{\beta}$=(β_1, β_1, …, β_p) is the parameter vector [38]. Compared to the simplified model Eq. (3), the regression model can provide more accurate estimation of HVAC energy consumption that is close to the "actual" simulated results, as shown by Figure 5.9. One cause of the difference between Eq. (3) and simulated energy consumption is the solar radiation that is not considered in Eq. (3). For example, to maintain room temperature at the set values between 10am and 14pm, no energy consumption is needed according to (3) but is required according to detailed home energy simulation.

5.4.3 Optimal DR policy based on Particle Swam

Conventional optimization technique depends strongly on the initial guess of a solution and is usually possible to get to a local optimal solution. Particle swarm optimization (PSO) is a

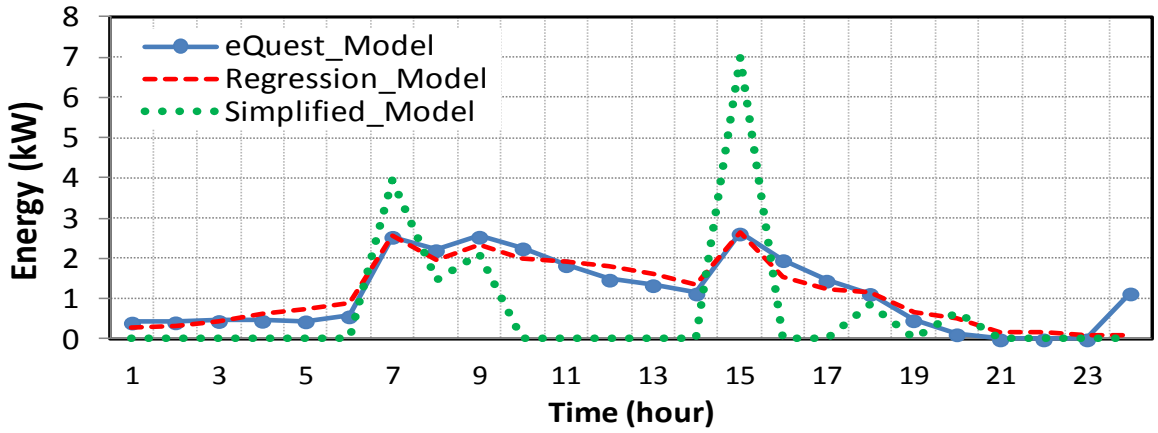

Figure 5.9 Comparison of HVAC energy consumption obtained from simulation, regression model and simplified model during a day

population based stochastic optimization technique developed by Drs. Eberhart and Kennedy in 1995 [39]. In PSO, each single solution is called a particle in the search space. All of particles have fitness values which are evaluated by the fitness function to be optimized, and have velocities which direct the flying of the particles. Each candidate solution can be thought of as a particle "flying" through the fitness space by updating the candidate velocity and position based on both global best fitness position and local best fitness position. By applying PSO to DR problems, it would help to identify potential difference among DR policies solved by using different optimization algorithms and determine whether there is a need to develop advanced optimization technique.

The algorithm to obtain a DR policy through the PSO is similar to Alg. 1, except that line 10 in Algorithm 1 is solved by using the PSO method. The pseudo code of the PSO is shown by Algorithm 2, which replaces line 10 in Alg. 1. In Algorithm 2, $\mathbf{T}(m)$, the position of a particle, represents a 24-hour thermostat setting during a day. $\tilde{\mathbf{T}}(m)$, the speed of a particle, represents the

thermostat adjustment during one iteration of the PSO algorithm. $\hat{\mathbf{T}}(m)$ and $\hat{\mathbf{T}}_G$ are the individual best thermostat setting associated with particle *m* and the global best thermostat setting of all the

Algorithm 2: PSO during the iteration of Alg. 1

1: Initialize particle position: $\mathbf{T}_{buf}(m) \in [T^{\min}, T^{\max}]$

2: Initialize particle speed: $\tilde{\mathbf{T}}_{buf}(m) \in [-\Delta T, \Delta T],\ m = 1,...,M$

3: {Calculate initial fitness values for all particles}
$\text{fitness}(m) = f\left(\mathbf{T}_{buf}(m)\right),\ m = 1,\cdots,M$

4: $\hat{\mathbf{T}}_G \leftarrow \mathbf{T}(k);\ if\ \text{fitness}(k) = \max\{\text{fitness}(m), m \in [1, M]\}$
$\hat{\mathbf{T}}(m) \leftarrow \mathbf{T}(m);$

5: **do**

6: {Update velocity for all particles}
$\tilde{\mathbf{T}}(m) = w\tilde{\mathbf{T}}_{buf}(m) + c_1 \cdot rand(0,1)\left[\hat{\mathbf{T}}(m) - \mathbf{T}_{buf}(m)\right]$
$+ c_2 \cdot rand(0,1)\left[\hat{\mathbf{T}}_G - \mathbf{T}_{buf}(m)\right]$

7: {Update position for all particles}
$\mathbf{T}(m) = \mathbf{T}_{buf}(m) + \tilde{\mathbf{T}}(m)$

8: *if* $\mathbf{T}(m)$ out of boundary $\rightarrow$ boundary handling $\mathbf{T}(m)$

9: {Calculate fitness values for all particles}
$\text{fitness}(m) = f\left(\mathbf{T}(m)\right),\ m = 1,\cdots,M$

10: $\hat{\mathbf{T}}_G \leftarrow \mathbf{T}(k);\ if\ \text{fitness}(k) = \max\{\text{fitness}(m), m \in [1, M]\}$
$\hat{\mathbf{T}}(m) \leftarrow \mathbf{T}(m);\ if\ \mathbf{T}(m) > \mathbf{T}_{buf}(m)$

11: $\mathbf{T}_{buf}(m) \leftarrow \mathbf{T}(m);\ \ \tilde{\mathbf{T}}_{buf}(m) \leftarrow \tilde{\mathbf{T}}(m)$

12: **while** maximum iterations or a stop criteria is not reached

particles, respectively. In line 6, c_1 and c_2 are the user defined coefficients, and *w* is the inertia weight used to balance global and local search. These parameters are determined through trial and error until a best possible result is obtained. For each updated particle position calculated in line 7, it is checked in line 8 whether the updated position is out of the boundary. If so, for any temperature setting beyond [T^{min}, T^{max}], it is reset to T^{min} or T^{max} depending on whether the temperature setting is smaller than T^{min} or larger than T^{max} [40]. The fitness function $f(\bullet)$is defined by

$$f(\mathbf{T}_{\mathrm{m}}) = \begin{cases} 1 \Big/ \left[\sum_{i=1}^{24} p_i \cdot \mathbf{Q}(m)_i \right], & Q^{\min} \le \mathbf{Q}(m)_i \le Q^{\max} \\ 0 & else \end{cases} \quad (3)$$

where $\mathbf{Q}(m)_i = q\left(T_{i+1}, T_i, T_i^o, \boldsymbol{\beta}\right)$ is the energy consumption of the HVAC for particle *m* at *i*th hour (*i*=1,…,24), and Q^{min} and Q^{max} stand for the minimum and maximum HVAC energy consumption corresponding to a practical HVAC unit.

5.4.4 Heuristic DR Policy

The heuristic DR strategy is a variable temperature setting approach developed by considering the utility RTPs. During the summer time, for instance, the air conditioner should be operated the coolest possible near the lower boundary, T_{lower}, of the ASHRAE summer comfort zone [41] when the RTP is lower than a predefined value. On the other hand, the HVAC should be operated the hottest possible near the upper boundary, T_{upper}, of the ASHRAE summer comfort zone. The HVAC should be operated between these two boundaries depending on the RTP tariff. One issue of the heuristic DR policy is that the algorithm is unable to take the advantage of low price periods to pre-cool down a house significantly.

The simplest heuristic thermostat setting strategy is a fixed lookup table approach [42]. For example, if the price is more than \$0.30/kWh, set the thermostat at 79°; if the price is between \$0.30/kWh and \$0.15/kWh, set the thermostat at 75°; if the price is lower than \$0.15/kWh, set the thermostat at 71°. However, it is found that this fixed DR strategy is unable to meet DR needs for diverse RTP distributions at different days. For instance, a fixed DR mechanism suitable for a highest RTP day is ineffective for a moderate RTP day.

Algorithm 3 shows a more efficient heuristic DR strategy. Assuming there are *n* temperature settings between T^{max} and T^{min}, then, the price and thermostat settings for summer time are calculated by (4) and (5). The basic concept is that the thermostat setting is determined

through a combined consideration of maximum and minimum day-ahead or real-time price, and price distribution over a day. In (4), k is a constant obtained from price distribution study for different seasons, and $PR_{diff}=PR^{max}-PR^{min}$, where PR^{max} and PR^{min} correspond to maximum and minimum electricity prices of RTP or DAP of a day. For winter time, a modification of Alg. 3 is necessary with T^{max} and T^{min} corresponding to PR^{min} and PR^{max}, respectively, and the price and thermostat settings are calculated by (4) and (6). Since PR^{max} and PR^{min} are usually not the same at different days, each day would have different thermostat settings in 24 hours.

$$PR_i = PR^{\max} - PR_{diff} \tanh\left(k \cdot i \cdot PR_{diff}\right) \tag{4}$$

$$T_i = T^{\max} - \left(T^{\max} - T^{\min}\right) \Big/ n \cdot i \tag{5}$$

$$T_i = T^{\max} + \left(T^{\max} - T^{\min}\right) \Big/ n \cdot i \tag{6}$$

Algorithm 3: Heuristic DR strategy during summer time

1: $PR^{max} \leftarrow$ Highest RTP during a day
2: $PR^{min} \leftarrow$ Lowest RTP during a day
3: **for** i = 1 to *24* **do**
4: Get real time price PR_{real} at ith hour.
5: **if** $PR_{real} \geq PR_{upper}$
6: Set thermostat at T^{max};
7: **else if** $PR_1 \leq PR_{real} < PR^{max}$
8: Set thermostat at T_1;
9: **else if** $PR_2 \leq PR_{real} < PR_1$
10: Set thermostat at T_2;
11: **else if** $PR_3 \leq PR_{real} < PR_2$
12: Set thermostat at T_3;
13: ⋮
14: **else if** $PR^{min} \leq PR_{real} < PR_n$
15: Set thermostat at T^{min};
16: **end if**
20: **end for**

5.5 Demand Response Studies Through Computational Experiments

This section provides a demand response study based on the DR algorithms developed in Section 5.4 and the house model shown in Section 5.2.2 (Figure 2). The real-life weather data [27] for a typical year in Springfield, IL is loaded into the program and the Ameren's RTP and DAP tariffs [37] for the same year is used in the computational experiment system.

5.5.1HVAC Demand Response Study

The study first focuses on how different algorithms affect the DR efficiency of HVACs by using RTP and DAP tariffs. For all the four different algorithms shown in Section IV, the upper and lower temperature settings are 71° and 79°, respectively. For the PSO algorithm, ΔT is set at 3°. For the heuristic algorithm, a 'nine-point' thermostat setting at 71°; 72°, 73°, 74°, 75°, 76°, 77°, 78° and 79° is used, in which 71° and 79° are the thermostat settings corresponding to PR^{min} and PR^{max} during a day, respectively.

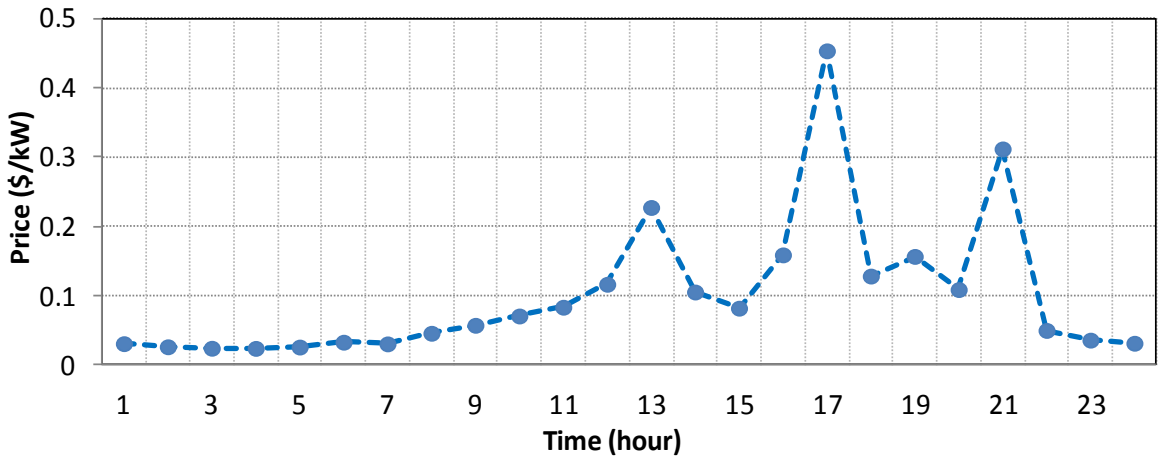

Figure 5.10 Real-time electricity price

Figures 5.7 and 5.8 compare HVAC energy and cost using the four different DR algorithms and a traditional constant 72° thermostat setting strategy for a highest RTP day and a highest DAP day in Summer 2011. In the figures, Model-OP, Reg-OP and PSO-OP stand for DR

strategies developed according to Sections 5.4.1, 5.4.2, and 5.4.3, respectively. All the DR policies are tested in the integrative computational experiment system. Table 5.1 shows a comparison of the HVAC cost for the highest RTP day, a moderate RTP day, and a low RTP day. The following remarks are obtained.

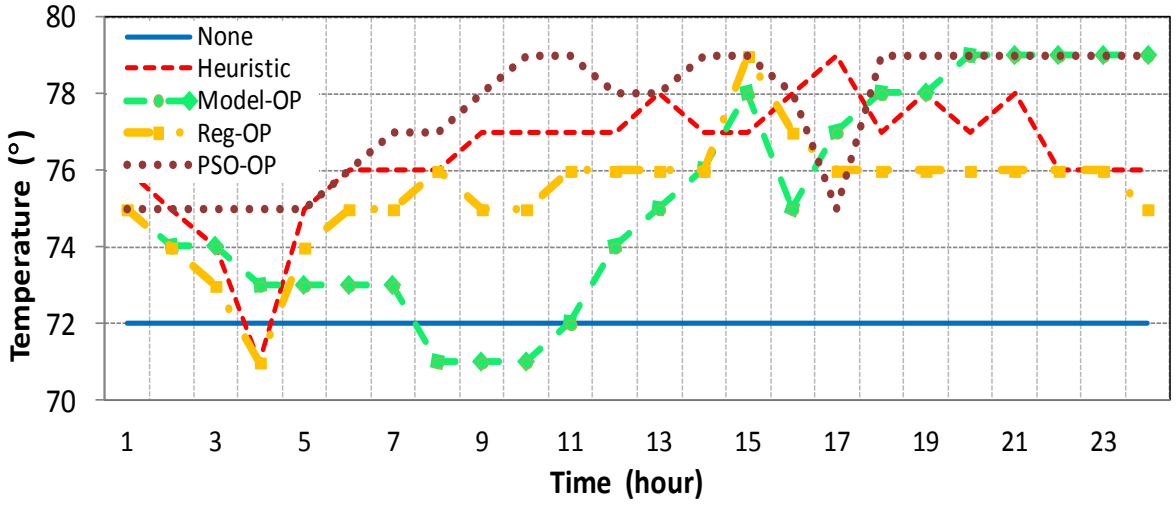

Figure 5.11 Thermostat setting

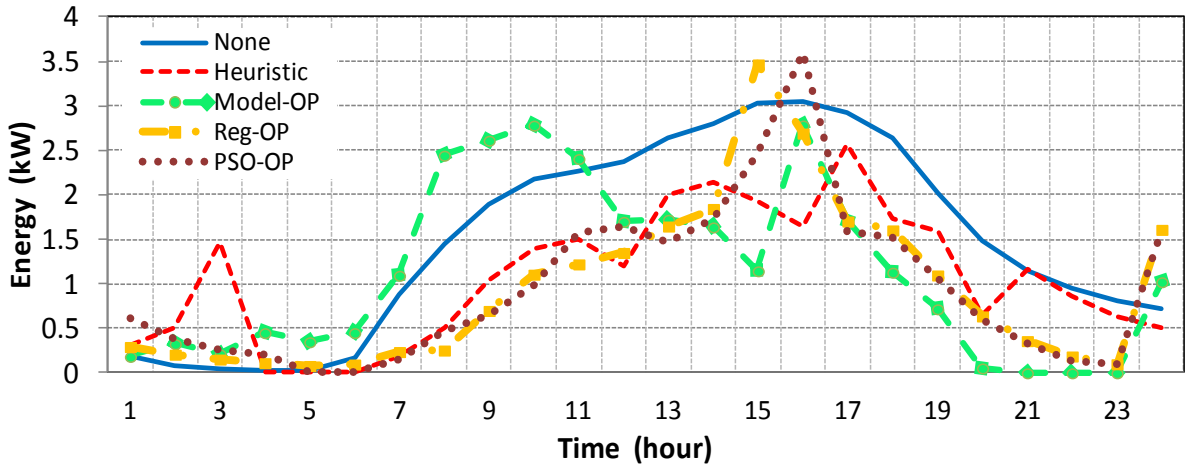

Figure 5.12 Energy consumption

1) For all the four algorithms, DR clearly reduces the energy consumption of the HVAC during peak hours using either RTP or DAP tariff structure (Figure. 6c and 7c).

	Highest		Mild		Low	
	RTP	DAP	RTP	DAP	RTP	DAP
None	$5.09	$3.44	$1.60	$1.57	$1.36	$1.32
Heuristic	$3.77	$2.28	$1.08	$1.38	$1.04	$0.88
Model-OP	$3.12	$2.05	$0.93	$0.80	$0.90	$0.82
Reg-OP	$3.12	$1.98	$0.73	$0.76	$0.73	$0.66
PSO-OP	$3.11	$1.94	$0.77	$0.56	$0.88	$0.76

Table 5.1 HVAC energy cost for high, mild and low price days

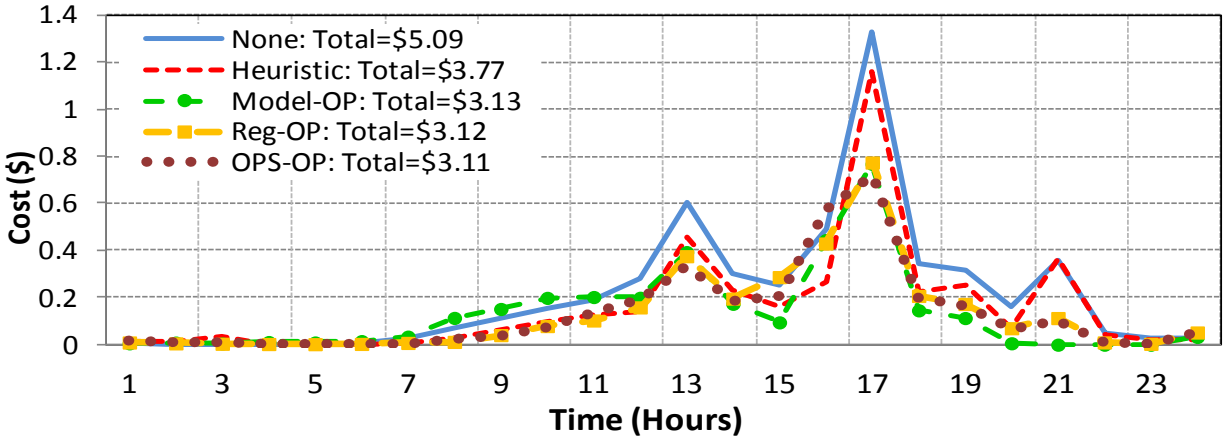

Figure 5.13 Hourly and total costs

2) DR using Model-OP, Reg-OP and PSO-OP requires HVAC energy consumption model while the heuristic algorithm does not need the energy consumption model, giving the heuristic algorithm an advantage in this perspective.

3) DR based on Model-OP, Reg-OP and PSO-OP requires detailed price information of a day, which is usually not available for RTP tariff structure.

4) For DAP tariff structure, HVAC energy consumption could still be high during actual utility peak hours because DAP tariff may be inconsistent with the real-time load demand. For both RTP and DAP binding customers, part of the energy consumption reduction during peak load periods is shifted to low price windows (Figures 5.12 and 5.13).

5) In terms of cost saving, DR is more effective for RTP binding loads than DAP binding loads (Figures 5.13 and 5.17). In terms of total cost, DAP is more economical but requires load binding one day before actual use of energy. Thus, a customer may need to take the risk of financial loss if the actual load level is lower or higher than the day-ahead binding load level.

6) For a high price day, DAP binding load is usually cheaper than RTP binding load (Table 1). For a moderate or a low price day, the cost for a RTP binding customer could be lower than that of a DAP binding customer. An examination of RTP and DAP tariffs shows that it is possible that RTP tariff is lower than DAP tariff during a day, indicating that DAP binding customers may need to pay more than RTP binding customers for those days.

7) According to Table 5.1, costs of Model-OP, Reg-OP and PSO-OP are close and better than that of the heuristic model. For some days, PSO-OP is better than Reg-OP. This is due to the fact that a global optimal solution cannot be guaranteed even using the well developed MATLAB optimization toolbox. In other words, the optimal solution solved by using Model-OP, Reg-OP or PSO-OP could be a local optimal solution, indicating a potential need for advanced algorithms that can guarantee a global optimal solution.

8) The energy consumption pattern of Reg-OP and PSO-OP is very close but is different from that of Model-OP. This is due to the fact that both PSO-OP and Reg-OP are based on the regression model using the simulated HVAC energy consumption data while Model-OP is based on energy consumption obtained from (3).

It is also investigated how adjusting the upper thermostat setting T^{max} would affect the energy and cost saving through the computational experiment. In a comparison study for upper thermostat settings of 80° and 81° using different DR strategies, it was found that although

modifying the upper thermostat setting could reduce the cost, proper management of HVAC energy usage during peak electricity price is still the most important factor.

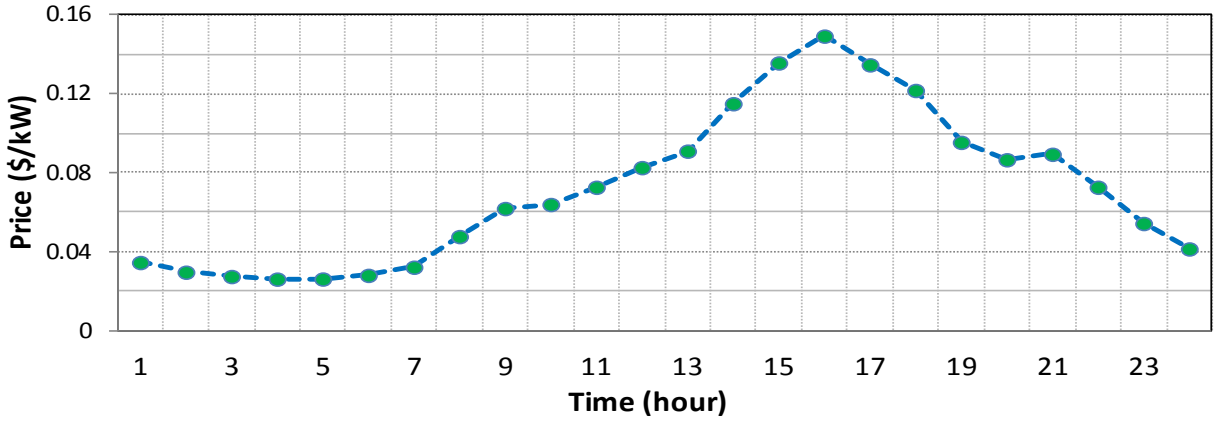

Figure 5.14 Day-ahead electricity price

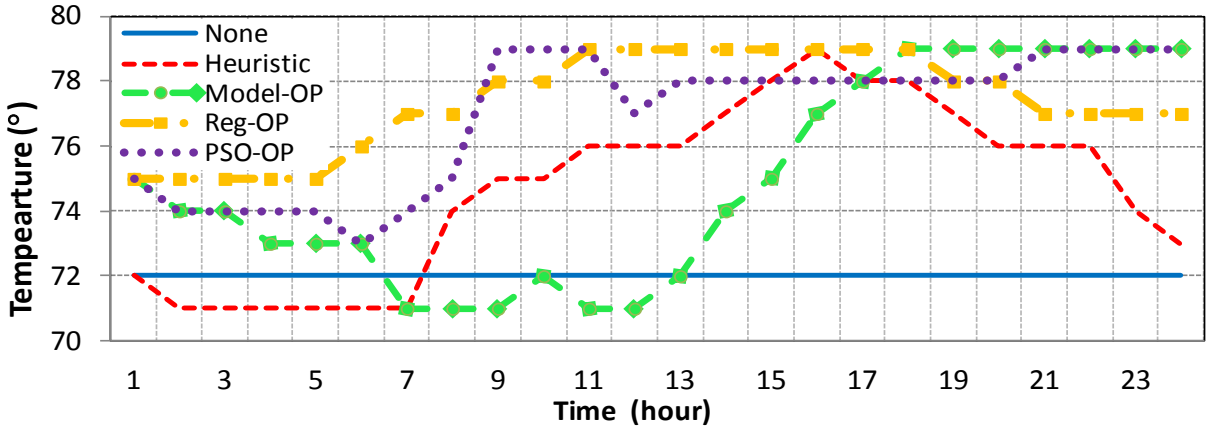

Figure 5.15 Thermostat setting

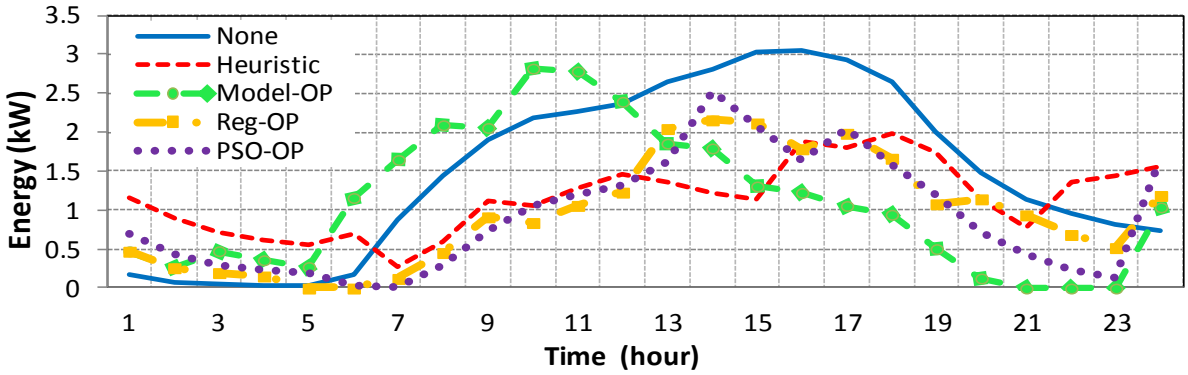

Figure 5.16 Energy consumption

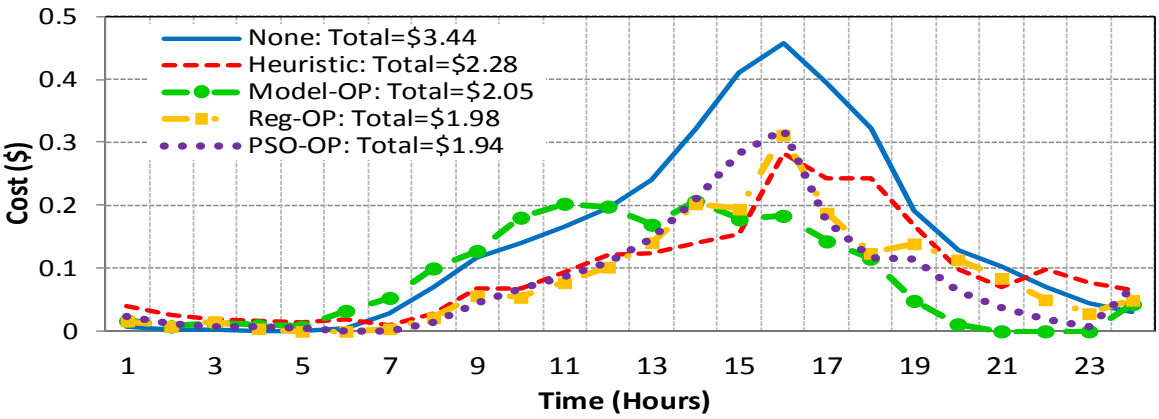

Figure 5.17 Hourly and total costs

5.5.2 Dishwasher and Dryer Demand Response Study

There are a large number of references on this topic [21], [25], [43], [44]. The basic principle is that within a customer acceptable time frame, these DR appliances operate if the electricity price is lower than a customer predefined price, otherwise those DR appliances operate at the time frame that has the lowest price within a customer preferred time window.

The simulation is conducted in the following way. For a conventional mechanism without DR, it is assumed that the dishwasher operates between 7pm to 8pm and the dryer operates between 6pm to 9pm on Monday, Wednesday, and Friday. On Sunday, 50% usage of dishwasher and dryer is defined between 7pm to 8pm and 6pm to 9pm, respectively, for consideration of general light load usage of those appliances during the weekend.

Both conventional and DR policies are generated in MATLAB and then loaded into the home energy simulator. Figures 5.18 and 5.19 compare total energy and cost of the house using conventional and DR policies during a high DAP day on a Wednesday in July 2011. In both cases, the 9-point heuristic DR policy of HVACs is considered. Similar results were also obtained when using the other three DR policies for HVACs. As it can be seen from the figure,

with DR, peak load is clearly reduced and the energy usage of dishwasher and dryers is shifted to low cost time period of the day.

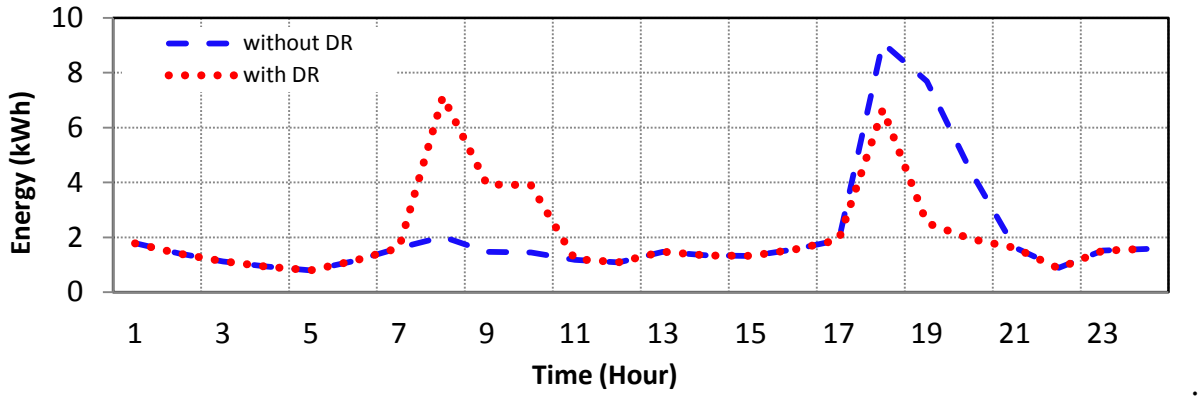

Figure 5.18 Energy consumption

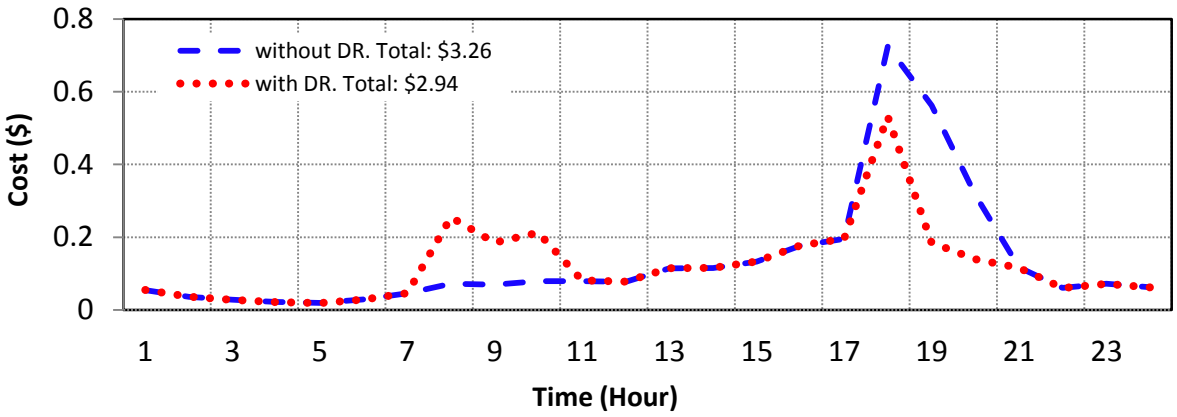

Figure 5.19 Total energy consumption and cost of a house in a high price day

The energy and cost saving are also affected by the number of people in the house. For the same condition shown in Figures 5.18 and 5.19, the corresponding energy and cost for 2, 4, 8 and 11 people in the house are 47.35kWh, 48kWh, 49.33kWh and 50.44kWh, and $2.74, $2.78, $2.86 and $2.94, respectively. In general, with more people in a house, the energy consumption and cost increase. But, the impact is not significant.

5.6 Conclusion

This paper presents a computational experiment approach to develop and investigate demand response strategies for a typical residential house.

The analysis presented in this paper illustrates that the real-time market is usually more expensive and changes more sharply than the day-ahead market. However, it is also found that the real-time market could be cheaper than the day-ahead market for a number of days.

For HVACs, how to define thermostat settings is critical. The paper investigates DR policies that are obtained by using four different approaches. For all the four DR algorithms, the demand response clearly reduces HVAC energy consumption during the peak hours using RTP or DAP tariff structure. In general, optimization-based DR algorithms are more efficient than the heuristic DR algorithm. However, demand response based on Model-OP, Reg-OP and PSO-OP requires detailed price information of a day, which is usually not available for RTP tariff structure, giving the heuristic algorithm an advantage in this perspective. It is also found that an optimal solution obtained by using Model-OP, Reg-OP and PSO-OP methods could be a local optimal solution, indicating a potential need for advanced algorithms that can guarantee a global optimal solution. This is one of our ongoing interdisciplinary research activities in this area.

For dishwashers and dryers, the DR strategy is to reschedule the energy usage of these appliances to a later time if the electricity price is high. Although the total energy consumption of a house does not change, the peak load reduction is clear and the overall energy cost drops obviously depending on the price of a day.

5.7 References

[1] T. Joseph Lui, Warwick Stirling, and Henry O. Marcy, “Get Smart,” *IEEE Power & Energy Mag.*, Vol. 8, No. 3, 66-78, May/June 2010.

[2] "Demand Response Discussion for the 2007 Long-Term Reliability Assessment," North

American Electric Reliability Corporation, February 2007. Accessed on May 18, 2013 http://www.naesb.org/pdf2/dsmee052407w4.pdf

[3] "Benefits of Demand Response in Electricity Markets and Recommendations for Achieving them," A report to the United States Congress, U.S. Department of Energy, February 2006. Accessed on May 18, 2013 http://eetd.lbl.gov/ea/EMS/reports/congress-1252d.pdf

[4] M.H. Albadi and E. F. El-Saadany "Demand Response in Electricity Markets: An Overview," *Proc. of IEEE Power Engineering Society 2007 General Meeting*, Tampa FL, June 24-28, 2007.

[5] S.A. Pourmousavi and M.H. Nehrir, "Real-Time Central Demand Response for Primary Frequency Regulation in Microgrids," *IEEE Trans. on Smart Grid*, Vol. 3, No. 4, December 2012, pp. 1988-1996.

[6] Z. Fan, "A Distributed Demand Response Algorithm and Its Application to PHEV Charging in Smart Grids," *IEEE Trans. on Smart Grid*, Vol. 3, No. 3, September 2012, pp. 1280-1290.

[7] N. Navid-Azarbaijani and M.H. Banakar, "Realizing load reduction functions by aperiodic switching of load groups," *IEEE Trans. Power Syst.*, vol. 11, no. 2, pp. 721–727, 1996.

[8] K. Y. Huang, H. C. Chin, and Y. C. Huang, "A model reference adaptive control strategy for interruptible load management," *IEEE Trans. Power Syst.*, vol. 19, no. 1, pp. 683–689, 2004.

[9] D. Westermann and A. John, "Demand matching wind power generation with wide-area measurement and demand-side management," *IEEE Trans. Energy Convers.*, vol. 22, no. 1, pp. 145–149, 2007.

[10] D. T. Nguyen, M. Negnevitsky, and M. de Groot, "Pool-based demand response exchange-concept and modeling," *IEEE Trans. Power Syst.*, vol. 26, no. 3, pp. 1677–1685, 2011.

[11] P. Faria, Z. Vale, J. Soares, and J. Ferreira, "Demand response management in power systems using a particle swarm optimization approach," *IEEE Intell. Syst.*, 2011.

[12] A.J. Conejo, J.M. Morales and L. Baringo, "Real-Time Demand Response Model," *IEEE Trans. on Smart Grid*, vol.1, no.3, pp. 236-242, Dec. 2010.

[13] M. Parvania andM. Fotuhi-Firuzabad, "Integrating load reduction into wholesale energy market with application to wind power integration," *IEEE Syst. J.*, vol. 6, no. 1, pp. 35–45, 2012.

[14] K.Dietrich, J.M. Latorre, L.Olmos, andA. Ramos, "Demand response in an isolated system with high wind integration," *IEEE Trans. Power Syst.*, vol. 27, no. 1, pp. 20–29, 2012.

[15] M. Carrión, A. B. Philpott, A. J. Conejo, and J. M. Arroyo, "A stochastic programming approach to electric energy procurement for large consumers," *IEEE Trans. Power Syst.*, vol. 22, no. 2, pp. 744–754, 2007.

[16] E. Gómez-Villalva and A. Ramos, "Optimal energy management of an industrial consumer in liberalized markets," *IEEE Trans. Power Syst.*, vol. 18, pp. 716–723, 2003.

[17] A. B. Philpott and E. Pettersen, "Optimizing demand-side bids in day-ahead electricity markets," *IEEE Trans. Power Syst.*, vol. 21, pp. 488–498, 2006.

[18] W.W. Hogan, "Electricity Market Reform: Market Design and Resource Adequacy," Harvard University, Cambridge, Massachusetts, June 2011.

[19] M. Carrión, A. J. Conejo, and J. M. Arroyo, "Forward contracting and selling price determination for a retailer," *IEEE Trans. Power Syst.*, vol. 22, no. 4, pp. 2105–2114, 2007.

[20] S. P. Holland and E. T. Mansur, "The short-run effects of time-varying prices in competitive electricity markets," *Energy J.*, vol. 27, no. 4, pp. 127–155, 2006.

[21] Jason W. Black, "Integrating Demand into the U.S. Electric Power System: Technical, Economic, and Regulatory Frameworks for Responsive Load," PhD dissertation, Massachusetts Institute of Technology, June 2005.

[22] Z.T. Taylor, K. Gowri, and S. Katipamula, "GridLAB-D Technical Support Document: Residential End-Use Module Version 1.0," Pacific Northwest National Laboratory, Richland, Washington, July 2008.

[23] Z. Zhou, F. Zhao, and J. Wang, "Agent-Based Electricity Market Simulation with Demand Response from Commercial Buildings," *IEEE Trans. on Smart Grid*, vol. 2, no. 4, pp.580-588, Dec. 2011.

[24] Energy Performance of Buildings—Calculation of Energy Use for Space Heating and Cooling, ISO 13790:2008.

[25] T.T. Kim and H.V. Poor, "Scheduling Power Consumption With Price Uncertainty," *IEEE Trans. on Smart Grid*, vol.2, no.3, pp.519-527, Sept. 2011.

[26] H. Farhangi, "The Path of the Smart Grid," *IEEE Power & Energy Mag.*, Vol. 8, No. 1, January/February 2010.

[27] "Weather Data & Weather Data Processing Utility Programs," Accessed on May 19, 2013 http://doe2.com/index_wth.html

[28] S. Li, R. Challoo, and Robert A. McLauchlan, "Heat Transfer Simulation Using PSpice",

Proc. of 2003 ASME Summer Heat Transfer Conf., July 21–23, 2003, Las Vegas, Nevada, USA.

[29] A. F. Mills, "Heat Transfer," 2nd Ed., Upper Saddle River, NJ: Prentice Hall, (1999).

[30] K. D. Hangen, "Heat Transfer with Applications," Upper Saddle River, NJ: Prentice Hall, (1999).

[31] A.G. Thomas, C. Cai, D.C. Aliprantis, and L. Tesfatsion, "Effects of Price-Responsive Residential Demand on Retail and Wholesale Power Market Operations," Proceedings of 2012 IEEE Power & Energy Society General Meeting, San Diego, CA, July 22-26, 2012.

[32] "eQUEST Introductory Tutorial, version 3.64," James J. Hirsch & Associates, Camarillo, CA, December 2010.

[33] S. Kavanaugh, "HVAC Simplified," American Society of Heating, Refrigerating, and Air-Conditioning, Atlanta, GA, 2007.

[34] Residential Energy Consumption Survey (RECS), U.S. Energy Information Administration. Accessed on May 26, 2013 <http://www.eia.gov/consumption/residential/index.cfm>

[35] Estimating Appliance and Home Electronic Energy Use, United States Department of Energy; Office of Energy Efficiency and Renewable Energy. Accessed on May 26, 2013 <http://www.energysavers.gov/your_home/>

[36] Edward G. Pita, "Air Conditioning Principles and Systems: An Energy Approach," 2th Ed. Upper Saddle River, NJ: Prentice Hall, 2001.

[37] Real-Time Pricing for Residential Customers, Ameren Focused Energy. http://www.ameren.com/sites/aiu/ElectricChoice/Pages/ResRealTimePricing.aspx.

[38] S. Li, D.C. Wunsch, E. O'Hair, and M.G. Giesselmann, "Comparative Analysis of Regression and Artificial Neural Network Models for Wind Turbine Power Curve Estimation ", *Transactions of the ASME, Journal of Solar Energy Engineering*, Vol. 123, No. 4, November 2001, pp. 327-332.

[40] J. Kennedy and R.C. Eberhard, "Particle swarm optimization", *Proc. of IEEE Int. Conf. on Neural Networks*, Piscataway, NJ, USA, 1995, pp. 1942-1948.

[41] N. Padhye, K. Deb, and P. Mittal, "Boundary Handling Approaches in Particle Swarm Optimization", Advances in Intelligent Systems and Computing, Vol. 201, Springer, 2013, pp. 287-298.

[42] Advances in Intelligent Systems and Computing Volume 201, 2013, pp 287- 298"

Conditions of Thermal Comfort: Influence of Humidity and Temperature on Personal Well-Being," SENSIRION, 2010.

[43] H. Sæle and O.S. Grande, "Demand Response from Household Customers: Experiences From a Pilot Study in Norway," *IEEE Trans. on Smart Grid*, Vol. 2, No. 1, March 2011, pp. 102-109.

[44] National Action Plan for Energy Efficiency (2010). "Coordination of Energy Efficiency and Demand Response," prepared by C. Goldman, M. Reid, R. Levy, and A. Silverstein, www.epa.gov/eeactionplan

[45] K. Spees and L.B. Lave, "Demand Response and Electricity Market Efficiency," *The Electricity Journal*, Vol. 20, Issue 3, April 2007, pp. 69-85

6 CONCLUSIONS AND FUTURE WORK

With the development of smart grid, a novel computational system is required to solve the competitive power market issue and assist the market participants to make proper decisions. By converting the power market mathematical models into PowerWorld simulator, it is possible to use the optimal power flow add-ons in PowerWorld simulator to maximize overall net surplus. The designed computational system is validated through Matlab. The piecewise linear and cubic generators' cost models have been evaluated. There are no significant differences between the results of the two models. For DC and AC OPFs, if the transmission line loss is negligible, the LMPs and real power generations would not diverge much from each other. The transmission line congestion can directly affect the LMPs on each bus. During the peak load period, LMPs on each bus will increase seriously. The amount of LSE net surplus depends on the load real power demand, the constant bidding rates, and the correspondence LMP. Therefore, during the peak load period, LSEs can only draw a small amount of net surplus which stands in sharp contrast to the off peak periods. GenCos' net surplus is highly reliant on both the real power generations of the generators and the corresponding LMPs on the generator buses. Hence, GenCos' net surplus is consistent with the changes of LMPs. The ISO net surplus is determined by the overall load profiles and the divergence of LMPs on each bus. During the daily power system operation, the utility companies also need to consider the start-up and turn-down costs for each generation units in the UC program. By combining PowerWorld simulator and the self-developed Matlab UC toolbox, it is convenient to perform UC and visualize the results. If the power transmission line loss is large, the simulation results show that the operation schedules can be very different for

running UC under the AC or DC power flow. Due to the large transmission loss, extra units need be added into the operational list during the peak load period. Future work will be directed towards developing the distributed optimal power flow (DOPF) and integrating DOPF into PowerWorld simulator.

Due to the dynamic nature of the competitive power market, each generation companies must be able to make offers or bids to ensure their own economic profits and avoid any potential risks. Therefore, the stochastic reinforcement learning (SRL) technique has been used into GenCo Learning. By equipping GenCo Learning, each GenCo can adjust their bidding strategies along with the changes in daily net surplus. GenCo Learning includes the online and offline learning methods. For both the online and offline learning, the number of bidding strategies can impact the GenCo's net surplus, since more strategies will lead to less possibility of choosing a certain strategy of high net surplus potential. Whereas using GenCo learning always has better gain in the net surplus than without using any learning technique or just report the true marginal cost of the generator. Unlike the online learning, the offline learning consists of two steps of procedure. The training procedure allows the GenCos to use the historical data (net surplus) to train the agent in order to get the trained strategies profile or distribution. The testing procedure is same as the online learning. The amount of training data can directly affect the trained strategy. In general, by using more data for training, the GenCo will have the better bidding strategies and get more net surplus in the testing procedure. Further work should be directed towards applying GenCo learning larger into some larger power systems and also including the LSE learning.

By converting two market policies into PowerWorld simulator, the optimal power dispatch can be applied for managing the power generation of the DGs. In order to make the MG

studies more comprehensive, both the power inverter and economic constraints has been considered in the simulation. In the grid connected condition, by using the minimum cost or maximum profit policy, the MG is able to operate more economically than the normal power flow study by taking the necessary operation on curtail loads. For the minimum cost policy, MG will shed all the curtail loads if the compensation costs of the specific curtail loads are lower than the electricity price of main grid. In contrast, for the maximum profit policy, load shedding is not preferable since any compensation cost will lower the overall profit in MG. In the islanding condition, the load shedding operation becomes more complicated that grid connected mode. Due to the limitations of DGs' generation capacities, both minimum cost and maximum profit policies will shed a large amount of curtail load to maintain the power balance. For the minimum cost policy, since it always shed the cheaper curtail load, the amount of load shedding is more than maximum profit policy. For the maximum profit policy, in order to gain more profit, MG will utilize the DGs' power to support as much curtail load as possible. Regarding the voltage regulation and power losses, using DGs' generation in MG network have better performance under PV mode than PQ mode. Also, due to the rated power constraints of DG power converters, the preference voltage may not be achieved in PV mode. Further work should be directed towards developing other optimal energy management methods by using artificial intelligence to achieve better performance on voltage regulation and operational cost.

For the HVAC's DR strategies, the proposed heuristic DR algorithm and optimization-based DR algorithms has been presented. For the heuristic DR algorithm, it can operate based on the RTP or DAP and adjust the thermostat settings to reduce the energy consumption of the peak price interval. For the optimization-based DR algorithms, the Model-OP, the proposed Reg-OP, and PSO-OP have been evaluated. Based on the results, Reg-OP and PSO-OP have the lowest

costs under both RTP and DAP conditions, since both of their optimization methods were applied into the more accurate regressed thermal model of a single house system. The results of Reg-OP and PSO-OP are very close to each other. Moreover, the Reg-OP uses the Penalty and Barrier Methods, its optimal solution is highly depend on the initial condition which can be hardly obtained in real situation. In contrast, PSO-OP doesn't require any initial condition and can achieve a near global optimal solution after reaching the termination condition. Future work should be directed towards adding the solar panel, energy storage devices (battery), and other home appliances into the optimization program to investigate the more comprehensive solution of demand response for a single house system.